

CONCERT–Japan Research and Innovation Joint Call

Efficient Energy Storage and Distribution
Resilience against Disasters

RAPSODI Project

Risk Assessment and design of Prevention Structures
for enhanced tsunami Disaster resilience

Deliverable D7 – Results of the
laboratory analysis and wave
flume tests
2nd year of funding

20120768–07–R
28 May 2015
Revision: 0



This work was supported by funding received from the
CONCERT–Japan Joint Call on Efficient Energy Storage
and Distribution/Resilience against Disasters



Project information

Name of the project:	RAPSODI
Start of the project:	01 July 2013
Duration (no. of months):	24
End of the project	30 June 2015
Name and country/region of each partner	NGI, Norway; PARI, Japan; TU-BS, Germany; METU, Turkey
Overall budget	383 k€

Client

Client:	CONCERT-Japan Joint Call Secretariat
Client's contact persons:	CONCERT-Japan Coordinator Projektträger im deutschen Zentrum für Luft- und Raumfahrt, Europäische und Internationale Zusammenarbeit, Germany Ms. Dr. Sabine Puch (sabine.puch@dlr.de) Phone: +49 228 3821 1423
	CONCERT-Japan Joint Call Secretariat Centre national de la recherche scientifique (CNRS) Ms. Lucie Durocher (lucie.durocher@cns-dir.fr) Phone: + 33 (0)1 44 96 47 14 Fax: + 33 (0)1 44 96 48 56

Contract reference:	http://www.concertjapan.eu NGI 229578/H20; METU 113M556; TUBS 01DR13016;
Settlement numbers	PARI 2013 H25国際第1-33号 2014 H26国際第1-17号

For NGI

Project manager:	Carl B. Harbitz
Prepared by:	Dr.-Ing. A. Strusińska-Correia, Dr.-Ing. A. Kortenhaus
Reviewed by:	Dr.-Ing. A. Strusińska-Correia, Dr. C.B. Harbitz

Publishable summary

The main objectives of the multilateral research project “Risk Assessment and Design of Prevention Structures fOr enhanced tsunami Disaster resilience (RAPSODI)” is to develop an enhanced method for the tsunami risk assessment and design of tsunami mitigation structures, contributing to the improved resilience against tsunami hazard in the tsunami-prone areas. The methods developed within the framework of the project are based on the results and findings from three project stages, including: (i) evaluation of existing knowledge and comparison of mitigation strategies, (ii) numerical and experimental studies, and (iii) methodology for tsunami vulnerability assessment and risk management.

The improved design of structural tsunami countermeasures required laboratory experiments on tsunami-loading and tsunami-induced damage in the wave flume of the Technical University of Braunschweig (TU-BS) in cooperation with the Middle East Technical University (METU) and TU-BS. The study was constrained to one type of the structure, namely the rubble-type of breakwater, identified as a research gap by a thorough literature study. Its performance under tsunami impact (generated as a solitary wave and a bore) was examined for its four configurations: (i) breakwater with a crown wall unit and a berm, (ii) breakwater without a crown wall unit and without a berm, (iii) breakwater with a crown wall unit and without a berm, (iv) breakwater with a shifted crown wall unit and without a berm. The layout of the rubble layers and the breakwater geometry was based on a simplified cross-section of the Haydarpasa Breakwater, protecting the Haydarpasa Port in Istanbul (Turkey), for which tsunami loads were not taken into account for the design. A similar investigation with the original geometry of the Haydarpasa Breakwater was examined in a wave flume of the Port and Airport Research Institute (PARI) in a framework of a collaboration of the RAPSODI project partners PARI and METU (with solitary wave and constant overflow used to represent a tsunami). These experiments served as reference tests in the study conducted at TU-BS.

The experimental results indicated that the harbour (landward) side of the breakwater, regardless the configuration, was most prone to damage (displacement of the armour layers over the harbour slope as well as the crown wall unit). The processes governing the breakwater damage were directly related to the breakwater submergence conditions tested and to the wave generation method: in case of the solitary wave impact (submerged breakwater conditions) wave overtopping was dominant, while in case of bore impact (emerged breakwater conditions) - pressure difference at the both sides of the breakwater.

The most stable breakwater configuration was the one with the crown wall unit and without the berm, however it failed under the impact of higher solitary waves. Further improvement of its stability can be achieved by applying a doubled armour layer on the harbour side, as indicated by the reference tests at PARI (however, not examined at TU-BS). Larger overtopping flow depths were attributed to the breakwater configuration without crown wall unit. The configuration with shifted crown wall



Publishable summary (cont.)

Project no: 20120768-07-R
Date: 28.05.2015
Revision: re0v no.
Page: 5

unit was less stable under wave impact due to the lack of sufficient support of the unit by the armour layer. The effect of the berm presence on wave impact was not clearly observed, most likely due to the resulting freeboard.

Contents

1	Introduction	8
2	Description of experiments at TU-BS	10
2.1	Wave flume	10
2.2	Experimental setup	11
2.3	Measuring technique	18
2.4	Testing programme	21
3	Description of reference tests at PARI	22
3.1	Wave flume	22
3.2	Experimental setup	22
3.3	Measuring technique	25
3.4	Testing programme	26
3.5	Summary of experiments at TU-BS and PARI	26
4	Analysis of experimental data from tests at TU-BS	29
4.1	Observed processes	29
4.1.1	Experiments with bore	29
4.1.2	Experiments with solitary wave	29
4.2	Analysis of flow depth / wave height	31
4.2.1	Experiments with bore	31
4.2.2	Experiments with solitary wave	36
4.3	Analysis of wave-induced pressure	39
4.3.1	Experiments with bore	39
4.3.2	Experiments with solitary wave	40
4.4	Analysis of flow velocity	43
4.4.1	Experiments with bore	43
4.4.2	Experiments with solitary wave	44
4.5	Analysis of breakwater damage	49
4.5.1	Experiments with bore	50
4.5.2	Experiments with solitary wave	51
5	Analysis of experimental data from tests at PARI	59
5.1	Key findings from tests at PARI	59
5.2	Differences to tests at TU-BS	60
6	Summary and conclusions	63
7	References	65
Appendix A		66
	Evolution of bore and solitary wave profiles in experiments at TU-BS	66
Appendix B		97
	Pressure measurements in experiments at TU-BS	97
Appendix C		113
	Flow velocity measurements in experiments at TU-BS	113



Appendix D	129
Breakwater damage profiles in experiments at TU-BS	129
Appendix E	145
Photo documentation of breakwater damage in experiments at TU-BS	145
Review and reference page	



1 Introduction

The main objectives of the Project “**Risk Assessment and design of Prevention Structures fOr enhanced tsunami DIaster resilience**” (RAPSODI <http://www.ngi.no/en/Project-pages/RAPSODI/>) is to provide an improved tool for tsunami risk assessment as well as an improved design of tsunami mitigation structures, based on the analysis of field surveys after the 2011 Tohoku Tsunami, numerical modelling and laboratory experiments. Analysis of structure failure under tsunami impact, its damage, and the exerted load is focus of the experimental work performed at the Technical University of Braunschweig (TU-BS) in the cooperation with the Middle East Technical University (METU) in the framework of project stage 2, Work Package 3 “Laboratory experiments on tsunami impact on structures” of the project. This report provides a detailed description of this investigation, including the model setup, experimental programme, and the gained results.

The type of the structure considered in this experimental study (a rubble mound breakwater) was selected on the basis of the failure matrix of tsunami mitigation structures in Japan, elaborated in RAPSODI Deliverable 1 “Existing tools, data, and literature on tsunami impact, loads on structures, failure modes and vulnerability assessment” (METU 2015), indicating the existing research gaps and potential research areas in the field of tsunami-induced load and damage to coastal structures.

Geometry of the Haydarpasa Breakwater, protecting the harbour in Istanbul (Turkey) was considered when determining the layout of the breakwater models investigated at TU-BS. Performance of the Haydarpasa Breakwater under tsunami impact (represented by solitary waves) was already investigated by the project partners METU and PARI in the facilities of PARI due to the fact that the tsunami load was not considered in its design (although it is constructed in a tsunami-prone area). By considering a slightly simplified geometry of the Haydarpasa Breakwater with further variations and including the additional type of tsunami impact source represented by a bore, the experiments at TU-BS were planned as an extension of the tests at PARI. The required simplifications of the breakwater cross-section as well as the bathymetry model as compared to the tests at PARI resulted predominantly from the limited time planned for the performance of the experiments.

The results generated from this study contribute to a better understanding of a failure mechanism and damage type of the investigated rubble-type breakwater under tsunami impact (under solitary wave and bore conditions). Based on the results, recommendations for an improved tsunami-resilient breakwater design for possible implementation in the tsunami risk modelling (Deliverable 8 “A GIS tsunami vulnerability and risk assessment model”, NGI 2015), will be given.

The report is structured as follows. In Chapter 2 a detailed description of the model setup and programme of the tests performed at TU-BS is provided. In Chapter 3 a brief overview of the experiments conducted at PARI is presented in order to highlight the similarities and the differences between these two studies. Chapter 4



contains the summary of the results gained from the experiments at TU-BS, including the analysis of wave height/flow depth, induced pressure, flow velocities/velocities at overtopping as well as the damage to the investigated breakwater models. The findings from the laboratory experiments at PARI are discussed in Chapter 5. The summary of the experiments and the most important results are provided together with the final conclusions and the recommendations for a tsunami-resistant breakwater geometry in Chapter 6.



2 Description of experiments at TU-BS

2.1 Wave flume

The experiments were conducted in the twin-wave flume of the LWI, which has a length of ca. 90 m and a maximum depth of 1.2 m. The wave flume consists of two individual parallel canals: one is 1.0 m wide and the second is 2.0 m wide (see Figure 2.1a and Figure 2.2); both have a horizontal bottom over the entire length.



Figure 2.1: Twin-wave flume at LWI, TU-BS with 1.0 m wide channel (left) and 2.0 m wide channel (right) with: a) wave maker, b) bore gate

A piston type of wave maker, used to generate solitary waves in the experiments, is installed at one end of the twin-wave flume. The required water depth for solitary wave generation ranges from ca. 0.5 to 0.8 m. Maximum height of solitary wave, which can be generated in the this facility for the given water depth conditions, yields ca. 0.24 m.

On the opposite end of the wave flume, there is a rubble mound slope absorbing waves and preventing from reflection of the waves from the end flume walls. Both flumes can be equipped additionally by removable bore gates, used for generation of a tsunami-like bore in a similar way to the break dam method (Figure 2.1b). The bore is triggered by a sudden release of the water stored behind the bore gate ($h_1=0.5 - 0.9$ m). The conditions at bore inundation can be varied by different water levels in front of the bore gate ($h_0=0.0, 0.1 - 0.3$ m).

For the purposes of the experiments, the 2.0 m wide wave flume was used.



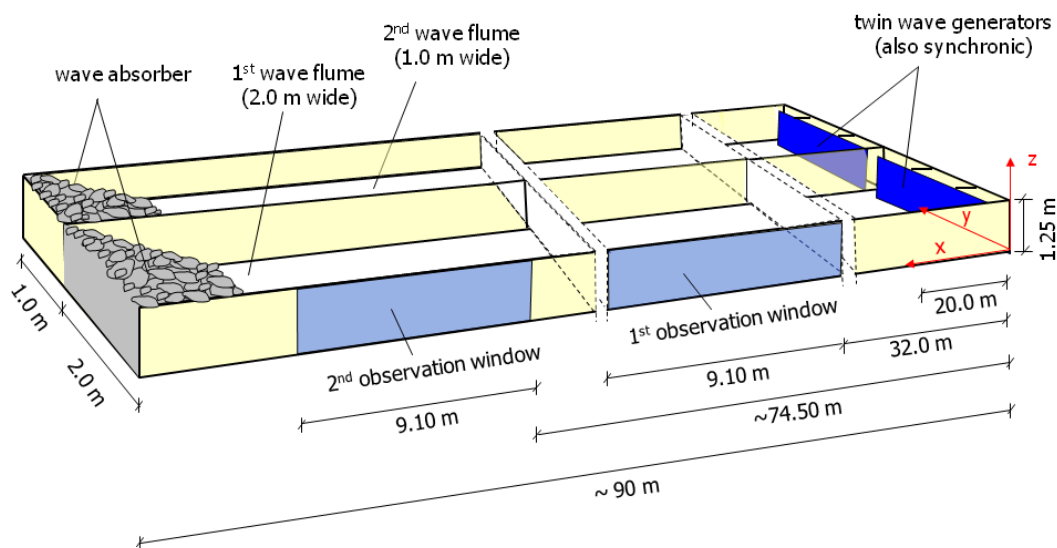


Figure 2.2: Geometry of the twin-wave flume at the LWI, TU-BS

2.2 Experimental setup

The model scale, based on the Froude similitude law, was chosen as 1:30, similarly to the reference experiments performed at the PARI (Guler et al., submitted). The scale factors to convert basic physical parameters are given in Table 2.1.

Table 2.1: Scaling factors using the similitude law of Froude

Parameter	Scale factor N_L	Conversion to model scale	Unit
Length	N_L	$1/N_L$	[m]
Time	$\sqrt{N_L}$	$1/\sqrt{N_L}$	[s]
Weight	N_L^3	$1/N_L^3$	[kg]

The experiments were conducted in the 2.0 m wide wave flume, which was divided into two parallel sections (ca. 1.0 m wide each) by means of a vertical plywood plate. All together four configurations of the simplified rubble-mound Haydarpasa Breakwater were tested (see Figure 2.3), with configuration 3 corresponding to the breakwater model tested at PARI:

- configuration 1: a rubble mound breakwater with a crown wall and a berm,
- configuration 2: a rubble mound breakwater without the crown wall,
- configuration 3: a rubble mound breakwater with a crown wall (based on the reference tests performed at PARI, see Guler et al., submitted),
- configuration 4: a rubble mound breakwater with a shifted crown wall.



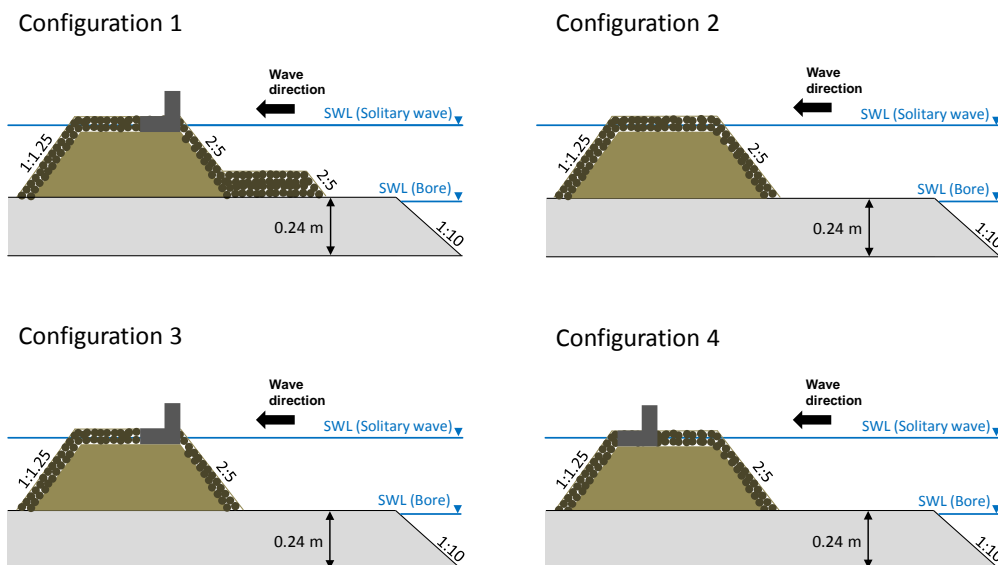


Figure 2.3: Breakwater configurations examined at TU-BS (scale 1:30)

The stones used for the construction of the rubble-mound breakwater were arranged manually in three layers, differing in the mass and their color:

- core layer (dark grey color): mass of stones between 0 and 10 g (mass of stones 0 – 0.2 t in prototype),
- filter layer (grey color): 0.07 m thick, mass of stones between 50 and 100 g (mass of stones 0.2 – 3 t in prototype),
- armour layer on the seaside (blue color): 0.09 m thick, mass of stones between 100 and 150 g (mass of stones 3 t in prototype),
- armour layer on the side of the port (yellow color): 0.07 m thick, mass of stones between 50 and 100 g (mass of stones 1.5 t in prototype),
- berm layer (red color): 0.2 m thick, mass of stones between 100 and 150 g (mass of stones 3 t in prototype).

The arrangement of the layers in the investigated breakwater configurations is shown in Figure 2.4, Figure 2.5 and Figure 2.6. While the stone mass, number of layers and their thickness was kept the same as in the reference tests at PARI, the arrangement of the core layer at the seaside and harbor sides was simplified to reduce the time effort needed for the breakwater model construction and reconstruction after the damage test – the core layer was not designed stepwise and thus the filter and the armour layers ran continuously from the breakwater top to its toe (see Chapter 3 for the comparison of the layer arrangement in the reference tests at PARI). In order to stabilize the harbor slopes, a wooden element was placed at the foot of the harbour slope (marked in black colour in Figure 2.7), which was also used in the reference experiments at PARI.



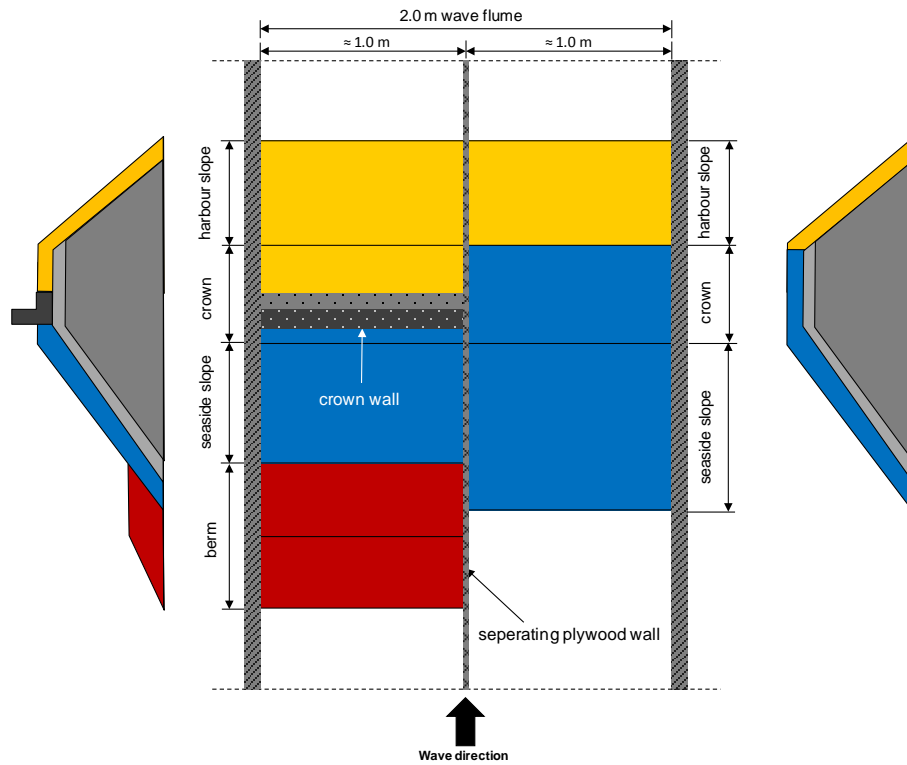


Figure 2.4: Layout of configurations 1 and 2 tested in wave flume of LWI, TU-BS



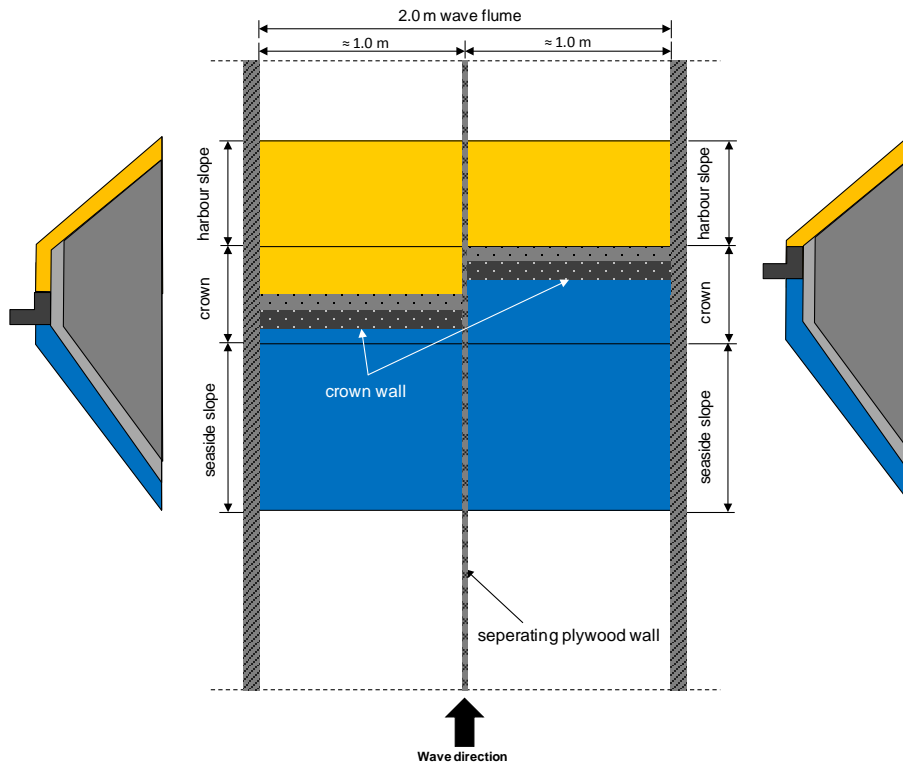
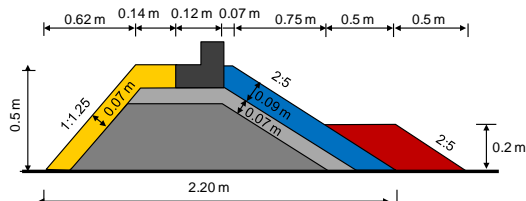


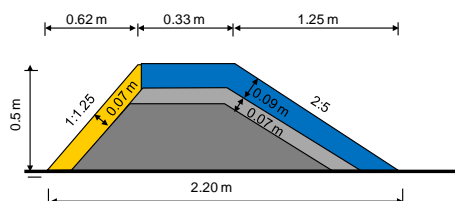
Figure 2.5: Layout of configuration 3 and 4 tested in wave flume of LWI, TU-BS



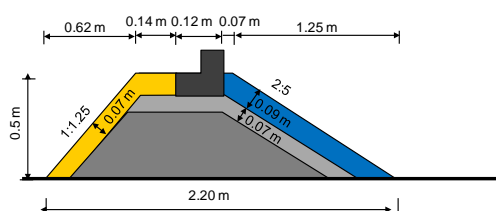
Configuration 1



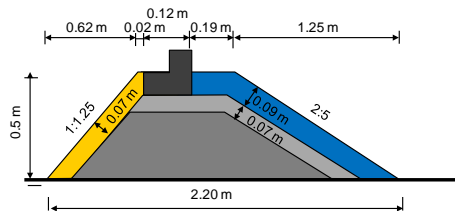
Configuration 2



Configuration 3



Configuration 4



Legend:

- | | | | |
|---|--|--|---------------------------|
|  | Armour layer at seaside (100 – 150 g) |  | Filter layer (50 – 100 g) |
|  | Armour layer at harbor side (50 – 100 g) |  | Core layer (0 – 10 g) |
|  | Berm (100 – 150 g) | | |

Figure 2.6: Geometry details of breakwater models tested at TU-BS (scale 1:30)

In contrast to the reference tests at PARI, the bathymetry model consisted solely of plywood horizontal platform of slope 1:10, on which the breakwater models were constructed (see Figure 2.7 and Chapter 3 for the comparison). Due to a significant length and a significant quantity of the material required for the construction, the slope 1:100 preceding the platform in the reference tests at PARI was not built in order to reduce the time for the construction works and to reduce the expenses in the budget. The platform geometry was different than that used in the reference tests at PARI, since its adjustments to the flume geometry, water depth conditions and breakwater model length were necessary. The platform height of 0.24 m resulted from the optimum water level required for the solitary wave generation and to maintain same water level above the platform (of 0.42 m) as in the reference tests at PARI. The horizontal length of the platform seaside slope was 2.32 m and the one of the horizontal part, on which the breakwater models were constructed, was 3.60 m (Figure 2.7). The horizontal length of the harbour side slope was 0.6 m, given the slope 2:5. The platform had a total length of 6.52 m. The foot of the platform began at a distance of 29.53 m from the wave maker. The void under the wood plate was filled with bricks to increase its capability of carrying the heavy breakwater models.

This platform was also used in the experiments with the tsunami bore in order to keep same bathymetry model in all test series. However, this led to less favourable submergence depth conditions of the breakwater models (the models were almost completely emerged in contrast to the tests with the solitary waves), with the water depth of 0.2 m reaching slightly below the horizontal part of the platform. Optimally,



construction of the breakwater models directly on the flume bottom would be preferred to provide more realistic submergence conditions of the models. This solution was however not possible due to the enormous time effort required for removing the platform and the re-construction of the breakwater models.

The geometry of the breakwater models was kept almost same as in the reference tests (for comparison see Chapter 3). All breakwater models were 0.5 m high and 2.2 m wide and had a slope of 2:5 on the seaside and 1:1.25 on the harbour side. The breakwater crown in all setups was 0.33 m long and was longer than in the reference tests in order to be able to investigate the configuration with a shifted crown wall. The following breakwater configurations were tested:

- Configuration 1 (Figure 2.7a): The breakwater with the crown wall and the berm started 0.5 m behind the end of the seaside platform slope. The berm had a total length of 1.0 m (including 0.5 m long seaside slope and 0.5 m long berm crown). The seaside slope of the berm was 2:5.
- Configuration 2 (Figure 2.7b): The breakwater without the crown wall and without the berm with seaside toe placed 1.0 m behind the end of the seaside platform slope.
- Configuration 3 (Figure 2.7c): The breakwater with the crown wall and without the berm with seaside toe placed 1.0 m behind the end of the seaside platform slope. The crown wall was placed at the start of the breakwater crown like in configuration 1. This configuration corresponds to that examined in the reference tests at PARI.
- Configuration 4 (Figure 2.7d): The breakwater with the crown wall and without the berm with seaside toe placed also 1.0 m behind the end of the seaside platform slope. The crown wall was shifted at the end of the breakwater crown.

The crown wall, used in configurations 1, 3 and 4, consisted of three similar concrete elements, which were 0.335 m, 0.335 m and 0.300 m wide (left element, element in the middle, and the right element in respect to the direction of wave propagation), 0.12 m long, and 0.12 m high (see Figure 2.8). The middle one had two holes for placing two pressure sensors – one in the front wall and another one at the bottom. As compared to the crown wall units used in the reference tests at PARI, all the walls were designed perpendicular to each other (i.e. at an angle of 90°), while in the reference tests the back part of the front was designed with a slope of 2.5:1.0 (for comparison see Chapter 3). The crown wall units in the reference tests were equipped with miniature pressure sensors, glued directly on the unit walls without the necessity of drilling a hole for these measuring devices.



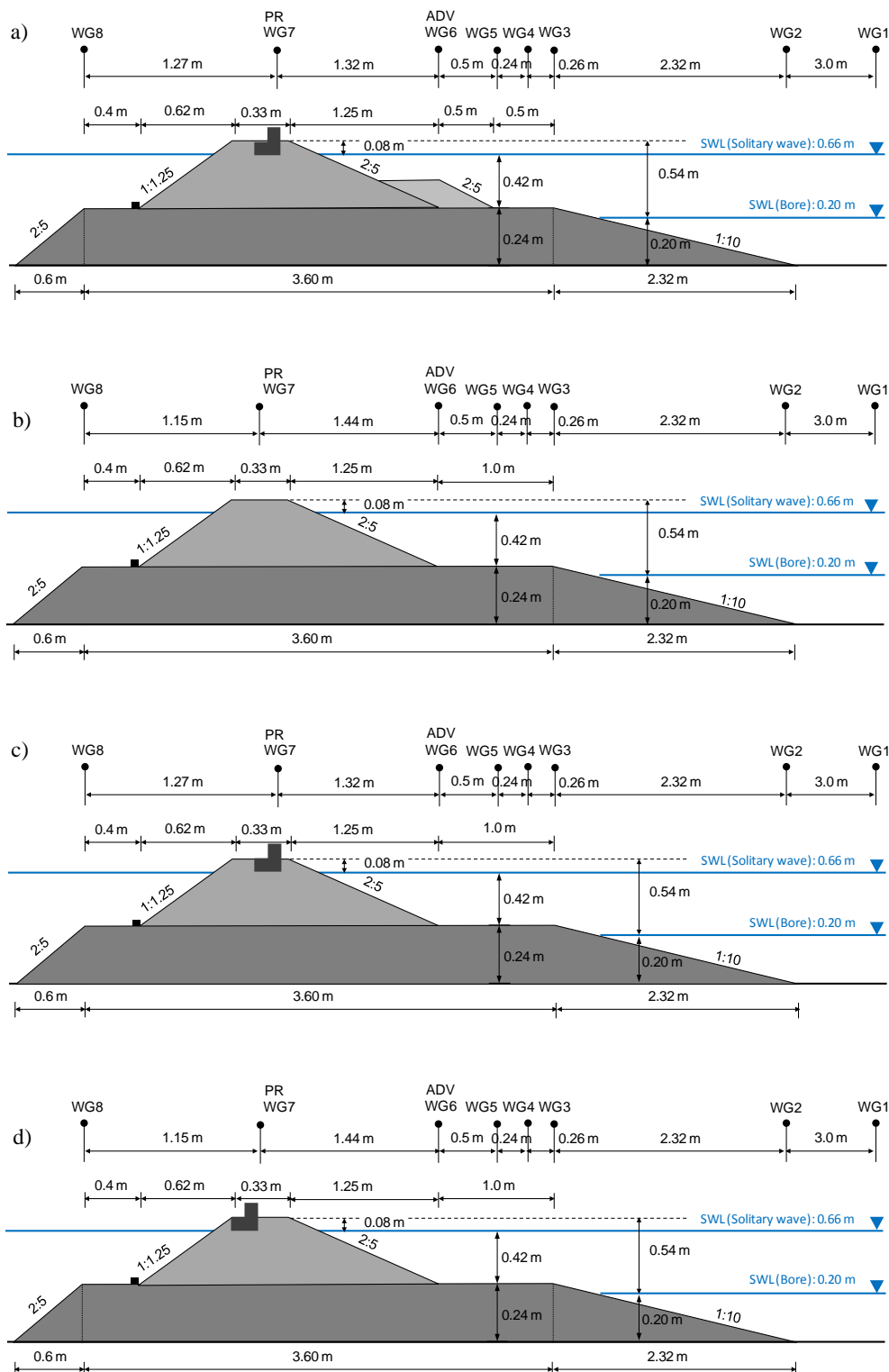


Figure 2.7: Experimental setup at TU-BS including measuring instruments: a) configuration 1, b) configuration 2, c) configuration 3 and d) configuration 4 (scale 1:30)



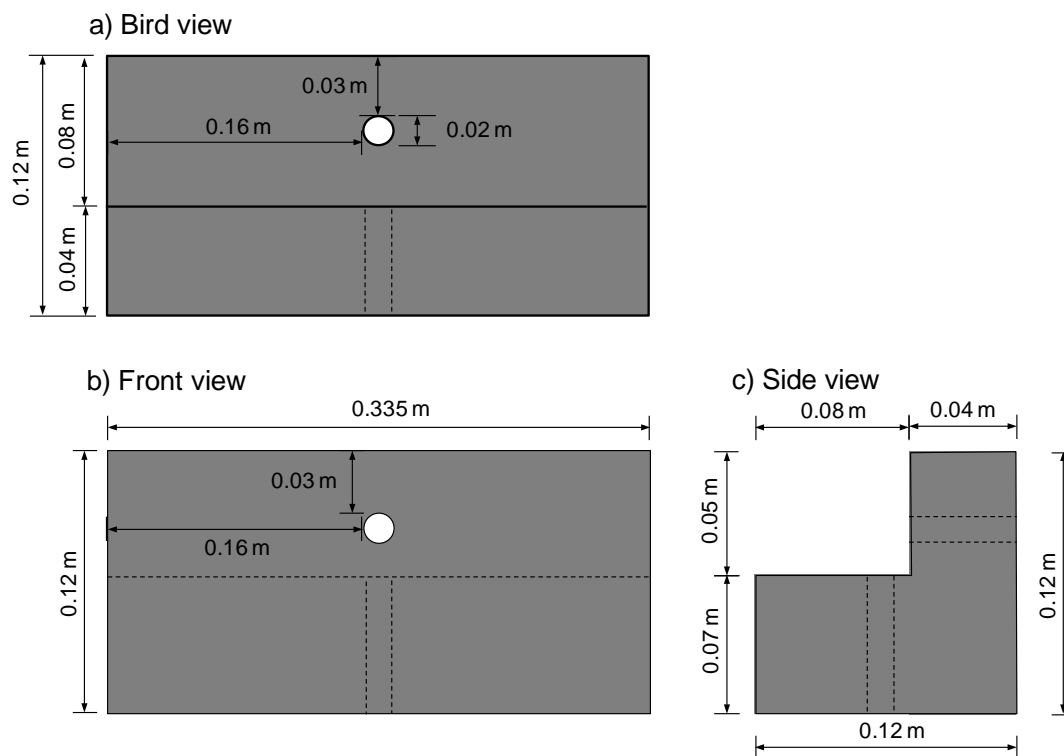


Figure 2.8: Layout of a middle crown wall element used in configurations 1, 3 and 4 in tests at TU-BS (scale 1:30)

2.3 Measuring technique

The following measuring devices were used in the tests at TU-BS for each breakwater configuration: (i) eight wave gauges, (ii) two current meters (one ADV-type and one propeller-type), (iii) two pressure sensors, as shown in Figure 2.7 - Figure 2.9 as well as in Table 2.2 and Table 2.3.

Wave gauges (WG) were installed along the wave flume and over the breakwater models. These wire type wave gauges were used to measure the water surface elevation (see Figure 2.7 and Figure 2.9). In each breakwater configuration, eight wave gauges were installed. Seven of them were normal (WG1 – WG6, WG8) and one (WG7) was shorter and was used for measuring the overflow depth. Therefore, it was installed above the crown wall in configurations 1, 3 and 4 and above the breakwater crown in configuration 2. Summarizing, the incident and reflected wave was measured by wave gauges WG1 to WG6, the overflow depth by WG7 and the transmitted wave by WG8. The wave gauges were fixed directly at the flume bottom/platform surface/ breakwater body/ crown wall element in the tests with the tsunami bore, while in the tests with the solitary wave they were submerged ca. up to half of the water depth of 0.66 m (apart from the overtopping wave gauge WG7, placed directly above the crown wall element in breakwater configurations 1, 3 and 4 and directly above the breakwater crown in configuration 2). In the reference tests at PARI, nine wave gauges were used: WG1 over the slope 1:100, WG2 – WG5 over



the slope 1:10, WG6 – 9 over the breakwater model with WG8 measuring the overtopping flow depth (for comparison see Chapter 3).

One propeller-type of current meter (PR) per configuration was used to record the flow velocity at overtopping. This current meter was placed above the crown wall in configurations 1, 3 and 4 and above the breakwater crown in configuration 2 (see Figure 2.7 and Figure 2.9). Moreover, there was one ADV-current meter (ADV) per configuration, installed at the berm slope in configuration 1 and at the breakwater seaside toe in configurations 2, 3 and 4 (see Figure 2.7 and Figure 2.9). It measured the horizontal flow velocity in direction of wave propagation, based on the Doppler effect. This current meter was installed 0.1 m above the berm in configuration 1 (i.e. 0.3 m above the horizontal platform) and 0.2 m above the horizontal platform in configurations 2, 3 and 4.



Figure 2.9: Exemplary arrangement of overtopping wave gauge (a), propeller current meter (b), pressure sensor (c), normal wave gauge (d) and ADV current meter (e) in tests at TU-BS

To record the wave pressure induced on the crown wall, two pressure sensors (PS) per configuration were installed at the front surface and the bottom of the crown wall in configurations 1, 3 and 4 (see Figure 2.8 and Figure 2.9). In contrast, eight miniature pressure gauges were used in the reference tests at PARI. Due to the required drilling of a hole in the crown wall element for placing the large pressure sensors in the tests at TU-BS (which led to reduced mass of the crown wall), it was not possible to perform more detailed pressure measurements with a larger number of these measuring devices.

Before and after each test the profiles of the breakwaters were measured manually by means of a scale (for the part of breakwater submerged in water) or a laser (for breakwater surface not covered by water). Furthermore, photos of the breakwaters were taken before and after each test to document the damage. Additionally, there were three video cameras recording the tests from different angles: one was installed



in front of the breakwaters, one behind the breakwaters and one at the observation window.

Table 2.2: Position of measuring devices in tests at TU-BS for configurations 1 and 2, related to initial position of wave maker

Configuration 1 (with crown wall and berm)		Configuration 2 (without crown wall and without berm)	
Device type	Position along wave flume related to wave maker [m]	Device type	Position along wave flume related to wave maker [m]
WG1_L	26.53	WG1_R	26.53
WG2_L	29.53	WG2_R	29.53
WG3_L	31.85	WG3_R	31.85
WG4_L	32.11	WG4_R	32.11
WG5_L	32.35	WG5_R	32.35
WG6_L	32.85	WG6_R	32.85
WG7_L	34.17	WG7_R	34.29
WG8_L	35.44	WG8_R	35.44
PR1_L	34.17	PR1_R	34.29
ADV1_L	32.85	ADV1_R	32.85
PS1_L	34.17	PS1_R	-
PS2_L	34.25	PS2_R	-

Note:
 L : Left, denotes configuration 1 (with crown wall and berm)
 R: Right, denotes configuration 2 (without crown wall and without berm)

Table 2.3: Position of measuring devices in tests at TU-BS for configurations 3 and 4, related to initial position of wave maker

Configuration 3 (with crown wall)		Configuration 4 (with shifted crown wall)	
Device type	Position along wave flume related to wave maker [m]	Device type	Position along wave flume related to wave maker [m]
WG1_L	26.53	WG1_R	26.53
WG2_L	29.53	WG2_R	29.53
WG3_L	31.85	WG3_R	31.85
WG4_L	32.11	WG4_R	32.11
WG5_L	32.35	WG5_R	32.35
WG6_L	32.85	WG6_R	32.85
WG7_L	34.17	WG7_R	34.29
WG8_L	35.44	WG8_R	35.44
PR1_L	34.17	PR1_R	34.29
ADV1_L	32.17	ADV1_R	32.85
PS1_L	34.17	PS1_R	34.29
PS2_L	34.25	PS2_R	34.36

Note:
 L : Left, denotes configuration 3 (with crown wall)
 R: Right, denotes configuration 4 (with shifted crown wall)



2.4 Testing programme

Tsunami was generated in the experiments as a solitary wave and a bore, for which different water depths in the wave flume were required, resulting from the two different generation methods, mentioned in Section 2.1. The tests with tsunami overflow, performed at PARI, were not conducted at TU-BS due to the fact that the facility required for this tsunami generation method is not available.

In the tests with the solitary waves, a constant water level of 0.66 m in front of the platform with the breakwater models was used. Due to uneven bottom of the wave flume, the water level at the wave maker was 0.68 m. Over the platform, in front of the breakwater models, the water level was 0.42 m (same as in the reference tests at PARI). A wider range of solitary wave height (0.05 – 0.15 m) was tested at TU-BS as compared to the reference tests at PARI (0.05 – 0.10 m).

The tsunami bore magnitude was differed by increasing water depth behind the bore gate h_0 from 0.75 to 0.85 m, while keeping water level in front of the bore gate h_1 constant (of 0.2 m).

The experimental programme is shown in Table 2.4 (see Chapter 3 for comparison).

Table 2.4: Experimental programme at TU-BS

Test number	Structure type in 2 m wave flume		Wave type	Wave height for wave maker	Water depth in front of bore gate	Water depth behind bore gate
	Left part of wave flume	Right part of wave flume				
			[-]	[m]	h_1 [m]	h_0 [m]
20140721_01	Configuration 3	Configuration 4	Tsunami bore	X	0.200	0.750
20140721_02			Tsunami bore		0.200	0.800
20140721_03			Tsunami bore		0.200	0.850
20140723_01	Configuration 1	Configuration 2	Tsunami bore		0.200	0.750
20140723_02			Tsunami bore		0.200	0.800
20140725_01	Configuration 1	Configuration 2	Solitary wave	0.050	X	
20140725_02			Solitary wave	0.075		
20140807_01			Solitary wave	0.100		
20140807_02			Solitary wave	0.125		
20140807_03			Solitary wave	0.150		
20150106_01	Configuration 3	Configuration 4	Solitary wave	0.050		
20150106_02			Solitary wave	0.075		
20150107_01			Solitary wave	0.100		
20150108_01			Solitary wave	0.125		
20150108_02			Solitary wave	0.150		



3 Description of reference tests at PARI

This study was performed in a framework of a joint research project between Japan and Turkey “Earthquakes and Tsunami Disaster Mitigation in the Marmara Region and Disaster Education in Turkey”, being a part of the programme Science and Technology Research Partnership for Sustainable Development (SATREPS; <http://www.jst.go.jp/global/english/about.html>). The focus of the experiments was to determine the performance of a rubble-mound type of breakwater protecting the most important port in Turkey – the Haydarpasa Port – under possible tsunami impact. For more details on this study see Guler et al. (submitted).

3.1 Wave flume

The reference tests were performed in a wave flume at PARI, which dimensions are 105×3.0×2.5 m. The flume was divided into two parallel channels of width of 0.78 m and 2.22 m. The breakwater model, tested in this study, was constructed in the 0.78 m wide channel.

3.2 Experimental setup

The reference experiments were performed at a scale of 1:30 and scaled according to the Froude similitude law.

Two configurations of the breakwater were considered: (i) the configuration corresponding to the prototype (i.e. to the existing Haydarpasa Breakwater) as shown in Figure 3.1a, (ii) an improved configuration in which the breakwater stability under tsunami impact was increased by doubling the thickness of the armour layer on the harbour side (from 0.07 m to 0.14 m), as presented in Figure 3.1b.

The breakwater body consisted of the following armour layers (see Figure 3.2):

- core layer (grey color): mass of stones between 0 and 10 g (mass of stones 0 – 0.2 t in prototype),
- filter layer (grey color): 0.07 m thick, mass of stones between 50 and 100 g (mass of stones 0.2 – 3 t in prototype),
- armour layer on the seaside (starting from breakwater toe: green, grey, red, blue and green color): 0.09 m thick, mass of stones between 100 and 150 g (mass of stones 3 t in prototype),
- armour layer on the side of the port (red color): 0.07 m and 0.14 m thick in the original and the improved configuration, respectively, mass of stones between 50 and 100 g (mass of stones 1.5 t in prototype).

The filter and the armour layers on both seaside and harbour side were not continuous from the breakwater toe to the breakwater crown, unlike the layer design in the experiments at TU-BS.



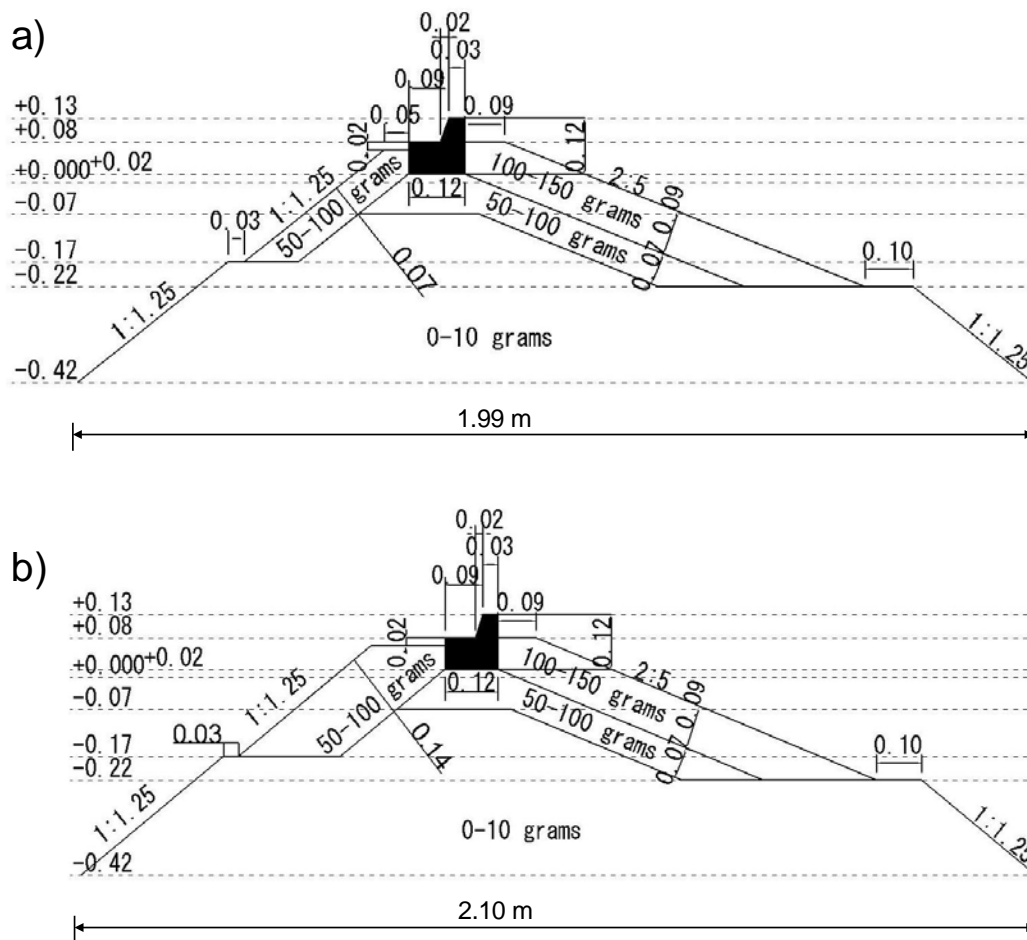


Figure 3.1: Breakwater model geometry tested in reference tests at PARI: a) original configuration, b) improved configuration (scale 1:30) (Guler et al., submitted)

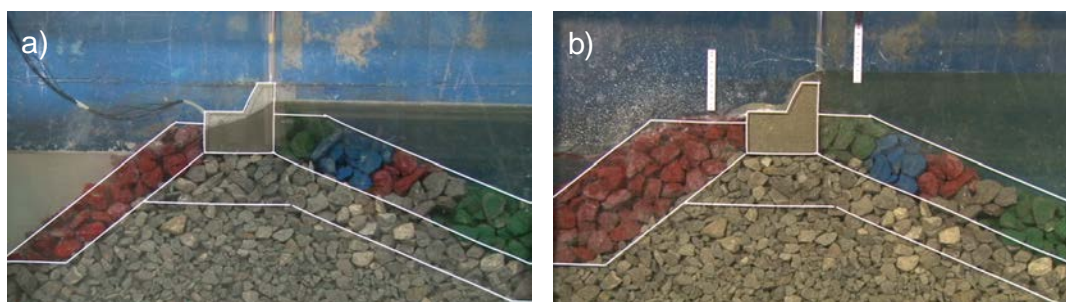


Figure 3.2: Layout of armour layers in reference tests at PARI: a) for original configuration, b) for improved configuration (Guler et al., submitted)

The setup consisted of three parts: (i) a slope of 1/100, (ii) a slope of 1/10 of length of 11.5 m and (iii) a horizontal platform of height of 1.15 m, on which the breakwater model was built, equipped with no slope at its rear side (see Figure 3.3).



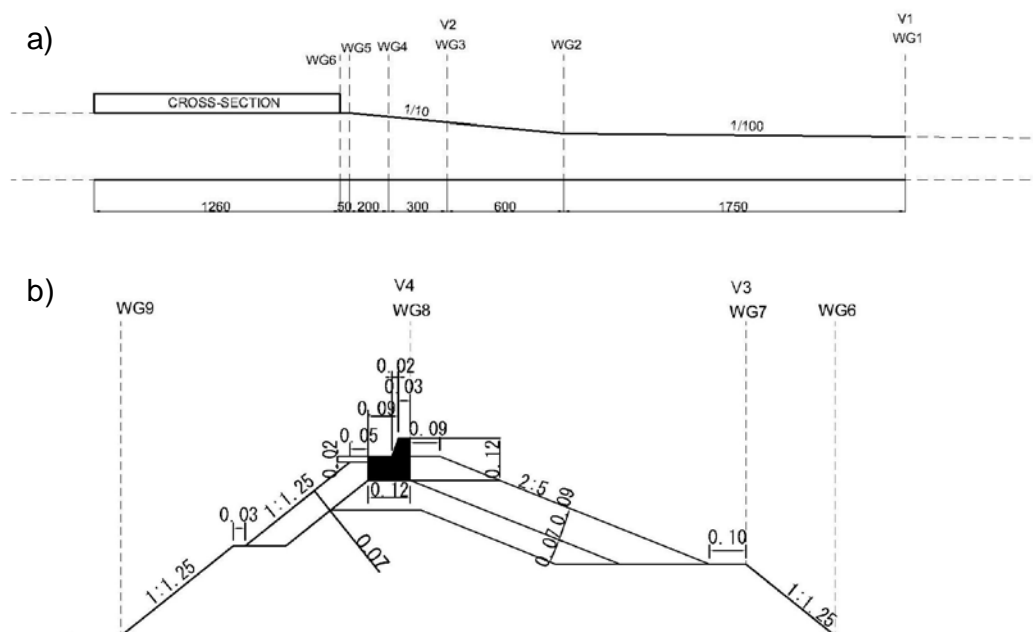


Figure 3.3: Model setup in reference tests at PARI with measuring instrumentation: a) location of wave gauges and current meters over the bathymetry model (dimensions in cm), b) location of wave gauges and current meters along breakwater model (model scale 1:30) (Guler et al., submitted)

The geometry of the breakwater models examined at PARI was more complex than those simplified, investigated at TU-BS (see Figure 3.1). The breakwater models were 0.5 m and 0.48 m high on the seaside and harbour side, respectively. The length of the breakwater crown was 0.12 m, while the total length of the breakwater basis yielded 1.99 m for the original breakwater geometry and 2.1 m for the improved breakwater model. The seaside breakwater slope was not uniform and yielded 1:1.25 for the core layer and 2:5 for the filter and armour layer. The breakwater slope at the harbour side was constant and yielded 1:1.25.

The crown wall was made of concrete and manufactured in four pieces. Every crown wall unit was 0.19 m wide, 0.12 m long, and 0.12 m high, as illustrated in Figure 3.4. Apart from the inclined upper, back part of the front surface with a slope 2.5:1.0, all the surfaces were perpendicular.



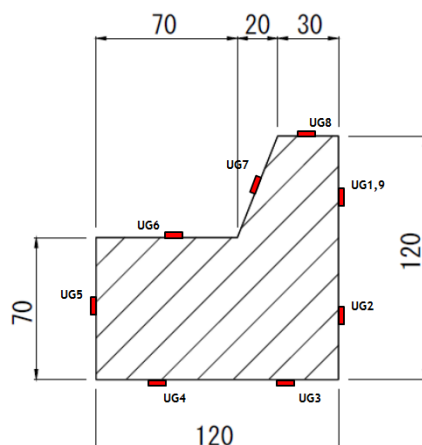


Figure 3.4: Geometry of crown wall unit in reference tests at PARI (model scale 1:30, dimensions in mm) (Guler et al., submitted)

3.3 Measuring technique

The measuring instrumentation, used in the experiments at PARI, was as follows: (i) nine wave gauges, (ii) four ADV-type current meters and (iii) nine miniature pressure sensors (see Figure 3.3 and Figure 3.4).

Wave gauges (WG) were employed to measure the height of the solitary wave/flow depth. Wave gauges WG1 – WG5 were placed above the both slopes constituting the bathymetry model: WG1 over the slope 1:100 and WG2 – WG5 over the slope 1:10 (with WG2 installed at the slope toe and WG5 at the end of the slope), as depicted in Figure 3.3a. Wave gauge WG6 was placed at the toe of the breakwater model, WG7 at the transition between 1:1.25 and 2:5 seaward slopes, WG8 over the crown wall unit to measure the water depth at the overtopping and WG9 at the harbour toe of the breakwater model to record the transmitted wave height/flow (see Figure 3.3b).

Four current meters (V), measuring flow velocity, were installed over the slope 1:100 of the bathymetry model (at WG1), over the slope 1:10 of the bathymetry model (at WG3), at the transition between 1:1.25 and 2:5 seaward slopes (at WG7) and over the crown wall unit (at WG8), as illustrated in Figure 3.3b.

Nine miniature pressure sensors (UG) were deployed on one crown wall unit to measure wave/flow-induced pressure (see Figure 3.4): three sensors (UG1, UG2 and UG9) were placed on the front surface, two of them (UG3 and UG4) on the bottom surface, one (UG5) on the rear surface and three (UG6 – UG8) on the upper surface of the crown wall element.

Video documentation of the experiments was done using three video cameras.



3.4 *Testing programme*

Two types of tsunami generation methods were used in the reference tests at PARI. First, experiments with solitary waves, generated by a piston-type wave maker, were performed solely for the original breakwater cross section with varying solitary wave height (0.05, 0.075 and 0.1 m). In order to examine the effect of the tsunami impact duration, overflow experiments with constant overflow were additionally conducted by using a pump system. In case of the original breakwater model, the overflow depth ranged from 1.1 to 1.95 cm, while in case of the improved breakwater model from 1.5 to 4.6 cm. The experimental programme is provided in Table 3.1.

Table 3.1: Experimental programme at PARI

Flow regime	Original breakwater model	Improved breakwater model
Solitary wave height [m]	0.05, 0.075, 0.1	No tests performed
Overflow depth [cm]	1.1, 1.15, 1.2, 1.3, 1.4, 1.7, 1.85, 1.9, 1.95	1.5, 1.6, 2.1, 2.7, 2.8, 3.4, 3.65, 4.3, 4.4, 4.6

3.5 *Summary of experiments at TU-BS and PARI*

A summary of the experimental setup and programme for the tests performed at TU-BS and at PARI is provided in



Table 3.2.

Table 3.2: Comparison of experiments at TU-BS and PARI

	Experiments at TU-BS	Reference experiments at PARI
Facility	Wave flume: 90×2.0×1.2 m, two parallel sections of width of 1.0 m for testing two configurations simultaneously	Wave flume: 105×0.78×2.5 m
Model scale	1:30	1:30
Breakwater configurations	<ul style="list-style-type: none"> • With crown wall unit and berm • Without crown wall unit and without berm • With crown wall unit • With shifted crown wall unit 	<ul style="list-style-type: none"> • Prototype of Haydarpasa Breakwater (original breakwater model) • Improved breakwater model with doubled armour layer on harbour side
Breakwater geometry	<ul style="list-style-type: none"> • Simplified • Seaside slope 1:1.25, 2:5 • Harbour slope 1:1.25 • Height: 0.5 m • Crown length: 0.33 m • Breakwater basis length: 2.2 m 	<ul style="list-style-type: none"> • Seaside slope 1:1.25, 2:5 • Harbour slope 1:1.25 • Height: 0.52 m on seaside, 0.5 m on harbour side • Crown length: 0.12 m • Breakwater basis length: 1.99 m (original cross-section), 2.1 m (improved cross-section)
Armour layers	<ul style="list-style-type: none"> • Simplified • Core layer: 0-10 g • Filter layer: 0.07 m thick, 50-100 g • Armour layer on seaside: 0.09 m thick, 100-150 g • Armour layer on harbour side: 0.07 m thick, 50-100 g • Berm layer: 0.2 m thick, 100-150 g 	<ul style="list-style-type: none"> • Core layer: 0-10 g • Filter layer: 0.07 m thick, 50-100 g • Armour layer on seaside: 0.09 m thick, 100-150 g • Armour layer on harbour side: 0.07 m and 0.14 m thick in the original and the improved configuration, respectively, 50-100 g
Crown wall units	<ul style="list-style-type: none"> • Concrete with 2 holes for pressure sensors • L-shape, all surfaces perpendicular • 3 units: 0.335/0.335/0.3 m wide, 0.12 m long, 0.12 m high 	<ul style="list-style-type: none"> • Concrete • L-shape, only upper back part of front surface inclined (2.5:1) • 4 units: 0.19 m wide, 0.12 m long, 0.12 m high
Bathymetry model	Horizontal platform of height of 0.24 m with seaside slope 1:10 and harbour slope 2:5	Slope 1:100; horizontal platform of height of 1.15 m with seaside slope 1:10
Measuring devices	<ul style="list-style-type: none"> • 8 wave gauges • 2 current meters • 2 pressure sensors 	<ul style="list-style-type: none"> • 9 wave gauges • 4 current meters • 9 miniature pressure sensors
Flow regime	<ul style="list-style-type: none"> • Solitary waves of height of 0.05-0.15 m, generated at water depth of 0.66 m • Bores with water depth in front of bore gate of 0.2 m and behind bore gate of 0.75, 0.8 and 0.85 m 	<ul style="list-style-type: none"> • Solitary waves of height of 0.05, 0.75, 0.1 m (only original breakwater model) • Overflow: (i) overflow depth from 1.1 to 1.95 cm for original breakwater model, (ii) overflow depth from 1.5 to 4.6 cm for improved breakwater model
Freeboard (till breakwater crown)	<ul style="list-style-type: none"> • Solitary wave: 0.08 m • Bore: breakwater fully emerged 	<ul style="list-style-type: none"> • Solitary wave and overflow: 0.06 m at harbour side, 0.08 m at seaside



4 Analysis of experimental data from tests at TU-BS

4.1 Observed processes

4.1.1 Experiments with bore

Flow through the porous body of the breakwater was the dominant phenomenon occurring in the tests with the tsunami bore, since the entire structure was emerged prior to bore impact. Overtopping of the crown wall/the breakwater crown took generally place in the most extreme conditions tested (i.e. $h_1=0.2$ m and $h_0=0.85$ m) for all tested breakwater configurations. In case of the weaker bores, there was no overflow for the breakwater with the crown wall unit, apart from the weak overflow observed for the breakwater without the crown wall element.

Due to the large water storage behind the bore gate, used for the bore generation, the bore impact was much longer as compared to the duration of the solitary wave attack, and yielded slightly more than 30 s (ca. 164 s in prototype), as recorded at wave gauge WG6 at the breakwater toe for the configurations 2, 3 and 4. In case of configuration 1, the presence of the berm in front of the breakwater reduced slightly the duration of the bore impact to ca. 27 s (ca. 148 s in prototype) at WG6 from ca. 30 s recorded at wave gauge WG5 at the berm toe.

The observed phenomena, wave impact duration as well as damage duration are provided in Table 4.1. Since a certain time was needed for the water flow through the breakwater, there was a time shift between the bore impact and the induced structure damage. This time shift is provided in brackets in column “Damage duration”.

4.1.2 Experiments with solitary wave

Unlike the experiments under tsunami bore conditions, overflow was the dominant process, leading to the breakwater damage, in the tests with solitary waves. No overtopping above the breakwater with the crown wall element and the berm (configuration 1) occurred solely in the experiment with the weakest solitary wave (i.e. wave height of 0.05 m).

The approximated duration of the solitary wave impact was 6 s (ca. 33 s in prototype).

The observed phenomena, wave impact duration as well as damage duration are provided in Table 4.1.



Table 4.1: Observed processes in tests with tsunami bore and solitary waves performed at TU-BS (model scale 1:30)

Test number	Overflow				Wave impact duration WG6 (WG5)				Damage duration			
	C1	C2	C3	C4	C1	C2	C3	C4	C1	C2	C3	C4
	[-]	[-]	[-]	[-]	[s]	[s]	[s]	[s]	[s]	[s]	[s]	[s]
TSUNAMI BORE												
20140721_01	X		no	no	X		34	34	X		no damage	no damage
20140721_02			weak	no			33	34			4 (4)	5 (4)
20140721_03			yes	yes			32	32			20 (3)	20 (3)
20140723_01	no	no	X		28 (34)	34	X		10 (4)	5 (4)	X	
20140723_02	yes	yes			27 (33)	33			18 (4)	16 (3)		
SOLITARY WAVE												
20140725_01	no	yes	X		7	7	X		no damage	no damage	X	
20140725_02	yes	yes			6	6			2	1		
20140807_01	yes	yes			5.5	5.5			3	3		
20140807_02	yes	yes			5	5			3	3		
20140807_03	yes	yes			5	5			2	2		
20150106_01	X		no	no	X		7	7	X		no damage	no damage
20150106_02			yes	yes			6	6			1	1
20150107_01			yes	yes			5.5	5.5			2	2
20150108_01			yes	yes			5	5			2	2
20150108_02			yes	yes			5	5			2	2



4.2 *Analysis of flow depth / wave height*

4.2.1 *Experiments with bore*

For each performed test, two different bore heights were determined for all wave gauges used: (i) incident bore height and (ii) maximum flow depth (see Figure 4.1). The incident bore height is specified as the distance between the flume bottom and the front of the arriving bore. Thus, it represents the actual bore height (see Table 4.2). The maximum flow depth is the maximum water elevation resulting from the water impoundment in front of the breakwater (



Table 4.3). The maximum flow depth is much higher than the incident bore height and therefore it determines the maximum pressure exerted on the crown wall element. For wave gauges located over the breakwater model (i.e. WG3 – WG6) it was very hard to distinguish the incident bore due to the aforementioned water impoundment. This cases are marked as “not determinable” in Table 4.2. In case of wave gauges WG7 and WG8, the incident bore height and the maximum flow depth were same.

The measured bore profiles, provided in Appendix A, show the water level elevation from the still water level (i.e. above the water depth of $h_1=0.2$ m in front of the bore gate). To determine the incident bore height, the value of 0.20 m has to be added to the water free surface elevation recorded by wave gauges WG1 and WG2, which were located in front of the breakwater model and were submerged in the water of depth of $h_1=0.20$ m. Other wave gauges (i.e. from WG3 to WG8) were either fixed over the platform or over the breakwater model. Therefore, in order to determine the incident bore height for these wave gauges, the value of 0.20 m does not have to be added to the measured water surface elevation.

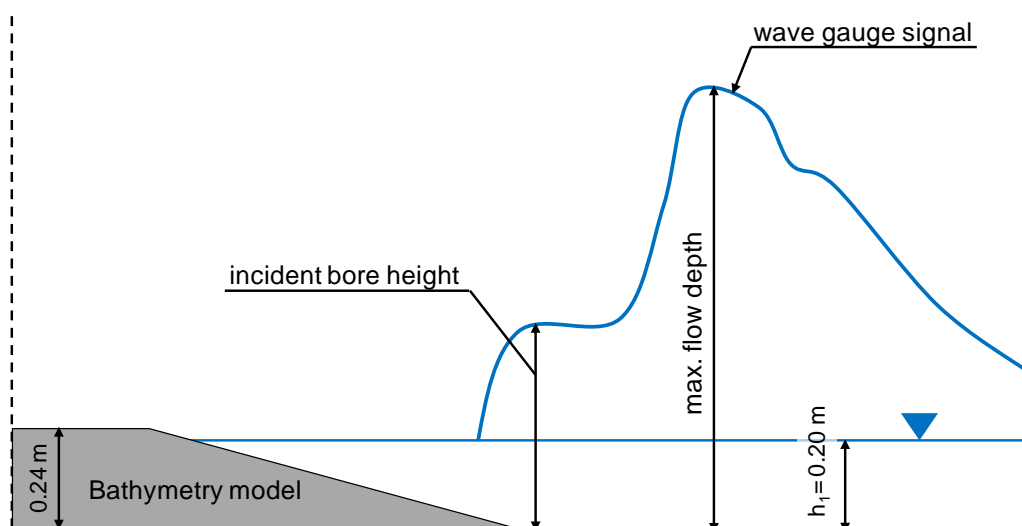


Figure 4.1: Explanatory sketch of bore heights determined in tests at TU-BS

It should be remarked that the overflow depth was measured from the top of the crown wall unit for configurations 1, 3 and 4, while in configuration 2 from the top of the breakwater crown.

The evolution of the bore profiles in each performed test is provided in Appendix A. The findings from the experiments are provided below:

- The generated bore conditions in front of the breakwater models (i.e. recorded at wave gauges WG1 and WG2) were almost same for all tested breakwater configurations. The differences might have been caused by slightly different water depth conditions in front of the bore gate (h_1) due to some leakage of the water impounded behind the bore gate.



- The incident bore height increased slightly with higher impoundment depth h_0 behind the bore gate. A more significant increase was noticeable for the maximum flow depth: from ca. 0.5 m for $h_0=0.75$ m, to ca. 0.56 m for $h_0=0.8$ m and further to ca. 0.66 m for $h_0=0.85$ m.
- The maximum flow depth at WG2 was of same order as those measured by WG3 – WG6 for breakwater configurations 2 and 4, while almost a half of that for breakwater configurations 1 and 3. This phenomenon cannot be reasonably explained through the different breakwater geometries tested.
- Starting from wave gauge WG3, the bore propagated over a dry bathymetry and breakwater models. Therefore, the values of the incident bore height are smaller than those measured by WG1 and WG2.
- The maximum flow depths recorded by wave gauges WG3 – WG6 were almost identical for all breakwater configurations: ca. 0.5 m for $h_0=0.75$ m, to ca. 0.56 m for $h_0=0.8$ m and further to ca. 0.66 m for $h_0=0.85$ m.
- The berm in breakwater configuration 1 did not increase the bore height, as indicated by the measurements at WG6 (despite the fact that the actual flow depth above the berm was lower than that measured at WG3 – WG5). The measured maximum flow depth, summed up with the height of the berm of $h_B=0.20$ m, corresponded to the maximum flow depths recorded at this wave gauge for other breakwater configurations examined. But the actual flow depth above the berm has decreased.

No overtopping was observed at WG7 for tests with $h_0=0.75$ m and all breakwater configurations as well as $h_0=0.8$ m and breakwater configuration 4 (marked as “no overflow” in Table 4.2 and



- Table 4.3). Despite this fact, there was some amount of the transmitted flow measured at WG8 due to the water infiltration through the breakwater body from the seaside to the harbour side.
- The values of the flow depth behind the breakwater model (i.e. at WG8) were not in agreement with the expected trends and it is difficult to draw general conclusions from the gained results. In cases with no overflow, similar flow transmission through the breakwater body would be expected for breakwater configurations 2, 3 and 4. In the tests with overflow, larger transmission for breakwater configuration 2 would be expected due to the removed crown wall unit. In the tests, the larger transmission was measured for breakwater configurations 1 and 3.

Table 4.2: Incident bore height measured in tests at TU-BS (model scale 1:30)

	Device	Unit	20140721_01 0.2, 0.75 m	20140721_02 0.2, 0.80 m	20140721_03 0.2, 0.85 m	20140723_01 0.2, 0.75 m	20140723_02 0.2, 0.80 m
Configuration 3	WG1_L	[m]	0.370	0.389	0.422	X	
	WG2_L	[m]	0.340	0.375	not working		
	WG3_L	[m]	0.225	0.251	0.291		
	WG4_L	[m]	0.193	0.223	0.262		
	WG5_L	[m]	0.173	0.200	0.266		
	WG6_L	[m]	0.165	0.240	0.305		
	WG7_L	[m]	no overflow	0.002	0.035		
	WG8_L	[m]	0.016	0.017	0.080		
Configuration 4	WG1_R	[m]	0.396	0.417	0.444		
	WG2_R	[m]	0.453	0.489	0.513		
	WG3_R	[m]	0.245	0.255	0.283		
	WG4_R	[m]	0.195	0.217	0.243		
	WG5_R	[m]	0.191	0.200	0.221		
	WG6_R	[m]	not determinable	not determinable	not determinable		
	WG7_R	[m]	no overflow	no overflow	0.029		
	WG8_R	[m]	0.006	0.009	0.080		
Configuration 1	WG1_L	[m]	X			0.393	0.404
	WG2_L	[m]				0.529	0.413
	WG3_L	[m]				0.259	0.300
	WG4_L	[m]				0.305	0.290
	WG5_L	[m]				not determinable	not determinable
	WG6_L	[m]				0.198	not determinable
	WG7_L	[m]				no overflow	0.003
	WG8_L	[m]				0.016	0.021
Configuration	WG1_R	[m]				0.411	0.423
	WG2_R	[m]				0.497	0.500
	WG3_R	[m]				0.235	0.278
	WG4_R	[m]				0.214	0.256
	WG5_R	[m]				0.200	0.217



WG6_R	[m]	0.253	not determinable
WG7_R	[m]	no overflow	0.010
WG8_R	[m]	0.005	0.006

NGI



Table 4.3: Maximum flow depth measured in tests with bore at TU-BS (model scale 1:30)

	Device	Unit	20140721_01 0.2, 0.75 m	20140721_02 0.2, 0.80 m	20140721_03 0.2, 0.85 m	20140723_01 0.2, 0.75 m	20140723_02 0.2, 0.80 m
Configuration 3	WG1_L	[m]	0.950	1.080	1.191	X	
	WG2_L	[m]	0.473	0.498	not working		
	WG3_L	[m]	0.524	0.600	0.714		
	WG4_L	[m]	0.497	0.531	0.534		
	WG5_L	[m]	0.532	0.574	0.689		
	WG6_L	[m]	0.525	0.603	0.681		
	WG7_L	[m]	no overflow	0.002	0.035		
	WG8_L	[m]	0.016	0.017	0.080		
Configuration 4	WG1_R	[m]	0.750	0.835	0.900		
	WG2_R	[m]	0.695	0.735	0.775		
	WG3_R	[m]	0.504	0.566	0.627		
	WG4_R	[m]	0.495	0.539	0.580		
	WG5_R	[m]	0.519	0.581	0.666		
	WG6_R	[m]	0.498	0.558	0.656		
	WG7_R	[m]	no overflow	no overflow	0.029		
	WG8_R	[m]	0.006	0.009	0.080		
Configuration 1	WG1_L	[m]	X			1.046	1.143
	WG2_L	[m]				0.568	0.508
	WG3_L	[m]				0.577	0.622
	WG4_L	[m]				0.517	0.533
	WG5_L	[m]				0.552	0.590
	WG6_L	[m]				0.316	0.327
	WG7_L	[m]				no overflow	0.003
	WG8_L	[m]				0.016	0.021
Configuration 2	WG1_R	[m]				0.815	0.854
	WG2_R	[m]				0.720	0.741
	WG3_R	[m]				0.556	0.583
	WG4_R	[m]				0.522	0.557
	WG5_R	[m]				0.553	0.602
	WG6_R	[m]				0.547	0.591
	WG7_R	[m]				no overflow	0.010
	WG8_R	[m]				0.005	0.006

4.2.2 Experiments with solitary wave

For each performed test, max. height of solitary wave was determined for all wave gauges used (see Table 4.4). It should be remarked that the overflow depth was measured from the top of the crown wall unit for breakwater configurations 1, 3 and 4, while in breakwater configuration 2 from the top of the breakwater crown.



The evolution of the solitary wave profiles in each performed test is provided in Appendix A. The findings from the experiments are provided below:

- Generally, the same incident wave conditions were generated for all breakwater configurations in the deeper portion of water in front of the breakwater models (i.e. at wave gauges WG1 and WG2).
- For two breakwater configurations tested parallel, a slightly higher wave (by ca. 1 – 3 mm, depending on the incident wave height), was generated in the left section of the wave flume (i.e. for breakwater configurations 1 and 3), as indicated by signals measured by WG1 and WG2. This could be due to a different calibration function or uneven flume bottom.
- Wave shoaling process over the platform seaside slope (at WG3) led to the increase of the wave height for all breakwater configurations. Solitary wave height over the horizontal part of the platform increased constantly (compare WG4 – WG6). The difference between the wave heights in both flume sections intensified (to 4 – 12 mm at WG4), which could be additionally caused by some slight differences in the platform construction in the left and right sections of the 2 m-wide flume. Maximum wave height was measured in the experiments at wave gauge WG6, placed at breakwater toe, and yielded: ca. 0.075 m for $H=0.05$ m, ca. 0.1 m for $H=0.075$ m, 0.12 – 0.14 m for $H=0.1$, ca. 0.15 – 0.17 m for $H=0.125$ m and ca. 0.18 m for $H=0.15$ m.
- No significant influence of the presence of the berm in breakwater configuration 1 on wave propagation was observed. The height of the berm of 0.2 m (and thus the corresponding freeboard over the berm) was apparently insufficient to cause further wave transformation over the berm (e.g. wave shoaling and/or breaking).
- There was no overtopping in tests with the smallest wave height of $H=0.05$ m for breakwater configurations 1, 3 and 4 (marked as “no overtopping” in Table 4.4).
- In case of the smallest wave height generated ($H=0.05$ m), the presence of the crown wall element in breakwater configurations 1, 3 and 4 definitely prevented from the wave overtopping. Under these conditions, there was wave overtopping solely over the breakwater model without the crown wall unit (i.e. breakwater configuration 2). The corresponding transmitted wave height was in this case around 0.007 m for the breakwater configurations with the crown wall element and 0.01 m for the breakwater model without the crown wall unit.
- No influence of shifting of the position of the crown wall unit (i.e. breakwater configuration 4) on the magnitude of the wave overtopping depth was observed as compared to that measured for breakwater configuration 3.
- In case of the non-damage tests ($H=0.05$ m) and tests with a minor damage ($H=0.075$, 0.1 and 0.125 m), the highest transmitted wave was always recorded for breakwater configuration 2 (i.e. breakwater without crown wall unit): 0.033 m for $H=0.075$ m, 0.066 m for $H=0.1$ m and 0.094 m for $H=0.125$ m. These values were higher by ca. 0.1 – 0.2 m as compared to the transmitted wave height recorded for breakwater configurations 1, 3 and 4.

NGI



- In case of tests with a major damage (H=0.15 m) there was almost no difference in the order of the transmitted wave height among the breakwater configurations, since the crown wall unit slid down the harbor breakwater slope upon the wave impact, what resulted in a free and intensified overtopping of the breakwater crown.

Table 4.4: Maximum wave height measured in tests with solitary wave at TU-BS (model scale 1:30)

	Device	Unit	20140725_01 H=0.050 m	20140725_02 H=0.075 m	20140807_01 H=0.100 m	20140807_02 H=0.125 m	20140807_03 H=0.150 m
Configuration 1	WG1_L	[m]	0.048	0.074	0.098	0.124	0.149
	WG2_L	[m]	0.052	0.078	0.103	0.129	0.155
	WG3_L	[m]	0.060	0.088	0.113	0.142	0.167
	WG4_L	[m]	0.063	0.091	0.117	0.146	0.171
	WG5_L	[m]	0.066	0.096	0.124	0.156	0.185
	WG6_L	[m]	0.070	0.098	0.122	0.150	0.176
	WG7_L	[m]	no overflow	0.030	0.063	0.114	0.121
	WG8_L	[m]	0.007	0.016	0.046	0.084	0.109
Configuration 2	WG1_R	[m]	0.049	0.074	0.099	0.125	0.151
	WG2_R	[m]	0.053	0.079	0.106	0.131	0.158
	WG3_R	[m]	0.058	0.084	0.107	0.134	0.159
	WG4_R	[m]	0.051	0.087	0.111	0.139	0.163
	WG5_R	[m]	0.065	0.092	0.116	0.143	0.167
	WG6_R	[m]	0.075	0.104	0.130	0.160	0.188
	WG7_R	[m]	0.023	0.056	0.070	0.092	0.128
	WG8_R	[m]	0.010	0.033	0.066	0.094	0.111
	Device	Unit	20150106_01 H=0.050 m	20150106_02 H=0.075 m	20150107_01 H=0.100 m	20150108_01 H=0.125 m	20150108_02 H=0.150 m
Configuration 3	WG1_L	[m]	0.047	0.073	0.098	0.123	0.149
	WG2_L	[m]	0.052	0.078	0.106	0.133	0.160
	WG3_L	[m]	0.059	0.085	0.113	0.139	0.166
	WG4_L	[m]	0.062	0.089	0.117	0.143	0.171
	WG5_L	[m]	0.067	0.095	0.125	0.154	0.183
	WG6_L	[m]	0.075	0.106	0.138	0.170	0.201
	WG7_L	[m]	no overflow	0.031	0.072	0.104	0.120
	WG8_L	[m]	0.007	0.013	0.048	0.096	0.119
Configuration 4	WG1_R	[m]	0.049	0.075	0.101	0.128	0.154
	WG2_R	[m]	0.053	0.800	0.107	0.134	0.163
	WG3_R	[m]	0.059	0.085	0.112	0.138	0.163
	WG4_R	[m]	0.062	0.090	0.117	0.143	0.166
	WG5_R	[m]	0.067	0.095	0.124	0.153	0.180
	WG6_R	[m]	0.076	0.108	0.140	0.171	0.202
	WG7_R	[m]	no overflow	0.029	0.059	0.063	0.070
	WG8_R	[m]	0.008	0.015	0.053	0.082	0.116



4.3 Analysis of wave-induced pressure

4.3.1 Experiments with bore

Maximum pressure induced by tsunami bore on the frontal and bottom surface of the middle crown wall unit (measured by pressure transducers PS1 and PS2, respectively) was determined for all tested breakwater configurations and is provided in Table 4.5. Breakwater configuration 2 (i.e. breakwater without crown wall and without berm) was not equipped with the crown wall units and thus with no pressure gauge (marked as “not installed” in Table 4.5). Therefore, no pressure measurements are available for this breakwater configuration.

The signals of the pressure sensors in the tests with the tsunami bore are shown in Appendix B for every experiment. The findings from the experiments are summarized as follows:

- Tests, in which the incident bore did not reach the crown wall unit are marked by “no overflow” in Table 4.5. In some tests, the bore reflected from the end wall of the wave flume exerted pressure on the crown wall unit, however this phenomenon and the resulting pressure was not the interest of this study.
- Generally, the pressure increased with the increase of the water storage behind the bore gate. However, there was no clear relationship between the magnitude of the pressure on the frontal/bottom surface of the crown wall unit and the bore conditions.
- Due to no overtopping, no pressure was measured by gauges PS1 and PS2 in tests with $h_0=0.75$ m and $h_1=0.2$ m for breakwater configurations 2, 3 and 4. For configuration 1 and same bore conditions as above, solely gauge PS1 did not measure the pressure exerted on the front surface of the crown wall unit, since the water impounded in front of the breakwater model was lower than the height at which this device was installed.
- Pressure exerted on the front surface of the crown wall unit by the dammed bore in front of the breakwater model, measured by transducer PS1, was generally positive and reduced gradually as the level of the dammed water sunk due to the water filtration through the breakwater body. This pressure corresponded to the moment, in which the mentioned filtrating water tried to lift up the crown wall element. In tests with stronger bores ($h_0=0.80$ m and $h_0=0.85$ m) for breakwater configurations 3 and 4, negative pressure of -0.09 kPa and -0.28 kPa was measured respectively and was most probably exerted by the sinking impounded water level. Tests, in which no negative pressure was measured at PS1, are marked as “no value” in Table 4.5.
- Pressure exerted on the bottom surface of the crown wall element (at PS2) was first positive and preceded the pressure recorded by PS1 by ca. 1 s. It became negative as the level of the infiltrating water lowered, trying to pull the crown wall unit down the breakwater crest and harbor slope.
- Maximum positive pressure, measured by PS1, was exerted for breakwater configurations 3 and 4 (0.81 and 0.89 kPa, respectively). Due to the shifting



of the crown wall in configuration 4, a smaller pressure would be expected, however this was not confirmed by the experimental data. Much smaller pressure of 0.32 kPa was attributed to breakwater configuration 1 due to the presence of the berm.

- Comparison of the maximum positive pressure at PS2 is difficult due to the scarce data, for example the pressure exerted by bore generated with $h_0=0.75$ m was measured solely for breakwater configuration 1 (0.16 kPa), while with $h_0=0.80$ m in breakwater configurations 1 and 3 (0.37 and 0.3 kPa, respectively) although some smaller pressure would be also expected in configuration 4. The largest pressure of 1.1 kPa was observed for configuration 3, however the pressure for the neighbouring breakwater configuration 4 was significantly lower (0.03 kPa).
- Generally, taking into consideration the scarce data and the discrepancies between the measurements, repeated tests would necessary to confirm the described trends.

Table 4.5: Maximum bore-induced pressure in tests at TU-BS (model scale 1:30)

	Device	Unit	20140721_01 0.2, 0.75 m	20140721_02 0.2, 0.80 m	20140721_03 0.2, 0.85 m	20140723_01 0.2, 0.75 m	20140723_02 0.2, 0.80 m		
C3	PS1_L	[kPa]	no overflow	0.175/-0.091	0.812/-0.280	X	X		
	PS2_L	[kPa]	no overflow	0.300/-0.204	1.100/-0.213				
C4	PS1_R	[kPa]	no overflow	no overflow	0.889/ no value				
	PS2_R	[kPa]	no overflow	no overflow	0.030/-0.180				
C1	PS1_L	[kPa]	X	X	X			no overflow	0.325/ no value
	PS2_L	[kPa]						0.158/-0.176	0.371/-0.180
C2	PS1_R	[kPa]				not installed	not installed		
	PS2_R	[kPa]				not installed	not installed		

4.3.2 Experiments with solitary wave

Maximum pressure induced by solitary wave on the frontal and bottom surface of the middle crown wall unit (measured by PS1 and PS2, respectively) was determined for all tested breakwater configurations and is provided in



Table 4.6. Pressure sensors were not installed in configuration 2 (i.e. breakwater without crown wall and without berm) and is marked as “not installed” in

NGI



Table 4.6.

The signals of the pressure sensors in the tests with the solitary wave are presented in Appendix B for each test. The findings from the experiments are summarized below:

- Despite the fact that no wave overtopping was observed in tests with breakwater configurations 1, 3 and 4 with smallest wave height of $H=0.05$ m, both pressure transducers PS1 and PS2 measured the pressure exerted by the wave. The wave reached the height at which the devices were installed, however was still too small to overtop the crown wall unit.
- Pressure exerted at the frontal surface (i.e. at PS1) was positive in all performed tests with all examined breakwater configurations and corresponded to the moment of hitting the crown wall unit by the wave. Pressure exerted at the bottom surface (i.e. at PS2) was negative for breakwater configurations 3 and 4. However, it was positive for breakwater configuration 1 what might have been caused by the presence of the berm. Incorrect calibration and installation of the sensor PS2 in this breakwater configuration can be definitely excluded.
- Pressure exerted at PS1 increased with the increasing height of the solitary wave from ca. 0.74 to 1.35 kPa for breakwater configuration 1, from ca. 0.5 to 1.44 kPa for breakwater configuration 2 and from ca. 0.2 to 1.7 kPa for breakwater configuration 4. The same trend was also observed for the pressure exerted at PS2, which ranged from ca. 0.17 to 1.53 kPa for breakwater configuration 1, from ca. -0.29 to -2.15 kPa for configuration 3 and from ca. -0.6 to -1.88 kPa for breakwater configuration 4.
- The lowest pressure at PS1 was recorded for breakwater configuration 4, which resulted from reducing the wave impact by shifting of the crown wall unit to the back of the breakwater crown. The highest pressure at PS1 was measured for the breakwater configuration 1, which was caused by increasing the flow velocity under the solitary wave through the presence of the berm (i.e. reducing the flow cross section).
- The lowest negative pressure at PS2 was observed for breakwater configuration 4 as a results of the changed position of the crown wall element. The highest negative pressure at PS2 was obtained for breakwater configuration 3 (apart from the test with $H=0.05$ m).
- Generally, pressure exerted at PS2 tended to be larger than the one exerted at PS1, which is particularly noticeable in the experiments with larger wave height.

NGI



Table 4.6: Maximum solitary wave-induced pressure in tests at TU-BS (model scale 1:30)

	Device	Unit	20140725_01 H=0.050 m	20140725_02 H=0.075 m	20140807_01 H=0.100 m	20140807_02 H=0.125 m	20140807_03 H=0.150 m
C1	PS1_L	[kPa]	0.739	1.006	1.189	1.274	1.354
	PS2_L	[kPa]	0.169	0.667	1.000	1.350	1.530
C2	PS1_R	[kPa]	not installed				
	PS2_R	[kPa]	not installed				
	Device	Unit	20150106_01 H=0.050 m	20150106_02 H=0.075 m	20150107_01 H=0.100 m	20150108_01 H=0.125 m	20150108_02 H=0.150 m
C3	PS1_L	[kPa]	0.491	0.804	1.193	1.384	1.441
	PS2_L	[kPa]	-0.289	-1.026	-1.614	-2.063	-2.417
C4	PS1_R	[kPa]	0.195	0.698	1.076	1.432	1.709
	PS2_R	[kPa]	-0.603	-0.778	-1.366	-1.639	-1.883

4.4 Analysis of flow velocity

4.4.1 Experiments with bore

Maximum horizontal flow velocity under the bore (measured by the ADV placed at breakwater seaside toe in configurations 2, 3, 4 and above berm in configuration 1) and at overtopping (measured by the propeller-type of current meter PR installed at wave gauge WG7 above the crown wall unit in configurations 1, 3, 4 and above breakwater crown in configuration 2) was determined for all examined breakwater configurations. These results are provided in Table 4.7.

The signals measured by the flow meters under tsunami bore impact are plotted for every test in Appendix C. The findings from the experiments are summarized below:

- Tests, in which no overflow occurred (with no measurements of velocity at overtopping available) are marked as “no overflow” in Table 4.7. Tests with weak overflow, however no velocity at overtopping measured, are marked as “overflow but no velocity measured” in Table 4.7.
- Due to the scarce experimental data, no clear relationship between the velocity at overtopping and breakwater configurations/bore intensity could be identified.
- Measurements of flow velocity under the bore by using ADV posed difficulties, since the device was employed in conditions unfavorable for the measurements (i.e. it was initially emerged in the tests). The recorded signal was very noisy and not similar for breakwater configurations 2, 3 and 4 (i.e. without berm). However, no other type of current meter was available at LWI at the time of the test performance. The velocity values in Table 4.7 represent averaged maximum values, since smoothing of the measured velocity profiles was necessary.



- Velocity measurements by ADV for breakwater configuration 1 (i.e. with berm) are significantly higher than for other examined breakwater configurations. This phenomenon corresponded to the fact of reducing the flow cross section by the berm presence, which resulted in the increase of the flow velocity.
- Increase of the flow velocity with impoundment depth h_0 would be expected, however the gained results did not confirm this trend. Overall, the velocity measurements by ADV have to be unfortunately considered as not reliable in the performed tests.

Table 4.7: Maximum flow velocity under bore in tests at TU-BS (model scale 1:30)

	Device	Unit	20140721_01 0.2, 0.75 m	20140721_02 0.2, 0.80 m	20140721_03 0.2, 0.85 m	20140723_01 0.2, 0.75 m	20140723_02 0.2, 0.80 m			
C3	PR_L	[m/s]	no overflow	overflow but no velocity measured	0.408	X				
	ADV_L	[m/s]	0.400	0.750	0.390					
C4	PR_R	[m/s]	no overflow	no overflow	overflow but no velocity measured			X		
	ADV_R	[m/s]	0.850	0.300	0.500					
C1	PR_L	[m/s]	X			no overflow	0.088			
	ADV_L	[m/s]				1.128	1.668			
C2	PR_R	[m/s]				X			no overflow	overflow but no velocity measured
	ADV_R	[m/s]							0.503	0.560

4.4.2 Experiments with solitary wave

Determined values of maximum flow velocity under solitary wave (measured by the ADVs placed at breakwater seaside toe in configurations 2, 3, 4 and above berm in configuration 1) and at overtopping (measured by the propeller-type of current meters PR installed at WG7 above the crown wall unit in configurations 1, 3, 4 and above breakwater crown in configuration 2) for all breakwater configurations investigated are given in



Table 4.8.

The measurements of flow velocity under solitary wave are shown for every test in Appendix C. The findings from the experiments are summarized below:

The propeller-type of current meter was not functioning properly in tests with breakwater configuration 2. These tests are marked as “not working” in

NGI



- Table 4.8.

The signals recorded by ADV were very noisy in the tests performed for breakwater configurations 1 and 2 despite signal filtering used. Velocity values provided in



Table 4.8 for these tests correspond to the averaged maximum values. Tests, in which no velocity value could be determined, are marked as “not determinable” in

NGI



- Table 4.8. In case of experiments with breakwater configuration 3 and 4, performed in later time, the ADV records were of very good quality. The reason for that was most probably the change of water properties in the common water supply system by other department by adding some fluid improving the reflection of the ADV signal from the water particles.
- The flow velocity (including the one at the overtopping) increased generally with the increasing incident solitary wave height. Velocity measured by the propeller-type of current meter ranged from ca. 0.13 to 0.31 m/s for breakwater configuration 1, from ca. 0.23 to 0.46 for breakwater configuration 3 and from ca. 0.23 to 0.4 m/s for breakwater configuration 4. In case of ADV, the velocity range was 0.25 – 0.75 m/s for breakwater configuration 1, 0.15 – 0.49 m/s for breakwater configuration 2, 0.09 – 0.28 m/s for breakwater configuration 3 and 0.08 – 0.29 m/s for breakwater configuration 4.
- While no clear difference between the velocity measurements for breakwater configurations 3 and 4 could be noticed, the presence of the berm in breakwater configuration 1 caused reduction of the velocity at overtopping, measured by PR.
- Values of flow velocity measured by ADV were almost same in breakwater configurations 3 and 4, however they differed from those for breakwater configuration 2 (also without the berm). The reason for that might be the not reliable device functioning in tests with breakwater configuration 2, as mentioned above. In case of breakwater configuration 1 (i.e. with berm), velocity measured by ADV was almost twice the one measured for other breakwater configurations.

NGI



Table 4.8: Maximum flow velocity under solitary wave in tests at TU-BS (model scale 1:30)

	Device	Unit	20140725_01 H=0.050 m	20140725_02 H=0.075 m	20140807_01 H=0.100 m	20140807_02 H=0.125 m	20140807_03 H=0.150 m
C1	PR_L	[m/s]	no overflow	0.135	0.245	0.292	0.314
	ADV_L	[m/s]	not determinable	0.250	0.400	0.450	0.750
C2	PR_R	[m/s]	not working				
	ADV_R	[m/s]	0.150	0.150	0.280	0.380	0.490
	Device	Unit	20150106_01 H=0.050 m	20150106_02 H=0.075 m	20150107_01 H=0.100 m	20150108_01 H=0.125 m	20150108_02 H=0.150 m
C3	PR_L	[m/s]	no overflow	0.226	0.371	0.416	0.461
	ADV_L	[m/s]	0.094	0.173	0.218	0.230	0.280
C4	PR_R	[m/s]	no overflow	0.235	0.385	0.361	0.402
	ADV_R	[m/s]	0.081	0.162	0.218	0.249	0.291

4.5 Analysis of breakwater damage

To determine the breakwater damage due to the bore/solitary wave impact, video and photo analysis as well as breakwater profile measurements before and after each test were performed. The video and photo documentation, in which the movement of the rubble and the crown wall unit were well recognizable, were used to classify the observed damage. The measurements of the breakwater profiles were performed manually using a distance laser (employed only for the emerged part of the breakwater model) and a scale (in case of underwater measurements). In first tests, three profiles in two breakwater models were measured. Since no significant differences among these three profiles were identified, measurement of the profile in the middle of the breakwater model was performed in the rest of the tests.

Based on these two methods, the breakwater damage was categorized in following five cases:

- no damage,
- minor damage, in which a few stones of the armour layer were moved and the crown wall element was not moved,
- medium damage, in which many stones of the armour layer were moved and the crown wall element was hardly moved,
- major damage, in which many stones of the armour, filter and core layers as well as the crown wall element were moved,
- total failure, in which the breakwater model was totally destroyed.



4.5.1 Experiments with bore

Detailed description of the breakwater damage induced by the bore is provided in Table 4.9. The damage description encompassed the damage observed for the seaside, the harbour side, the breakwater crown wall and the crown wall unit, which all determined the damage category mentioned in Section 4.5. The breakwater profiles, measured before and after the experiments, are given in Appendix D, while the photo documentation of the observed breakwater damage for every configuration is shown in Appendix E. The comparison of the breakwater profiles before the tests indicated some discrepancies in the breakwater geometries, which were caused by their manual construction. Particularly difficult was obtaining a uniform slope along the breakwater widths. The results of the damage analysis can be summarized as follows:

- No damage was observed for breakwater configurations 3 and 4 for tests with the weakest bore (i.e. with $h_1=0.2$ m and $h_0=0.75$ m). For same bore conditions, however configurations 1 and 2, a minor damage was observed, meaning that more rubble was moved at the breakwater harbor side. In case of tests with $h_1=0.2$ m and $h_0=0.8$ m, minor damage was observed for breakwater configurations 3 and 4, while major damage for breakwater configurations 1 and 2. Total damage of the breakwater models occurred under the strongest bore conditions ($h_1=0.2$ m and $h_0=0.85$ m), tested solely for breakwater configurations 3 and 4. The difference between the classified damaged might have resulted from the geometrical differences of the reconstructed breakwater models after every test, which was difficult to be performed uniquely every time.
- The breakwater damage resulted mainly due to the pressure difference at the seaside and harbour sides of the breakwater models. The water filtrating through the breakwater body exploded the armour layers from inside. The contribution of the overflow in the experiments with the overtopping to the breakwater damage was negligible as compared to the effect of the pressure difference.
- Generally, the seaside slope for all breakwater configurations in all experiments was not damaged at its lower part. Some stones were removed in breakwater configurations 3 and 4 in test with the strongest bore (i.e. $h_1=0.2$ m and $h_0=0.85$ m). Similarly, the berm geometry in breakwater configuration 1 remained almost intact – solely the rubble at its toe and slightly above was removed under bore impact in tests with $h_0=0.75$ m and $h_0=0.80$ m.
- The crown wall element was moved under the impact of the strongest bore (i.e. $h_1=0.2$ m and $h_0=0.85$ m) in breakwater configurations 3 and 4, however in configuration 1 already under weaker bore conditions (i.e. $h_1=0.2$ m and $h_0=0.80$ m). Despite loose arrangement of the crown wall unit elements on the breakwater crown wall, allowing for a free displacement, the units stucked together after rotation caused by flow impact and hanged at the flume walls.
- In case of configuration 2 (without the crown wall unit), there was no damaged to the breakwater crown under the weakest bore conditions (i.e.

NGI



$h_1=0.2$ m and $h_0=0.75$ m). The increase of the water level to $h_0=0.8$ m behind the bore gate caused displacement of many stones of the armour layer constituting the breakwater crown.

- Breakwater damage was focused mainly on the harbor side. A single stone on the breakwater harbor side was removed in breakwater configurations 3 and 4 in test with the weakest bore (i.e. $h_1=0.2$ m and $h_0=0.75$ m), while few stones were moved under same bore conditions in configurations 1 and 2. The increase of the impoundment water depth to $h_0=0.80$ m was accompanied by displacement of few stones in breakwater configurations 3 and 4 and many stones in breakwater configurations 1 and 2. Further, for $h_0=0.85$ m and breakwater configuration 3 and 4, the core layer was uncovered, since the armour layer was washed away.

4.5.2 *Experiments with solitary wave*

NGI



Table 4.10 shows a detailed description of the solitary wave-induced damage of the investigated breakwater models (including the damage of the seaside, the harbour side, the breakwater crown wall and the crown wall unit, determining the damage category mentioned in Section 4.5). The breakwater profiles, measured before and after the tests, are provided in Appendix D and the photo documentation of the observed breakwater damage for every configuration is presented in Appendix E.

During the construction of the breakwater models it was not possible to avoid some discrepancies in the breakwater profiles, as indicated by the comparison of these profiles before the experiments. Damage analysis results are as follows:

- There was no breakwater damage in tests performed for all breakwater configurations, impacted by the smallest wave height of $H=0.05$ m. Almost no damage was observed in breakwater configurations 1 and 2 with test with solitary wave height of $H=0.075$ m; for same conditions minor damage was observed in configurations 3 and 4. Minor damage occurred to breakwater configuration 1, 2 and 3 under impact of solitary wave of height of $H=0.10$ m, while major damage for breakwater profile 4. In test with $H=0.125$ m breakwater configurations 1 and 2 experienced minor damage, while configurations 3 and 4 major damage. Finally, for $H=0.15$ m all breakwater profiles suffered major damage. The more intensive damage for breakwater configuration 4 resulted from the fact that the crown wall unit was more unstable (i.e. not supported by the armour layer at the harbour side) as compared to the non-shifted crown wall element.
- Unlike the tests with tsunami-bore, the breakwater damage in the experiments with solitary wave was caused predominantly by wave overtopping, not wave transmission through the breakwater body.
- Generally, the seaside breakwater slope remained intact in almost all tests with almost all breakwater configurations. Displacement of a few stones in front of the crown wall element was observed solely in experiments with breakwater configurations 3 and 4, under impact of larger solitary waves of height $H=0.125$, and 0.15 m. In case of breakwater configuration 4, such stone displacement occurred also for solitary wave of height of $H=0.10$ m.
- The crown wall element remained stable in breakwater configurations 1, 2 and 3 under the impact of small solitary waves of height of $H=0.05$ and 0.075 m. In case of breakwater configuration 3, no displacement of the crown wall unit was also observed under impact of solitary wave of height $H=0.10$ m. In the tests with the higher solitary waves, the crown wall elements were displaced towards the harbour slope and slightly rotated, what led sometimes to the effect of sticking at the flume wall and crown wall unit corners (despite the loose units arrangement). Particularly in the experiments with the highest solitary wave (i.e. of $H=0.15$ m), the crown wall units in breakwater configuration 4 tended to be more unstable than in configuration 3, since they were not sufficiently support by the armour layer at the harbour side.
- The breakwater crown in breakwater configuration 2 did not suffer any damaged solely in test with the smallest solitary wave of height of $H=0.05$ m.

NGI



Few blue stones constituting the armour layer over the breakwater crown were moved in test with solitary wave height $H=0.075$ m. With the increase of the wave height, the number of the displaced stones and its transport distance increased, too (in case of solitary wave height of $H=0.15$ m, some stones were transported even over the breakwater toe at the harbor side).

- Similarly to the tests with the bore, the major damage to the breakwater occurred on the harbour slope. Under the smallest wave height conditions (i.e. of $H=0.05$ m), no damage to the harbour slope was observed in any of the breakwater configurations examined. For $H=0.075$ m few stones of the armour layer were displaced in all breakwater configurations and their number increased, together with its transport distance, in tests with a larger waves of height of $H=0.10$ and 0.125 m. Most of the rubble was displaced under the impact of the strongest wave of height of $H=0.15$ m.

NGI



Table 4.9: Overview of bore-induced breakwater damage in tests at TU-BS

Test number	Breakwater configuration	Breakwater damage				
		Seaside slope	Harbour slope	Crown wall element/ Breakwater crown	Berm	Damage classification
20140721_010.2, 0.75 m	C3	no damage	1 yellow stone moved a little bit	not moved	-	no damage
	C4	no damage	1 yellow stone moved within slope	not moved	-	no damage
20140721_020.2, 0.80 m	C3	no damage	some yellow stones moved within slope and few over toe and over platform toe	not moved	-	minor damage
	C4	no damage	some yellow stones moved within slope and few over toe and over platform toe	not moved	-	minor damage
20140721_030.2, 0.85 m	C3	armor, filter and core layer removed over 1/3 of slope length	armor layer washed away, core layer uncovered	moved in flow direction, fixed between flume walls, blue armor and filter layer removed completely, core layer removed partially	-	total failure
20140721_030.2, 0.85 m	C4	armor, filter and core layer removed over 1/3 of slope length	armor layer washed away, core layer uncovered	moved in flow direction, fixed between flume walls, blue armor and filter layer removed completely, core layer removed partially	-	total failure
20140723_010.2, 0.75 m	C1	no damage	some yellow stones moved within slope and few over toe and over platform toe	not moved	berm toe and berm crown moved over seaside slope	minor damage
	C2	no damage	some yellow stones moved within slope and few over toe	no stones moved	-	minor damage



Test number	Breakwater configuration	Breakwater damage				
		Seaside slope	Harbour slope	Crown wall element/ Breakwater crown	Berm	Damage classification
			and over platform toe			
20140723_020.2, 0.80 m	C1	no damage	many yellow stones moved within slope and over toe and platform toe	slightly moved in flow direction and tilted around front lower edge	berm toe and berm crown moved over seaside slope	major damage
	C2	slight damage	many yellow stones moved within slope and over toe and platform toe	many blue stones moved within slope, behind toe and behind platform toe	-	major damage



Table 4.10: Overview of solitary wave-induced breakwater damage in tests at TU-BS

Test number	Breakwater configuration	Breakwater damage				
		Seaside slope	Harbour slope	Crown wall element/ Breakwater crown	Berm	Damage classification
20140725_01 H=0.050 m	C1	no damage	no damage	not moved	no damage	no damage
	C2	no damage	no damage	no stones moved	-	no damage
20140725_02 H=0.075 m	C1	no damage	few yellow stones moved within slope	not moved	no damage	almost no damage
	C2	no damage	few yellow stones moved within slope	few blue stones moved within slope	-	almost no damage
20140807_01 H=0.10 m	C1	no damage	some yellow stones moved within slope	slightly moved in flow direction and tilted around front lower edge	no damage	minor damage
	C2	no damage	some yellow stones moved within slope	some blue stones moved within slope	-	minor damage
20140807_02 H=0.125 m	C1	no damage	some yellow stones moved within slope and 1-2 over toe	slightly moved in flow direction	no damage	minor damage
	C2	no damage	some yellow stones moved within slope and 1-2 over toe	some blue stones moved within slope	-	minor damage
20140807_03 H=0.15 m	C1	no damage	many yellow stones moved within slope and some over toe	left crown element moved in flow direction ca. 0.6 m, middle and left crown element rotated around right side, middle crown element stopped by pressure cell cable	no damage	major damage
	C2	no damage	many yellow stones moved within slope and some over toe	some blue stones moved within slope and some over toe	-	major damage
20150106_01 H=0.050 m	C3	no damage	no damage	not moved	-	no damage
	C4	no damage	no damage	not moved	-	no damage



Test number	Breakwater configuration	Breakwater damage				
		Seaside slope	Harbour slope	Crown wall element/ Breakwater crown	Berm	Damage classification
20150106_02 H=0.075 m	C3	no damage	few (about 4) yellow stones moved within slope	not moved	-	minor damage
	C4	no damage	few (about 4) yellow stones moved within slope, especially stones directly behind crown wall	not moved	-	minor damage
20150107_01 H=0.10 m	C3	no damage	many yellow stones especially from the top edge of the slope moved within slope	not moved	-	minor damage
20150107_01 H=0.10 m	C4	few blue stones in front of left and middle crown wall element moved in flow direction	many yellow stones moved within slope and over toe	moved in flow direction, left crown wall element moved by the farthest distance (about 30 cm), right crown wall element just rotated a little bit about right side	-	major damage
20150108_01 H=0.125 m	C3	few blue stones directly in front of crown wall moved a little bit in flow direction	many yellow stones moved within slope	left and right crown wall elements moved about 1 cm in flow direction, middle crown wall element moved about 2 cm in flow direction		major damage
20150108_01 H=0.125 m	C4	few blue stones directly in front of crown wall moved a little bit in flow direction	many yellow stones moved within slope and over toe, all stones directly behind crown wall moved in flow direction	slightly moved in flow direction and tilted around front lower edge		major damage
20150108_02 H=0.15 m	C3	few blue stones directly in front of crown wall moved in flow direction	many yellow stones moved within slope and over toe	moved in flow direction, right crown wall element just moved a little bit, middle and left crown wall elements moved in flow direction and rotated about right side		major damage



Test number	Breakwater configuration	Breakwater damage				
		Seaside slope	Harbour slope	Crown wall element/ Breakwater crown	Berm	Damage classification
	C4	few blue stones directly in front of crown wall moved in flow direction	many yellow stones moved within slope and over toe	slightly moved in flow direction and tilted around front lower edge		major damage



5 Analysis of experimental data from tests at PARI

The key objective of this report is to describe the physical model tests performed at LWI, TU-BS. However, similar model tests have been performed at PARI, the results of which will be summarised here for comparison. The chapter will first summarise the key findings in the tests performed at PARI in Section 5.1 and will then try to highlight the similarities and discrepancies between the model tests at TU-BS in Section 5.2.

5.1 Key findings from tests at PARI

Tests performed at PARI have used two different types of generation methods to simulate tsunamis, namely solitary waves and overflow conditions. These methods have been generated for testing the stability of two types of breakwaters, where the first one follows the principal design of the rubble mound structure at Haydarpasa Breakwater and the second is an improved version due to the observation of the first damages. The key findings of the tests at PARI can be summarized as follows:

- **Relevant failure mode:** regardless of the type of tsunami generation the key failure mode under all load conditions was the sliding of the crown wall of the breakwater (see Figure 5.1). This has happened for individual units first and then for the whole crown wall and was due to the large water level difference before and behind the breakwater. This failure was then often followed by failure of the armour layer, mostly on the harbour side of the breakwater and the top layer of the sea side of the breakwater.

However, if the crown wall proved to be stable under tsunami attack, the armour stones on the sea side were hardly damaged either.

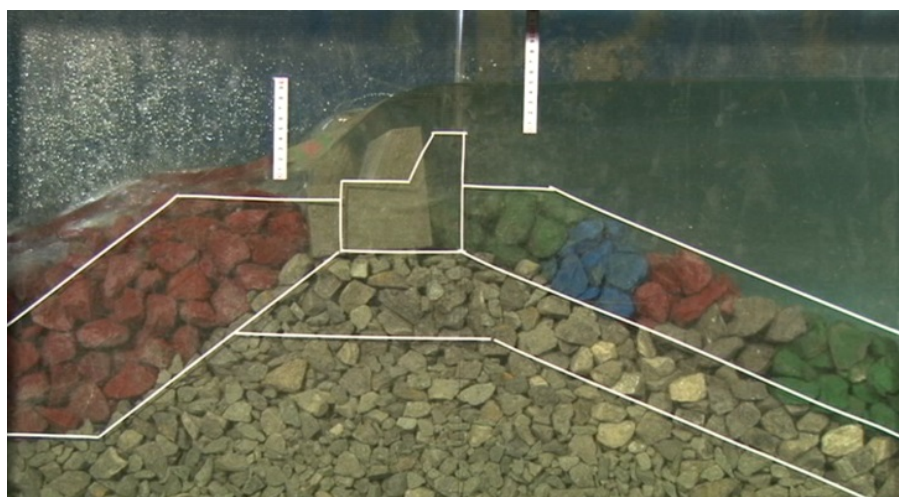


Figure 5.1: Sliding of crown wall units under overflow conditions during PARI tests (Guler et al., submitted)

NGI



- **Influence factors for stability of crown wall:** it has been observed that the (random) placement of armour stones, especially on the harbour side of the breakwater plays a crucial role in the stability of the crown wall and hence in the overall stability of the breakwater. Whenever tsunami loads reach a critical margin, small modifications of the armour stone layout on the breakwater may lead to either failure (with different times when this failure conditions are reached) or stable condition, respectively.
- **Stability of armour layers:** As mentioned before, the armour layers on both sides of the breakwater proved to be stable as long as the crown wall (units) did not start to slide. Any failure of these units resulted in subsequent damage of the armour units being washed away together with or after the failure of the crown wall. On the sea side of the breakwater in most of the cases the lower part of the armour layer proved to be stable even though the upper part was eroded.
- **Improvement of cross section:** after first evaluation of the failures and the relevant failure modes of the original cross section of the breakwater, the armour layer thickness at the harbour side of the breakwater has been doubled to improve the resistance strength against tsunami attack. This has increased the stability of the breakwater significantly so that overflow heights of up to 4.3 cm in the model caused small sliding only (1.85 cm with original design).

Further results of these model tests and more detailed analysis in terms of stability of the armour layer and comparison to existing stability equations can be found in Guler et al. (submitted).

5.2 Differences to tests at TU-BS

From results at PARI (see section 5.1) it became clear that more model tests with more variations of the hydrodynamic and structural parameters would be needed to derive more conclusive results and recommendations. This was one of the reasons for the tests performed at TU-BS and described in this report.



Table 3.2 in section 3.5 of this report shows already the key differences in the setup of the two models at PARI and at TU-BS where the key differences are:

- the simplified geometry of the breakwater of the TU-BS model,
- different layouts of the breakwater resulting in two configurations at PARI (original and improved) and four configurations at TU-BS (see Figure 2.6),
- differences in the bathymetry of the model,
- the differences in generating tsunami conditions (solitary wave and overflow at PARI and solitary wave and bore generation at TU-BS).

From Table 3.2 and the aforementioned comparison the following conclusions can be derived:

- a direct comparison between model tests cannot be performed since both the cross sections of the breakwater and the bathymetry at PARI and TU-BS were different,
- the closest comparable layout is the original configuration (PARI) and configuration 3 (TU-BS) for solitary waves,
- all other configurations should be used for deriving further influences of the geometric parameters of the breakwater layouts.

The results used here for comparison focus on the damage of the breakwater and disregard the layer thicknesses, velocities and pressures on the crown wall. The main reason for this limited comparison is the scarcity of the data in many of the observed parameters and the differences in the two model setups as discussed before. Regarding damages of the breakwater the following conclusions can be drawn:

- **Comparison of two flumes:** for the two breakwater configurations closest to each other in the two test setups (at PARI and TU-BS flumes) the observations of damages for solitary waves were very similar. Model structures in both flumes failed due to the sliding of the crown wall units and this happened for about the same wave height of the solitary waves (starting from about 10 cm corresponding to 3.0 m in prototype).
- **Failure mode:** the dominant failure mode in all cases, regardless of the configurations and the tsunami generation type (overflow, bore, or solitary waves) and regardless of the flume in which the tests have been performed was the sliding of the crown wall units; a second failure mode was observed during the TU-BS tests with the tsunami bore generation where the pressure difference between the sea side and the harbour side caused a significant seepage through the breakwater body and caused the armour stones of the harbour side to fail.
- **Stability of armour layer:** the stability of armour layer in both cases was very good as long as the crown wall did not fail. Major damages occurred only after failure of the crown wall which then left the armour stones, especially at the harbour side of the breakwater, exposed to the tsunami flow.



- **Sensitivity of results:** in both cases (PARI and TU-BS tests) results proved to be very sensitive to small changes, either in the layout of the armour stones, the way the crown wall was positioned on the breakwater, or the hydrodynamic boundary conditions. Any comparison should therefore be made very carefully and should not rely on accurate numbers but more on the order of magnitude of results.
- **Influence of a berm on the sea side:** the use of a berm on the sea side of the breakwater has been tested within the TU-BS tests (cf. configuration 1 against configuration 3). For a tsunami bore the comparison of two different bore height showed that the berm damage starts earlier than any damage of the main breakwater but seem to have a negative influence on the stability of the breakwater as well. More damage was observed in case of the berm than in case without it. However, in the case of solitary waves (and where the still water level was high) the berm did not show any damage regardless of the solitary wave height, even when the main breakwater experienced significant damage.
- **Influence of the crown wall:** configuration 2 of the TU-BS tests did not have a crown wall and can therefore be directly compared to configuration 3. In case of a bore generation the damage without a crown wall starts earlier which means that the crown wall gives additional stability to the breakwater. In case of the solitary waves the behaviour was very similar between both configurations although the crest for the case without the crown wall was also damaged whereas it was not for the case of a crown wall.
- **Position of the crown wall:** configuration 4 of the TU-BS tests used a different position than configuration 3. As for the tsunami bore this difference did not result in any significant difference of the damage patterns whereas for the solitary waves it seemed that the damage of the backward position of the crown wall starts slightly earlier than the one with the standard position. This could be explained by less support from the armour stones behind the crown wall and is therefore understandable although these results are almost within the sensitivity of the parameters used.

Overall, the comparison of results show that the key issues are the type of generation of the tsunami waves and the sensitivity of the structural parameters (position of armour stones, placement of crown wall units, etc.). The tests seem to support the same type of failure mode (sliding of crown wall units) and suggest to use the standard rubble mound configuration (crown wall, no seaward berm), but with a modified armour layer thickness on the harbour side to provide additional support for the crown wall.



6 Summary and conclusions

Laboratory experiments on the performance of the rubble-type of a breakwater under tsunami impact, with the focus on the induced breakwater damage, were performed in a wave flume at TU-BS in a framework of the cooperation between METU and TU-BS in the RAPSODI project. This investigation was a continuation and extension of the tests conducted at PARI, in which the stability of the Haydarpasa Breakwater in the Haydarpasa Port in Istanbul (Turkey), subject to impact of solitary waves and constant overflow, was analysed. Three additional variations of the breakwater prototype with simplified geometry were examined at TU-BS, resulting in a total of four breakwater geometries considered: (i) breakwater with a berm and a crown wall unit (configuration 1), (ii) breakwater without crown wall unit (configuration 2), (iii) breakwater with crown wall unit (configuration 3, corresponding to the prototype), (iv) breakwater with shifted crown wall unit (configuration 4). Two breakwater configurations were always examined simultaneously (configurations 1 and 2, 3 and 4) to optimize the performance time. Apart from the additional breakwater configurations examined, the extension of the reference experiments at PARI encompassed also larger load induced by solitary waves (wave height range from 0.05 to 0.15 m in the model scale) and another flow regime – the tsunami bore, representing a broken, propagating tsunami (with a water depth in front of the bore gate of 0.20 m and behind the bore gate of 0.75 – 0.85 m).

For the comparison purposes of the experimental results, the model scale was kept the same in the tests at PARI and TU-BS (1:30), and the model setup was designed with some minor modifications of the bathymetry/breakwater models geometry, resulting from a limited time for the performance of the investigation (however, keeping the same thickness and mass of the rubble layers, breakwater model height and geometry of the crown wall units).

The determination of the performance of the breakwater models was based on the analysis of the observed processes, the properties of the incident and transmitted wave/flow (including wave height/flow depth, pressure induced on the crown wall unit, and flow velocity) as well as the breakwater damage (damage classification, photo/video analysis, and comparison of the breakwater profiles before and after tests).

The water depth conditions in the tests with solitary wave and tsunami bore, defining the initial breakwater model submergence (i.e. breakwater submerged up to the crown, breakwater emerged, respectively), resulted from the different methods of the flow regime generation and determined the mode of the breakwater failure. The conditions in the tests with the bore corresponded in nature to a very strong withdrawal of the sea prior to tsunami impact (or to an onland embankment), which might not be very realistic. However, change of the water depth conditions by introducing other bathymetry profile was not favoured concerning the comparative result analysis and the limited duration of the experiments.

NGI



Breakwater model damage in case of the tests with the bore resulted predominantly from the pressure difference in front of and behind, as the water, released by the opening of the bore gate, dammed in front of the breakwater models. This led to the effect of blowing out the rubble layers at the harbour side from inside, with the seaside slope almost undamaged. The contribution of the overtopping of the crown wall units/breakwater crown to the overall breakwater model damage was not significant; it led to sliding of the crown wall unit down the breakwater harbour slope. Due to the fact that different damage extension was observed for the different breakwater configurations, not necessarily resulting from the different geometry (e.g. major damage observed for configurations 1 and 2 for bore of $h_0=0.80$ m, while minor damage to configurations 3 and 4 for same bore conditions), repetition of the experiments would be recommended to confirm the gained results.

In case of the tests with solitary wave, the failure mode of the breakwater models was sliding of the crown wall element and the rubble down the harbour breakwater slope, induced by wave overtopping. Unlike the experiments with the tsunami bore, the seaward breakwater slope as well as the berm remained generally stable under solitary wave attack as they were in submerged conditions.

The presence of the crown wall unit definitely increased the stability of the armour harbour slope, as indicated by the comparative result analysis for breakwaters with and without the crown wall unit. Therefore, the breakwater configuration without the crown wall element is not recommended for practical implementation. No particular advantage of the berm presence (for the geometry tested) was observed. Further tests should be performed to examine berm geometries different from the one applied to the experiments at TU-BS, including berm lengthening and heightening (i.e. reducing the freeboard over the berm). This would be expected to have more influence on wave transformation over the berm, resulting in a lesser wave transmission to the harbour side.

Both the experimental investigation at PARI and TU-BS indicated that the conventional breakwater design (i.e. configuration 3 in tests at TU-BS with the crown wall unit placed at the seaside edge of breakwater crown) is stable under weak tsunami conditions (up to ca. 3 m in prototype – 0.1 m in model scale). Further improvement of breakwater stability under more severe tsunami impact can be achieved by thickening the armour layer at the harbour breakwater slope as indicated by the experimental results at PARI with the improved breakwater.



7 References

METU (2015): Existing tools, data, and literature on tsunami impact, loads on structures, failure modes and vulnerability assessment. Deliverable D1 of the RAPSODI Project. Norwegian Geotechnical Report 20120768-01-R, 108 pp.
<http://www.ngi.no/en/Project-pages/RAPSODI/Reports-and-Publications/>

NGI (2015): A GIS tsunami vulnerability and risk assessment model. Deliverable D8 of the RAPSODI Project. Norwegian Geotechnical Report 20120768-08-R.
<http://www.ngi.no/en/Project-pages/RAPSODI/Reports-and-Publications/>

Guler H.G., Arikawa T., Oei T., Yalciner A.C. (submitted): Performance of rubble mound breakwaters under tsunami attack, a case study: Haydarpasa Port, Istanbul, Turkey. *Journal of Coastal Engineering, Elsevier*.



Appendix A

Evolution of bore and solitary wave profiles in experiments at TU-BS



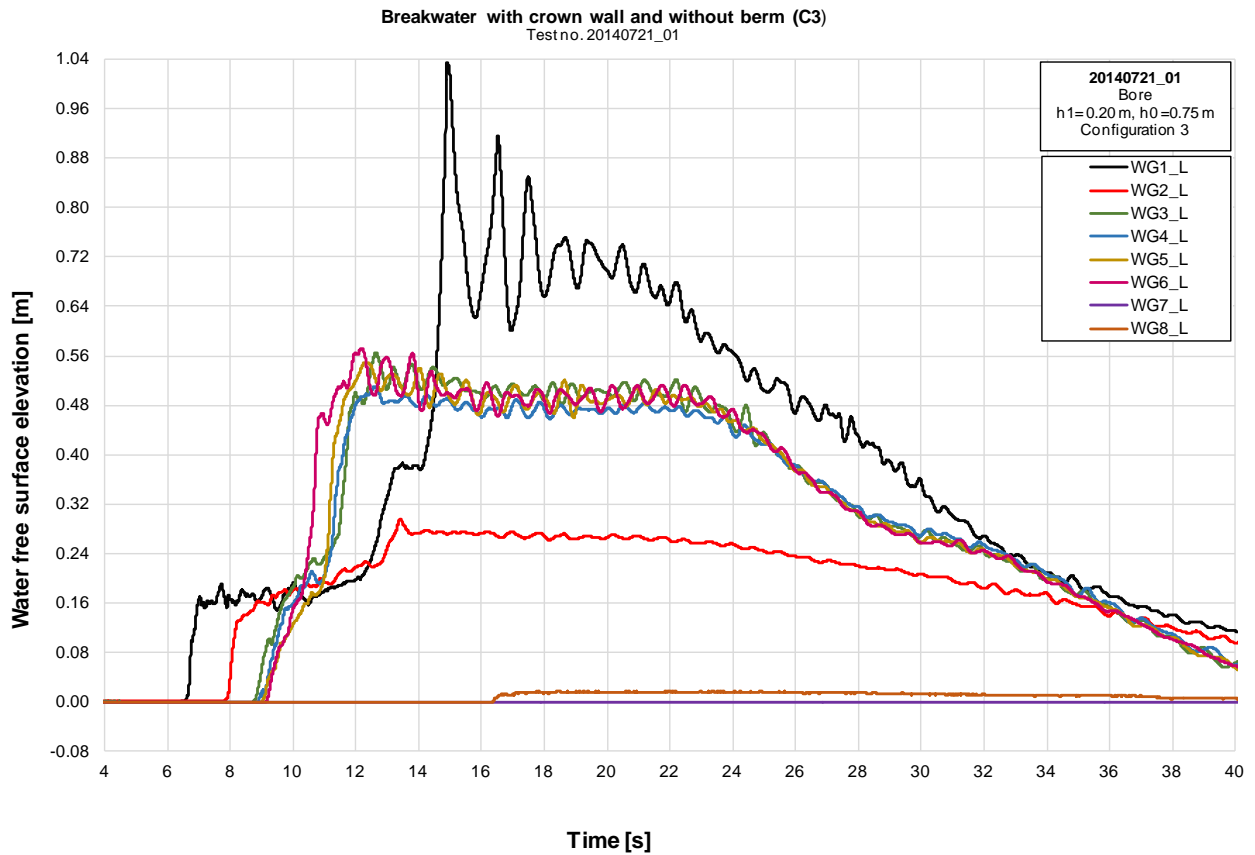


Figure A 1: Bore profiles for configuration 3 with $h_0=0.75\text{ m}$ and $h_1=0.20\text{ m}$ (Test 20140721_01)



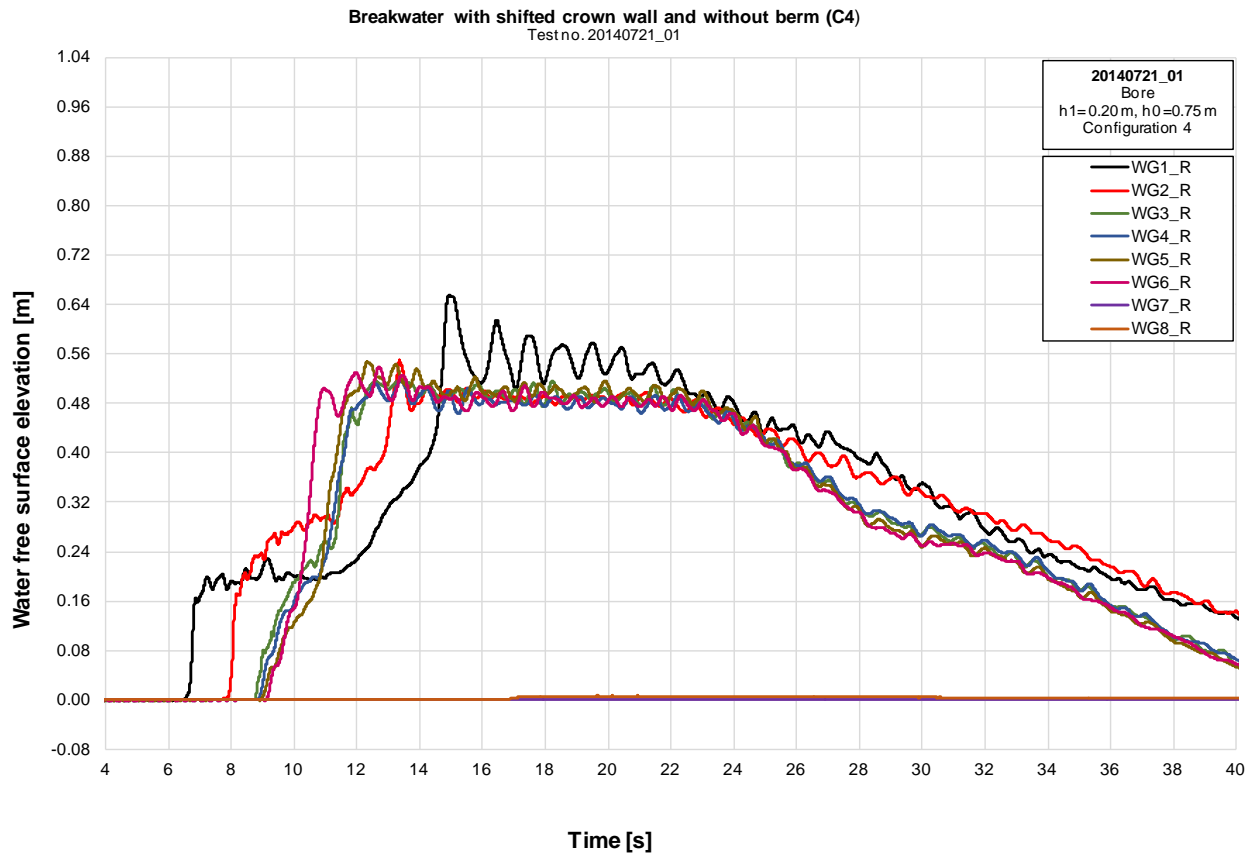


Figure A 2: Bore profiles for configuration 4 with $h_0=0.75\text{ m}$ and $h_1=0.20\text{ m}$ (Test 20140721_01)



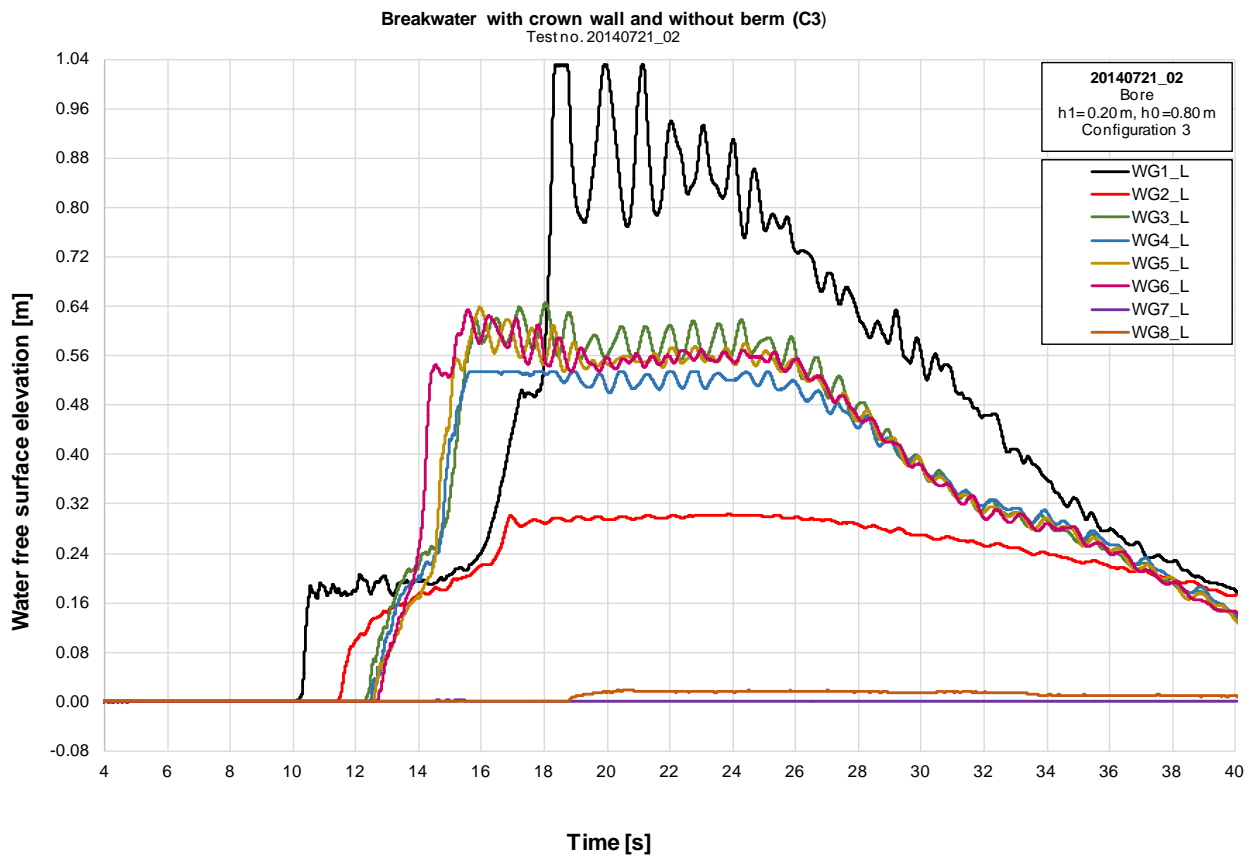


Figure A 3: Bore profiles for configuration 3 with $h_0=0.80\text{ m}$ and $h_1=0.20\text{ m}$ (Test 20140721_02)



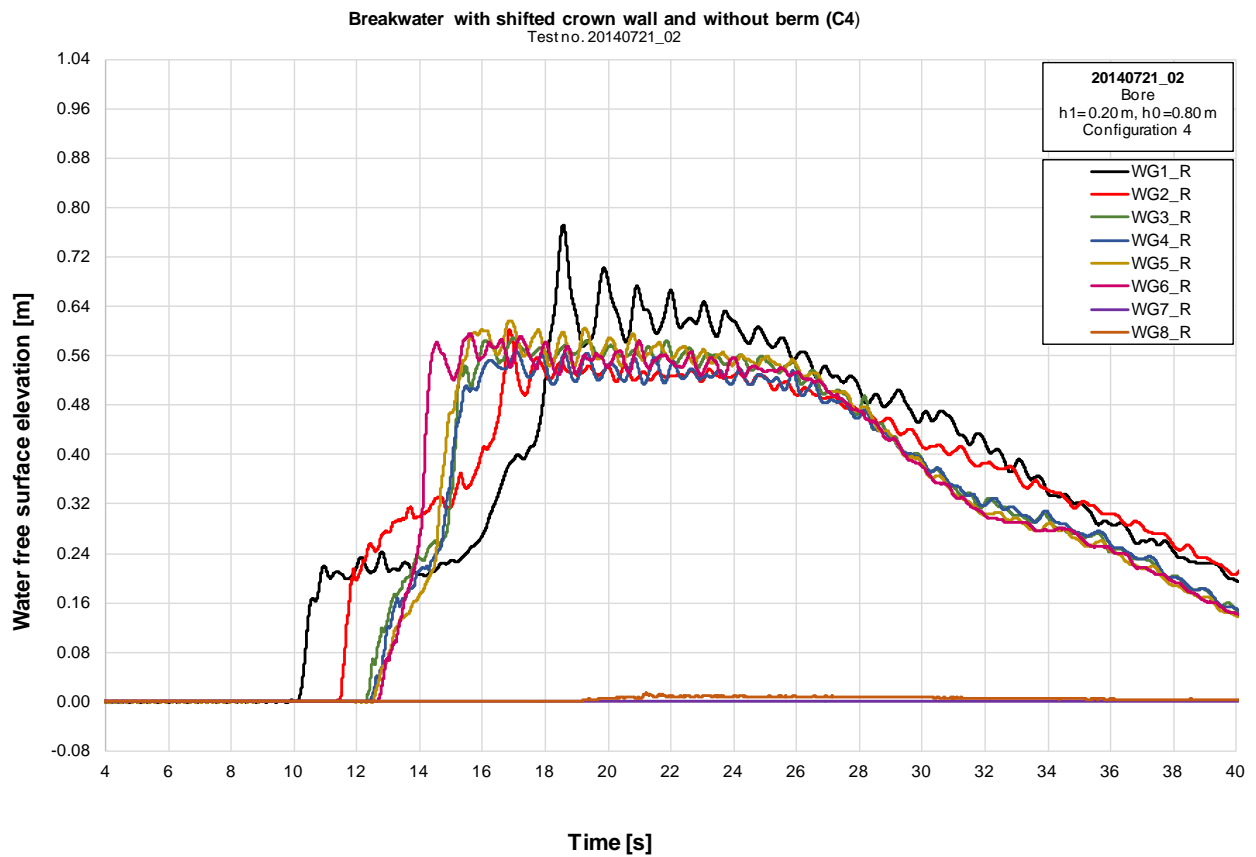


Figure A 4: Bore profiles for configuration 4 with $h_0=0.80\text{ m}$ and $h_1=0.20\text{ m}$ (Test 20140721_02)



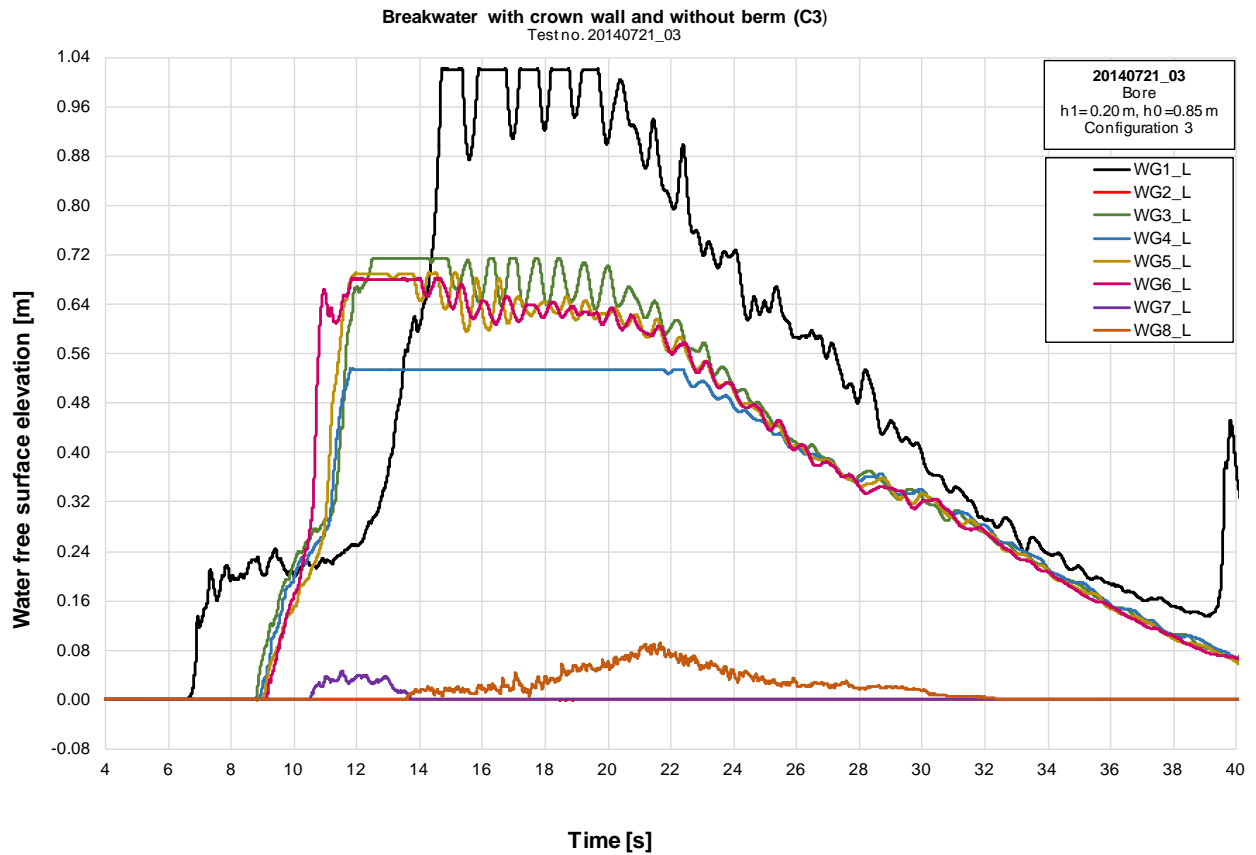


Figure A 5: Bore profiles for configuration 3 with $h_0=0.85$ m and $h_1=0.20$ m (Test 20140721_03)



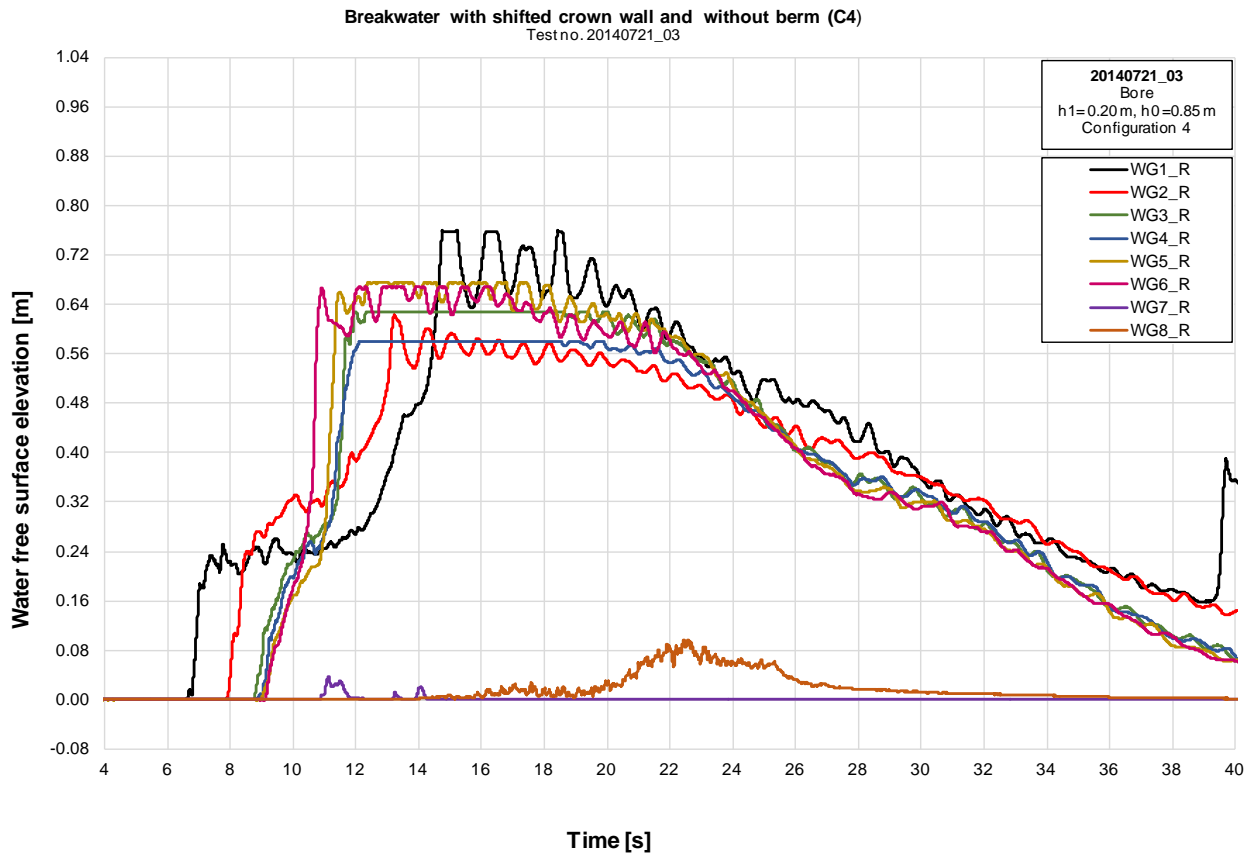


Figure A 6: Bore profiles for configuration 4 with $h_0=0.85\text{ m}$ and $h_1=0.20\text{ m}$ (Test 20140721_03)



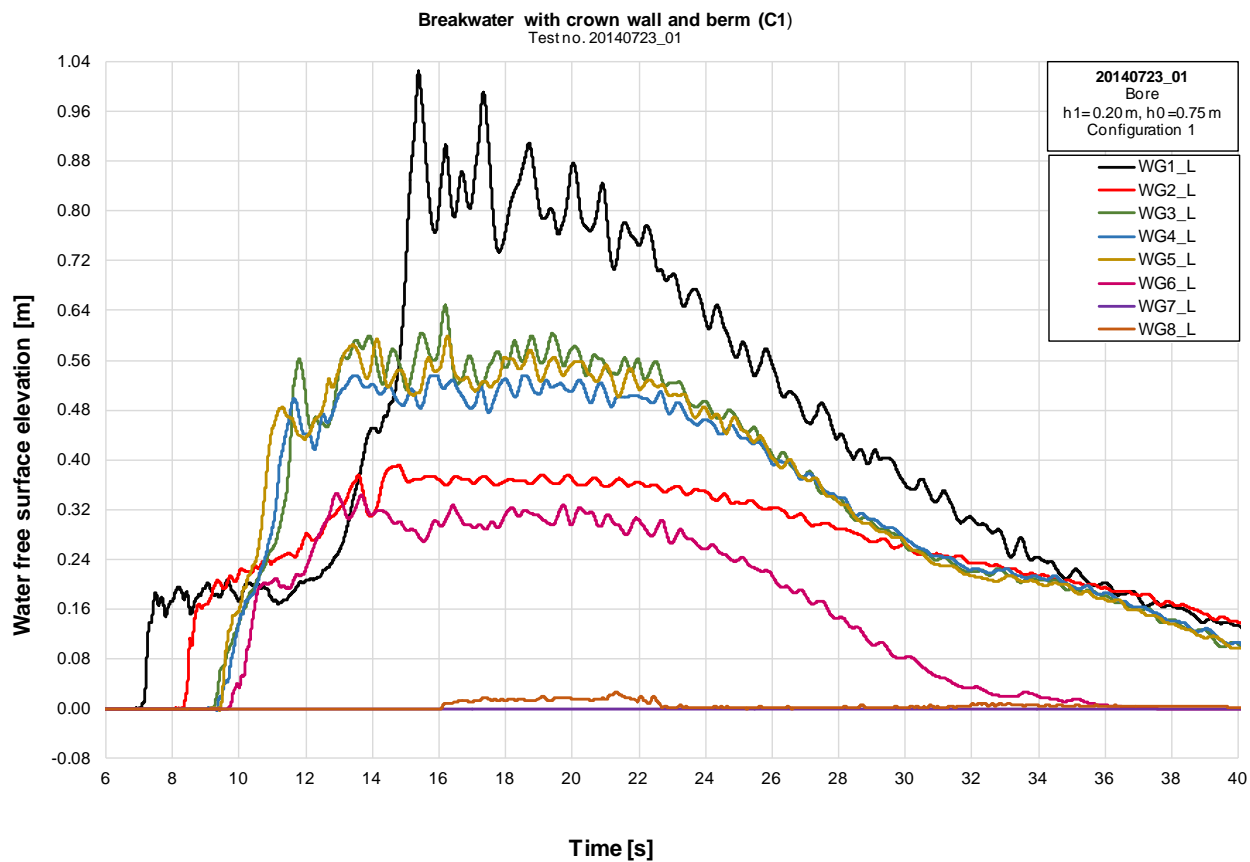


Figure A 7: Bore profiles for configuration 1 with $h_0=0.75\text{ m}$ and $h_1=0.20\text{ m}$ (Test 20140723_01)



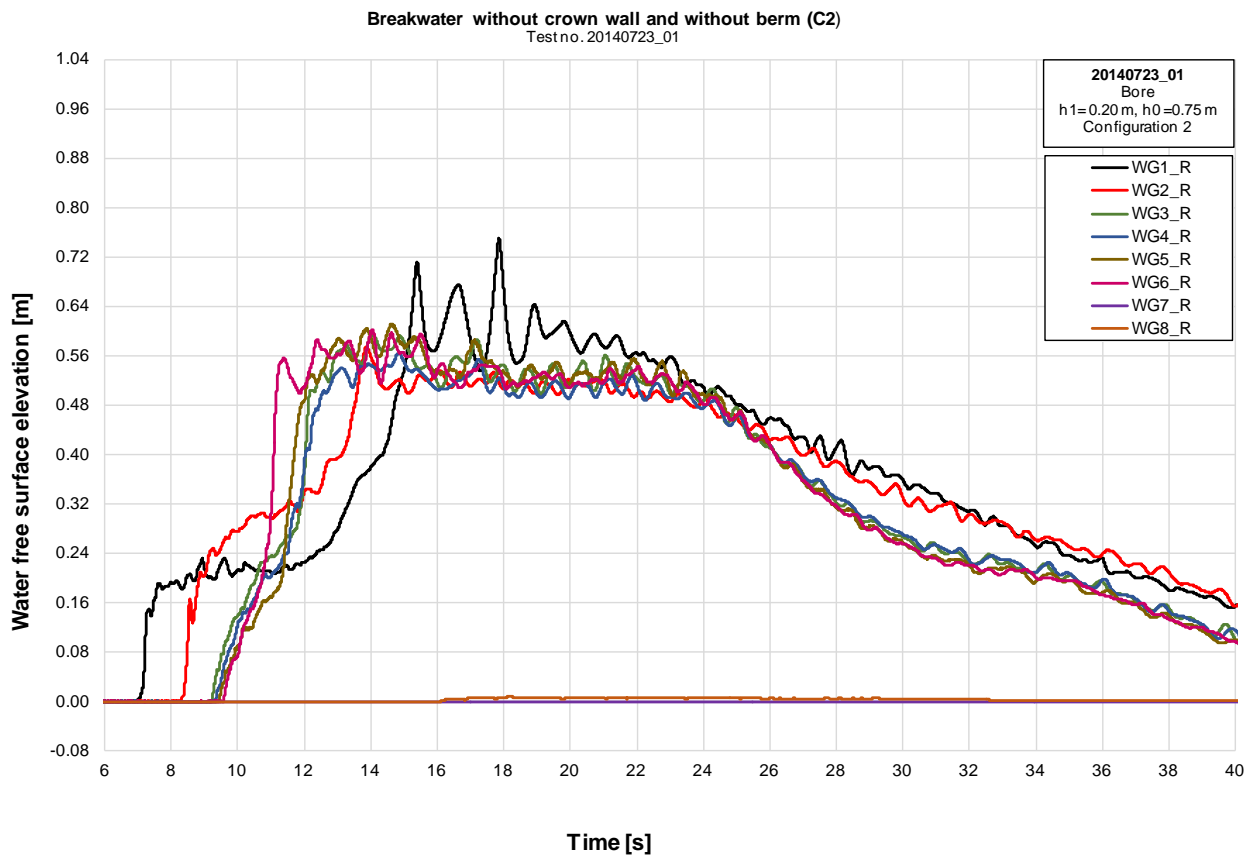


Figure A 8: Bore profiles for configuration 2 with $h_0=0.75\text{ m}$ and $h_1=0.20\text{ m}$ (Test 20140723_01)



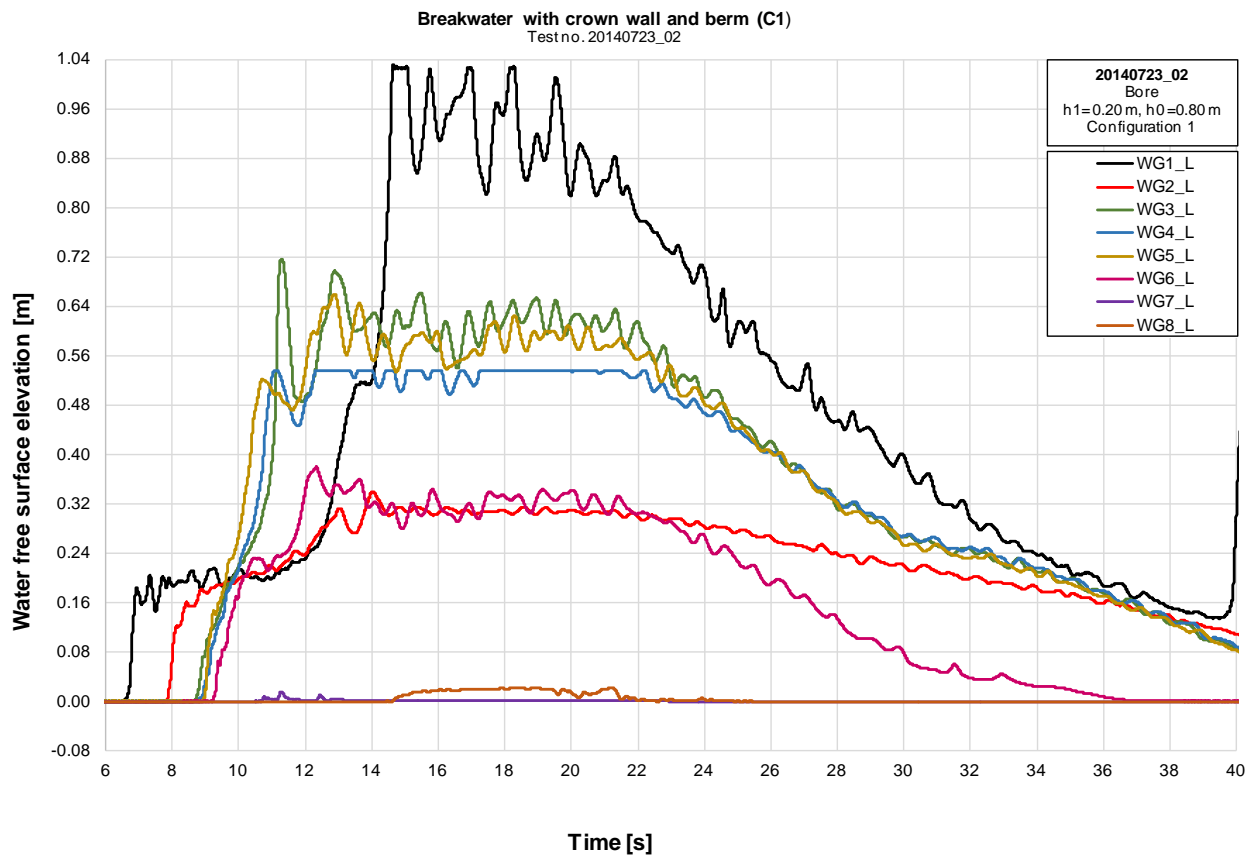


Figure A 9: Bore profiles for configuration 1 with $h_0=0.80\text{ m}$ and $h_1=0.20\text{ m}$ (Test 20140723_02)



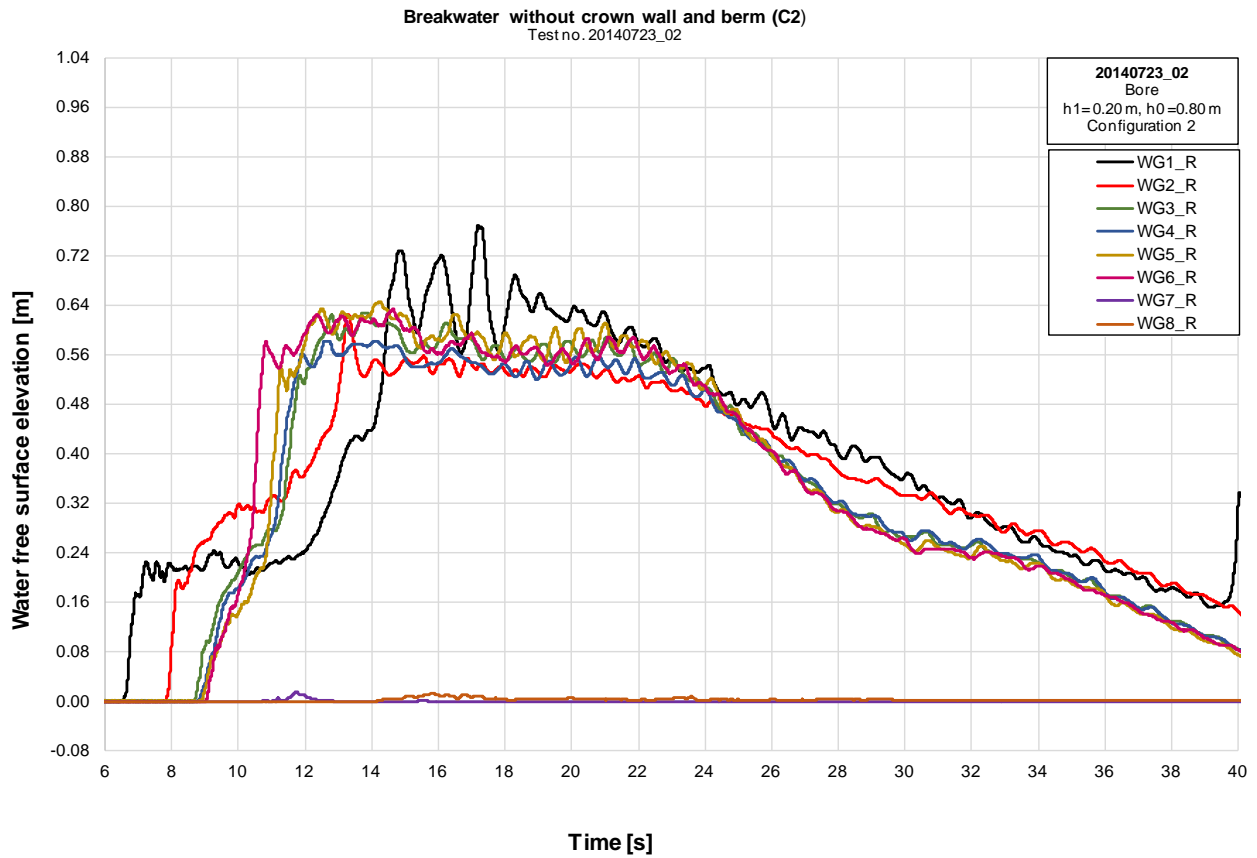


Figure A 10: Bore profiles for configuration 2 with $h_0=0.80\text{ m}$ and $h_1=0.20\text{ m}$ (Test 20140723_02)



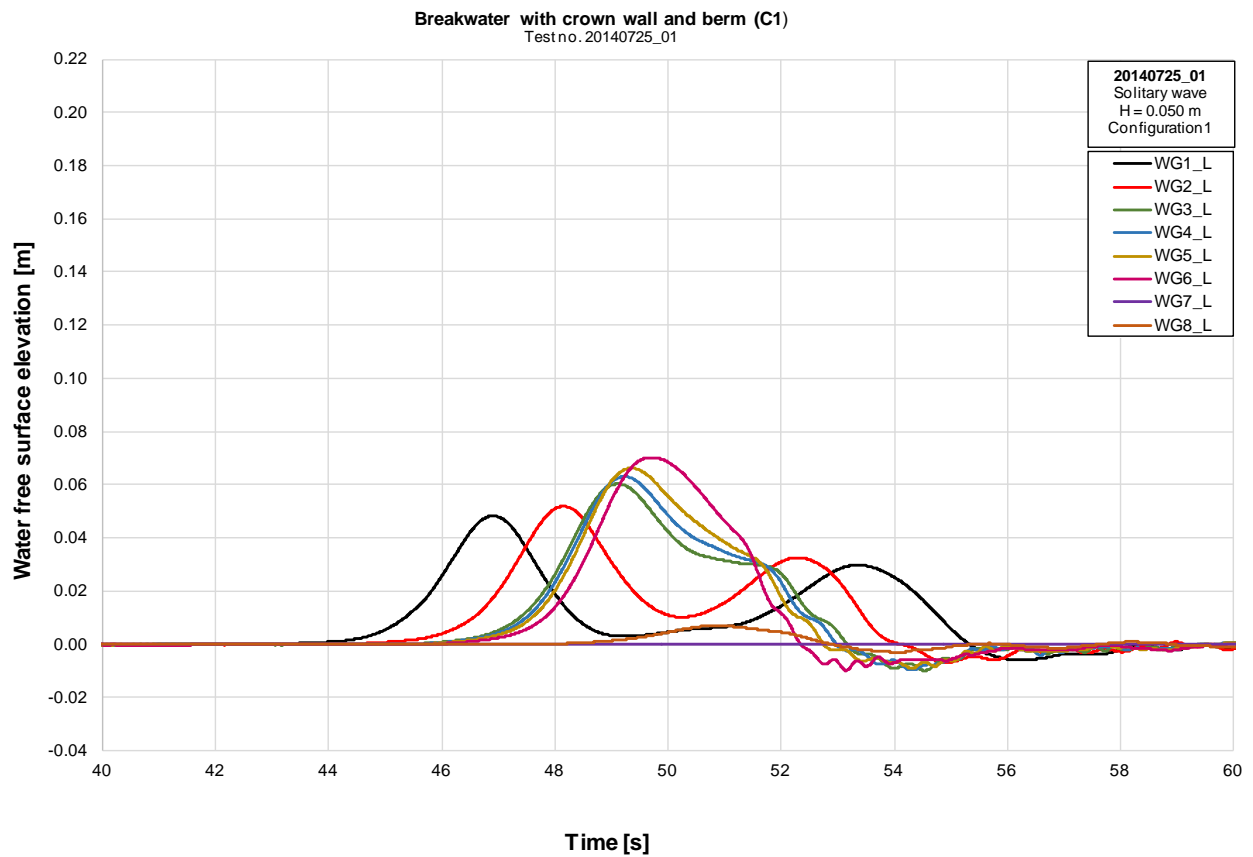


Figure A 11: Solitary profiles for configuration 1 with $H=0.050$ m (Test 20140725_01)



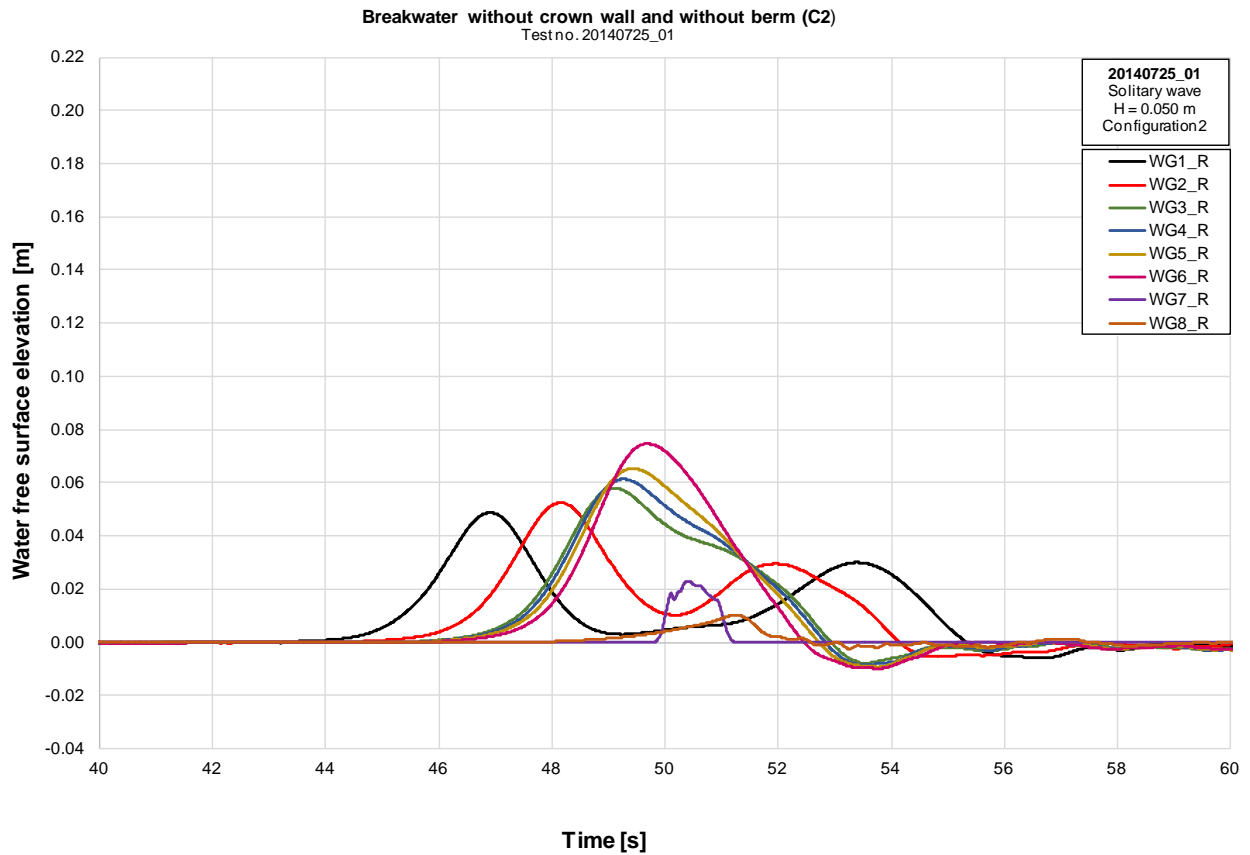


Figure A 12: Solitary profiles for configuration 2 with $H=0.050$ m (Test 20140725_01)



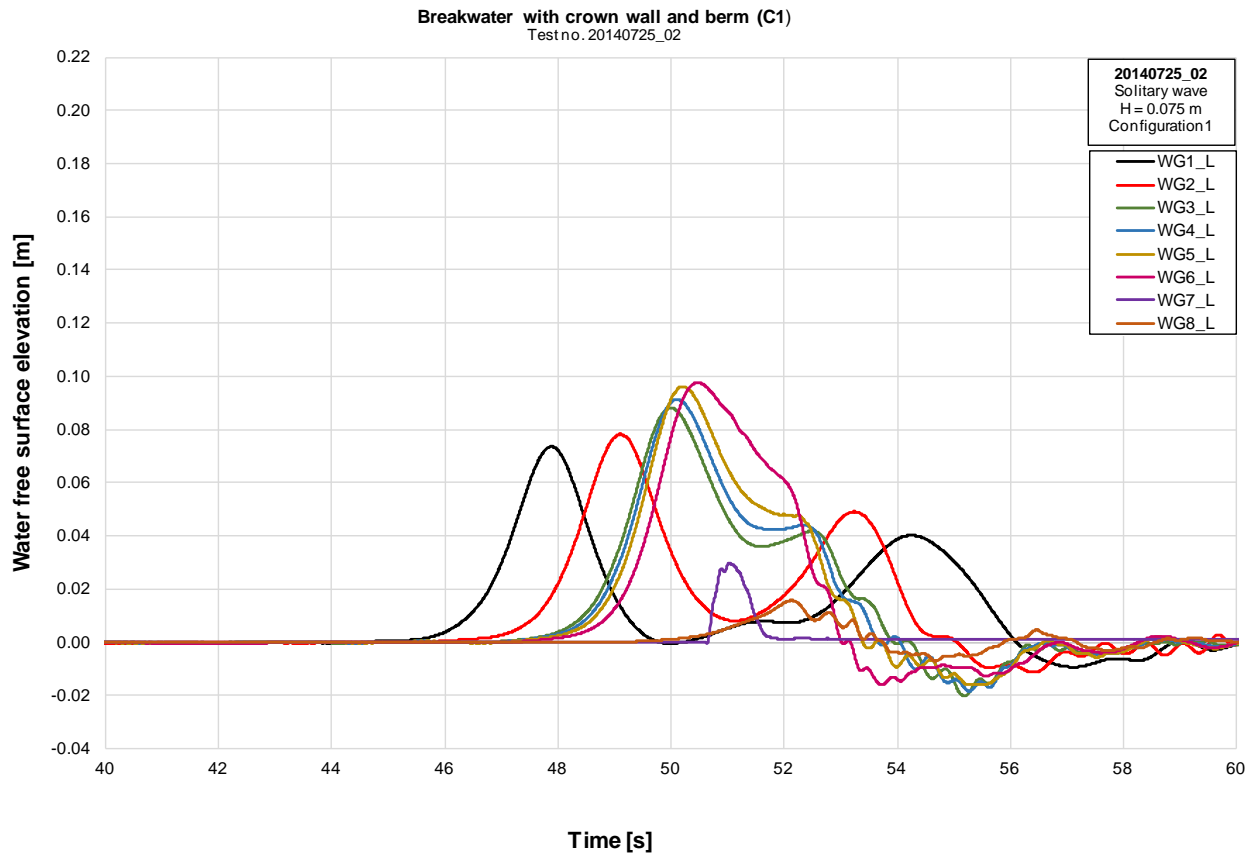


Figure A 13: Solitary profiles for configuration 1 with $H=0.075$ m (Test 20140725_02)



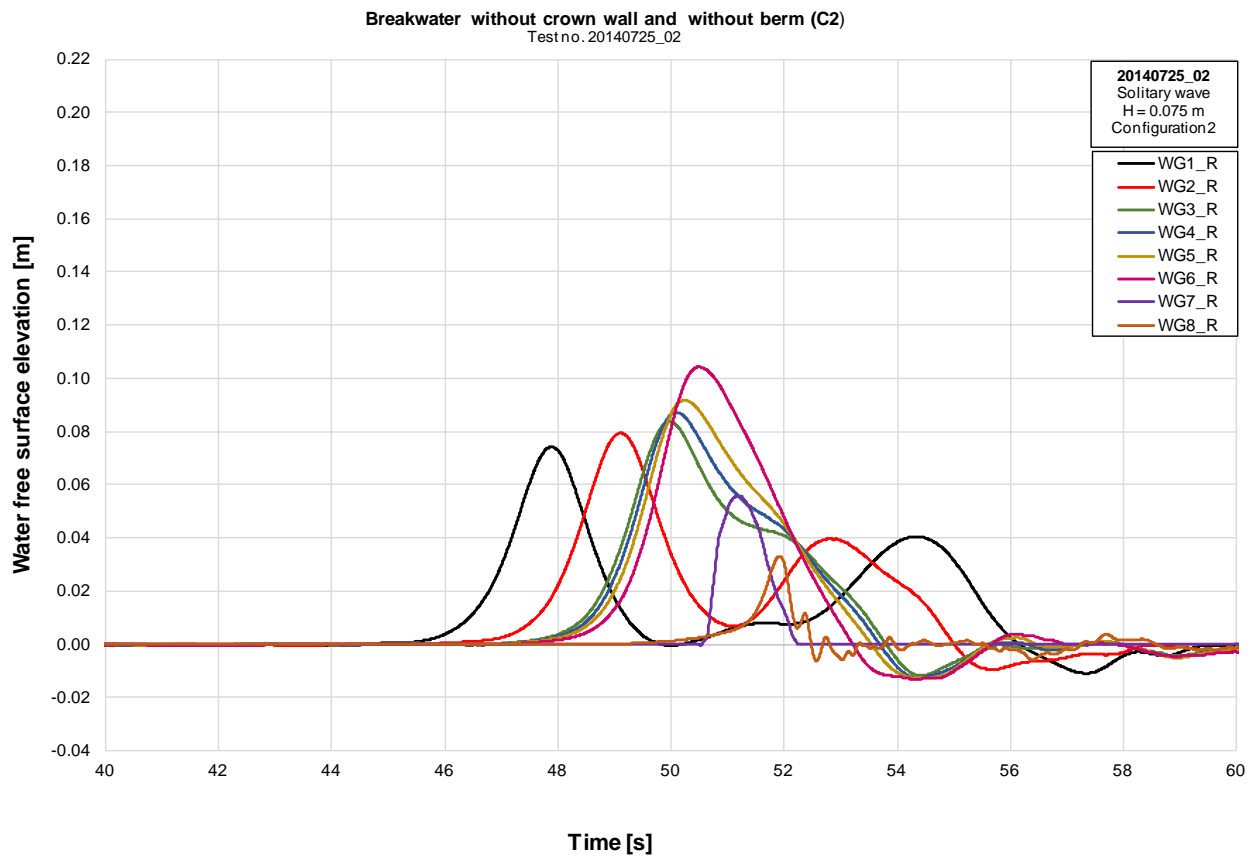


Figure A 14: Solitary profiles for configuration 2 with $H=0.075$ m (Test 20140725_02)



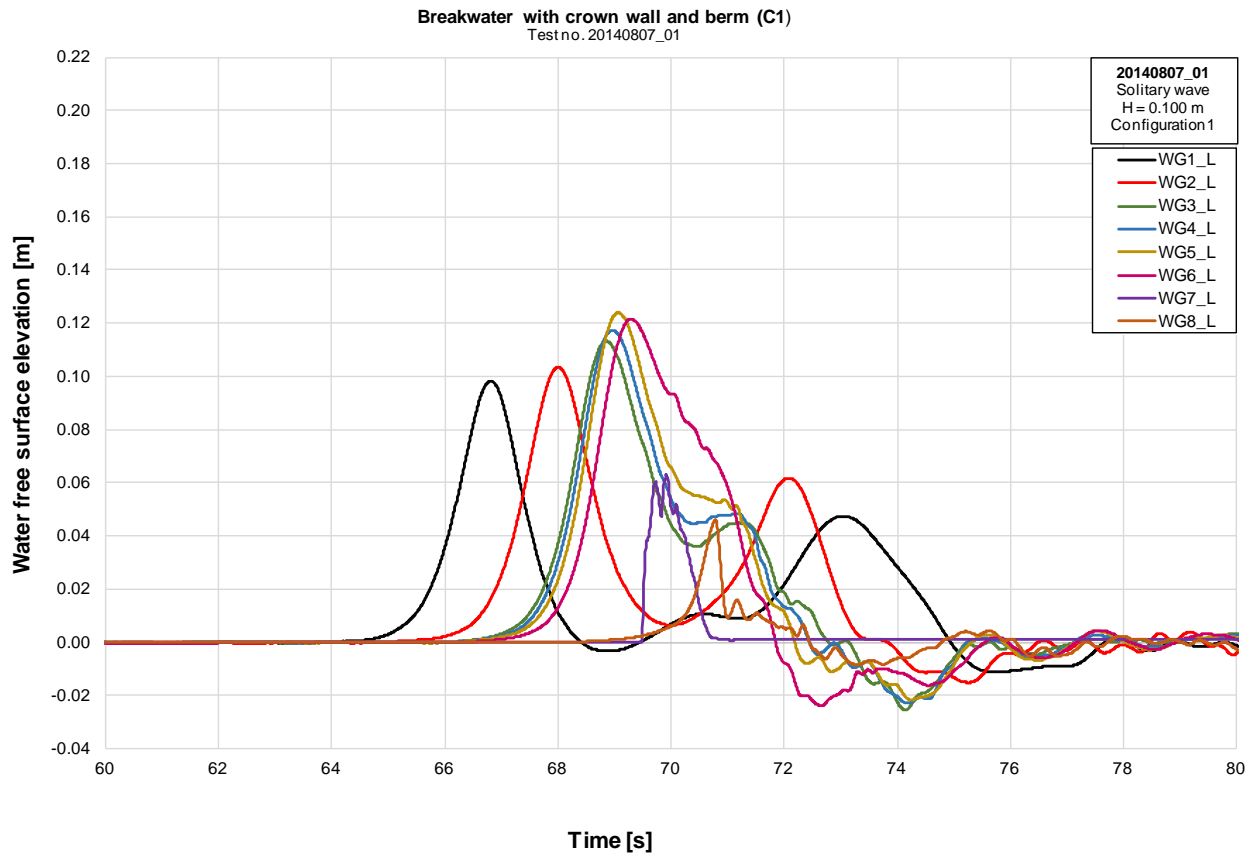


Figure A 15: Solitary profiles for configuration 1 with $H=0.100$ m (Test 20140807_01)



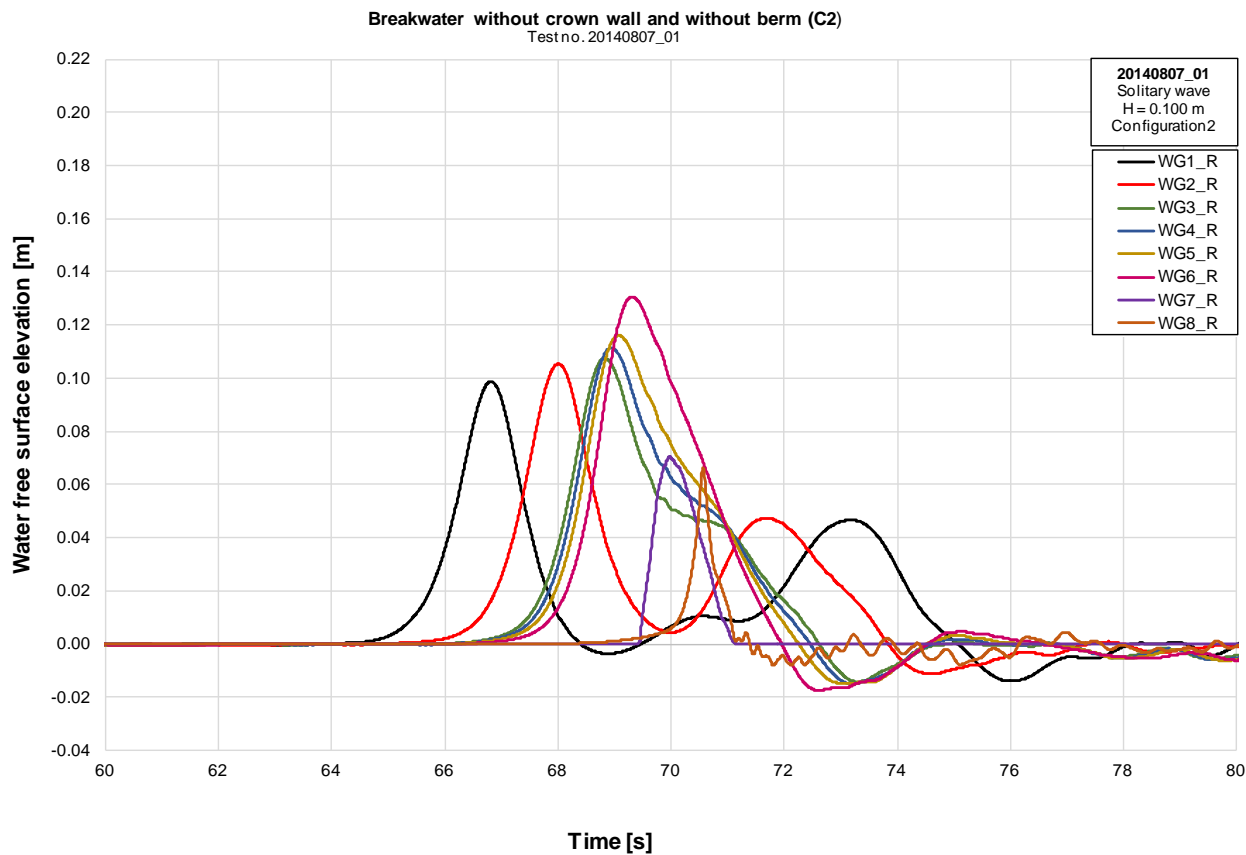


Figure A 16: Solitary profiles for configuration 2 with $H=0.100$ m (Test 20140807_01)



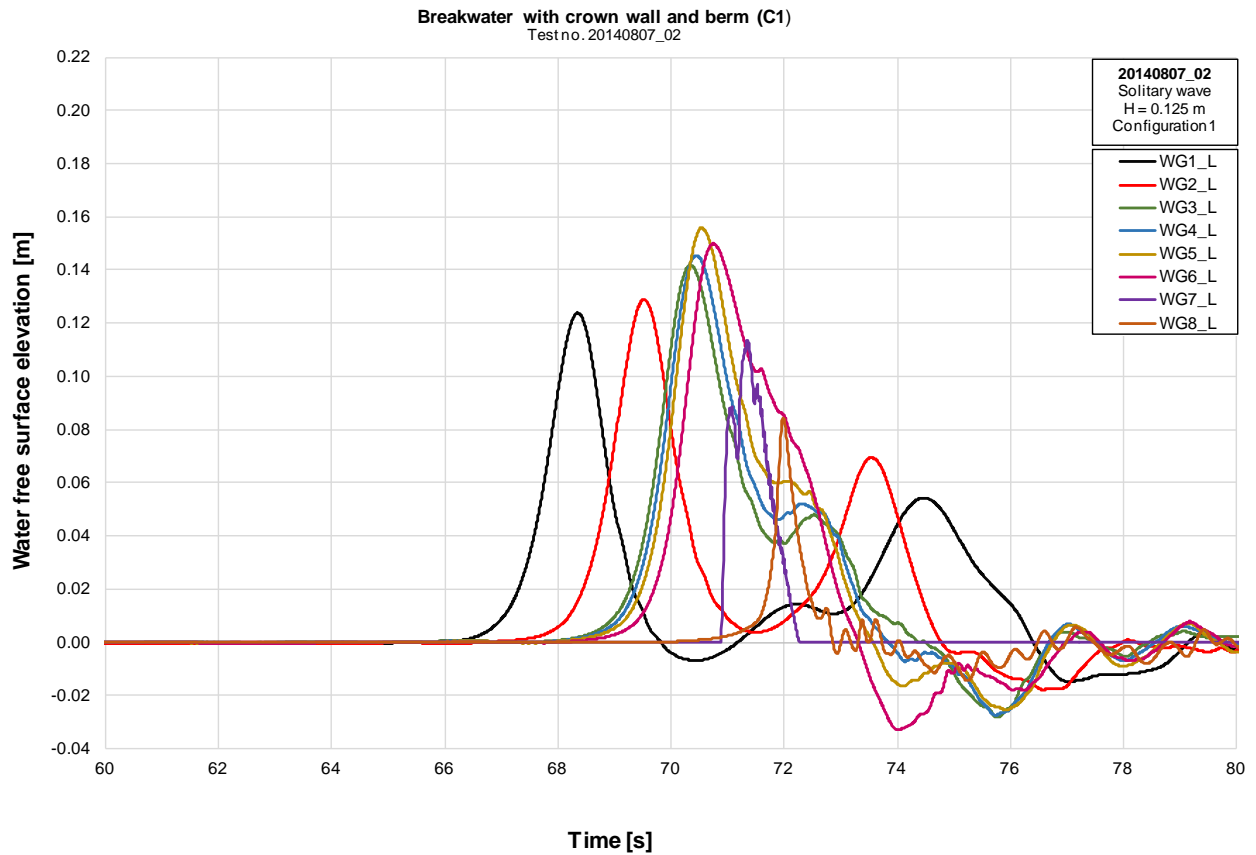


Figure A 17: Solitary profiles for configuration 1 with $H=0.125$ m (Test 20140807_02)



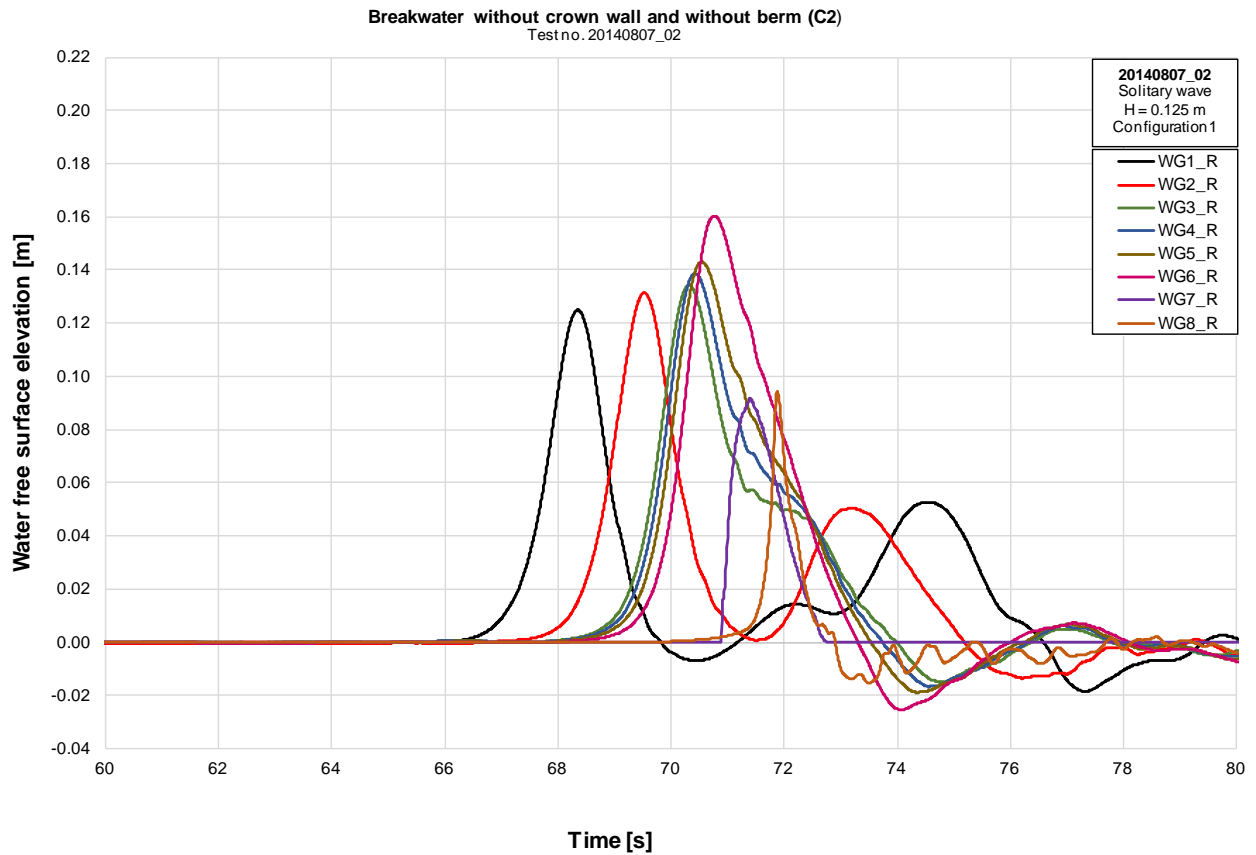


Figure A 18: Solitary profiles for configuration 2 with $H=0.125$ m (Test 20140807_02)



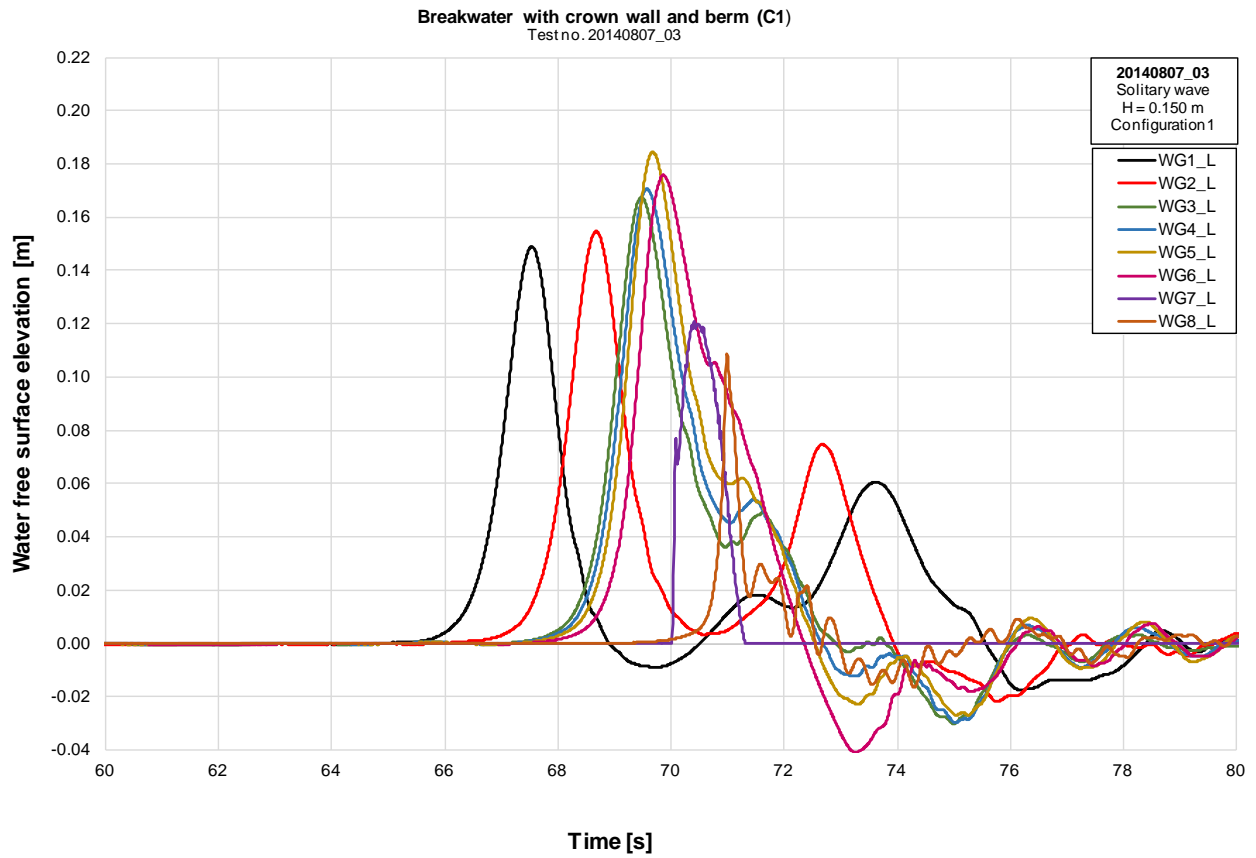


Figure A 19: Solitary profiles for configuration 1 with $H=0.150$ m (Test 20140807_03)



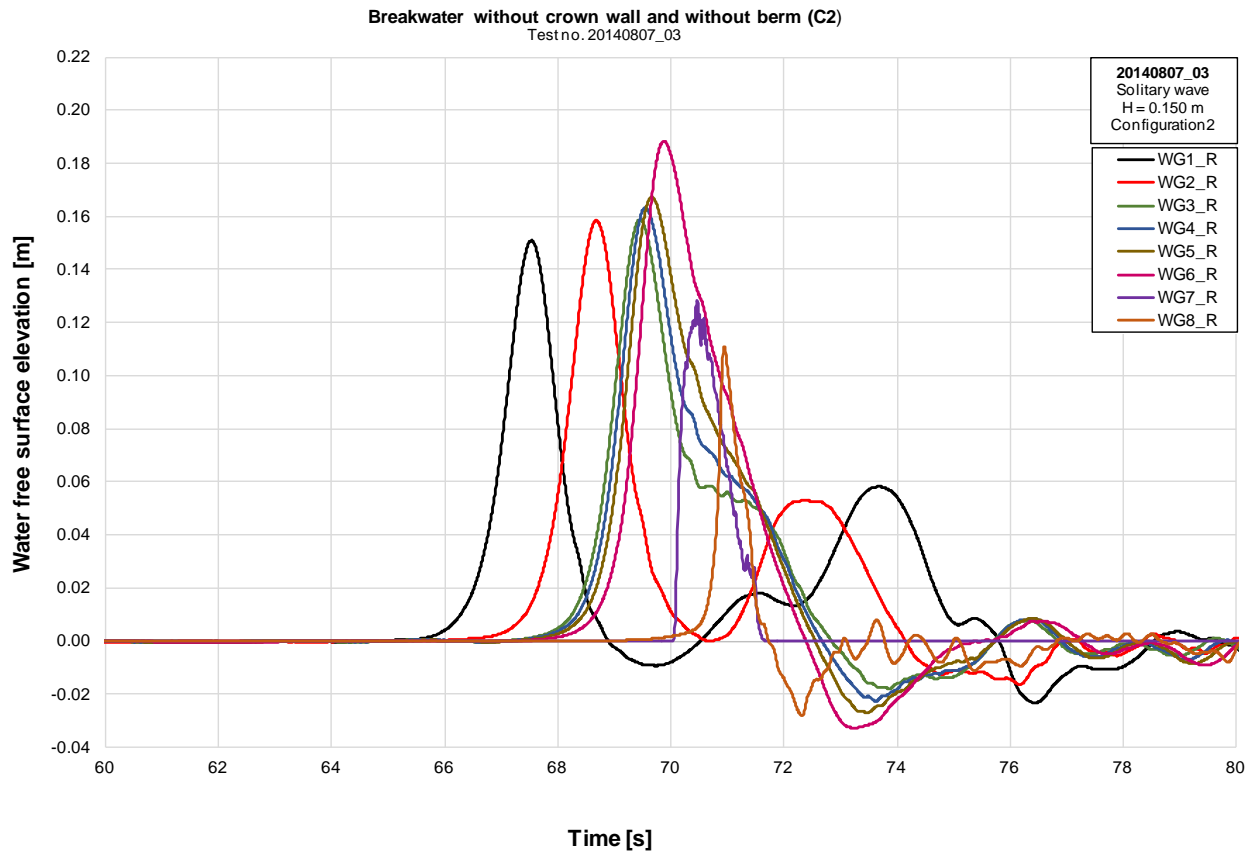


Figure A 20: Solitary profiles for configuration 2 with $H=0.150$ m (Test 20140807_03)



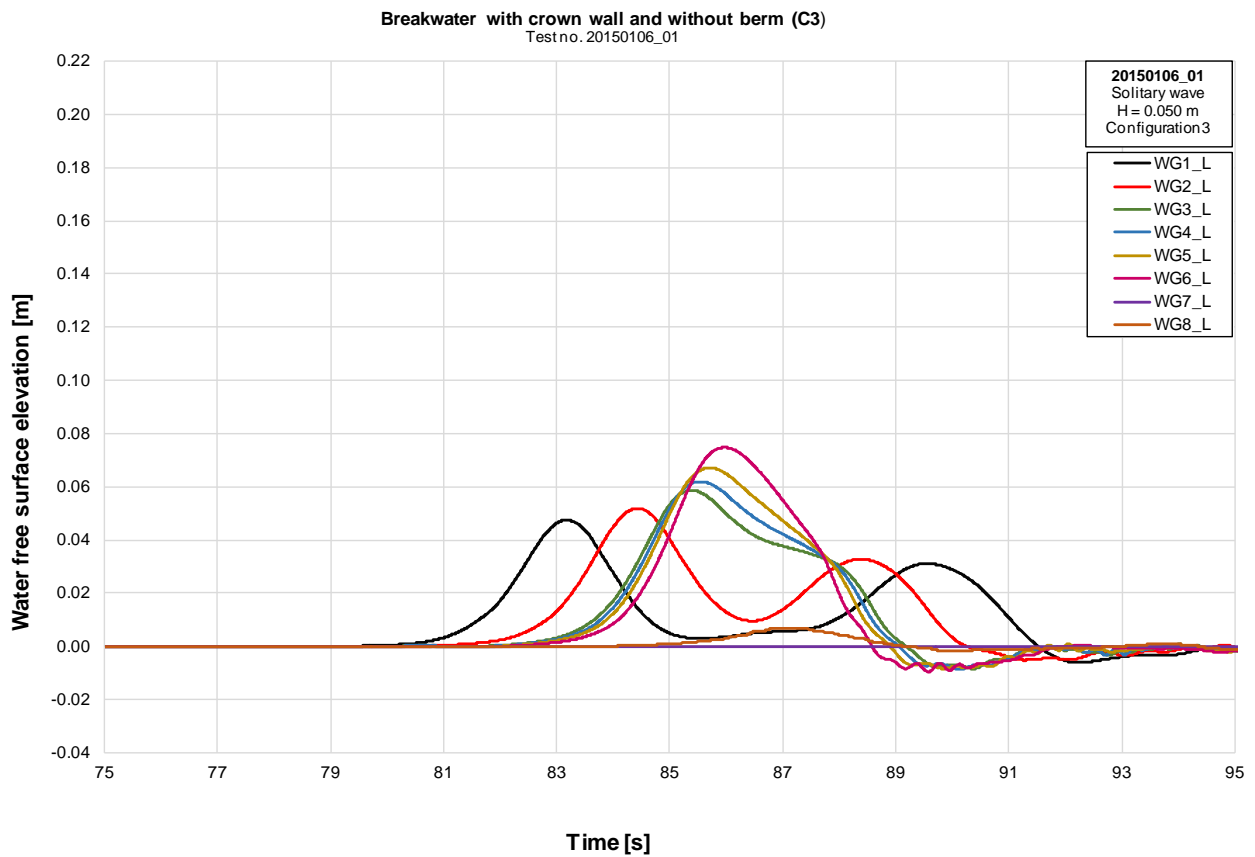


Figure A 21: Solitary profiles for configuration 3 with $H=0.050$ m (Test 20150106_01)



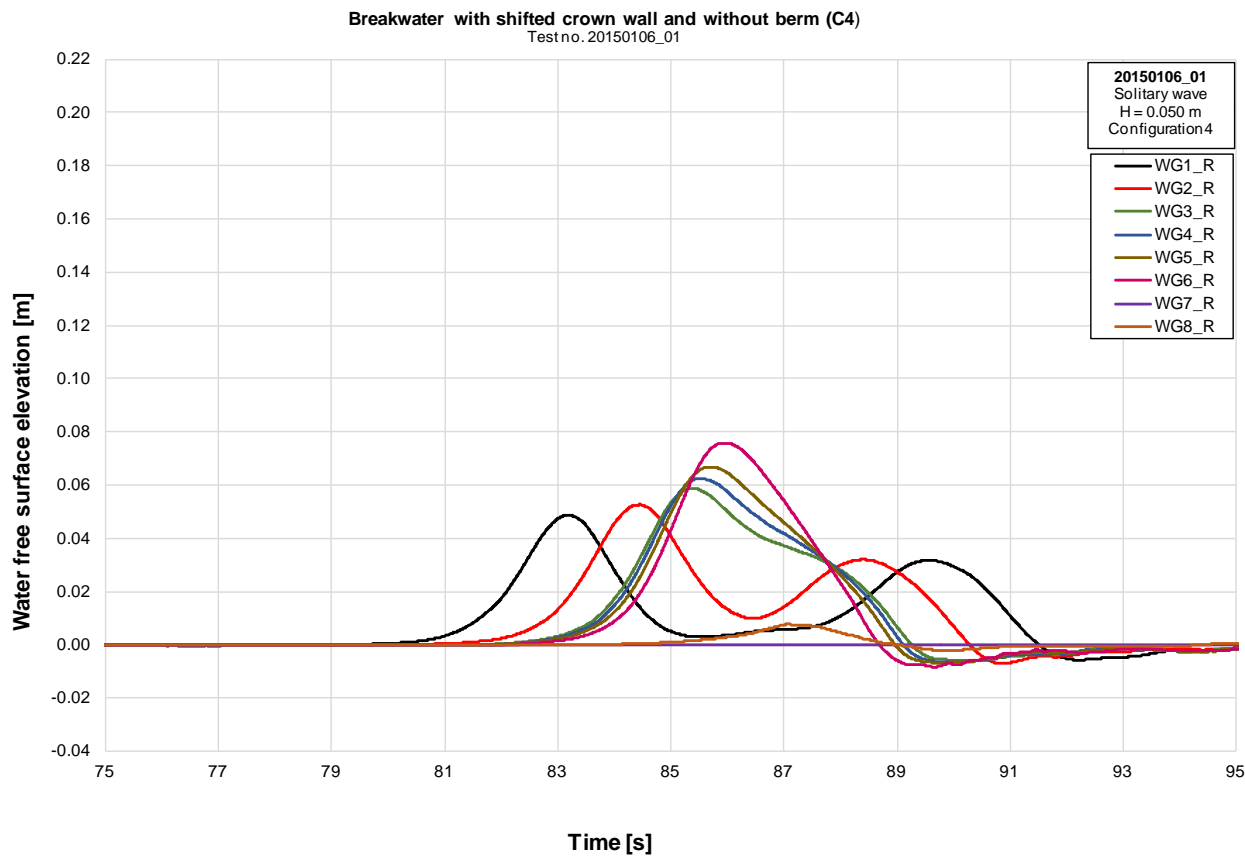


Figure A 22: Solitary profiles for configuration 4 with $H=0.050$ m (Test 20150106_01)



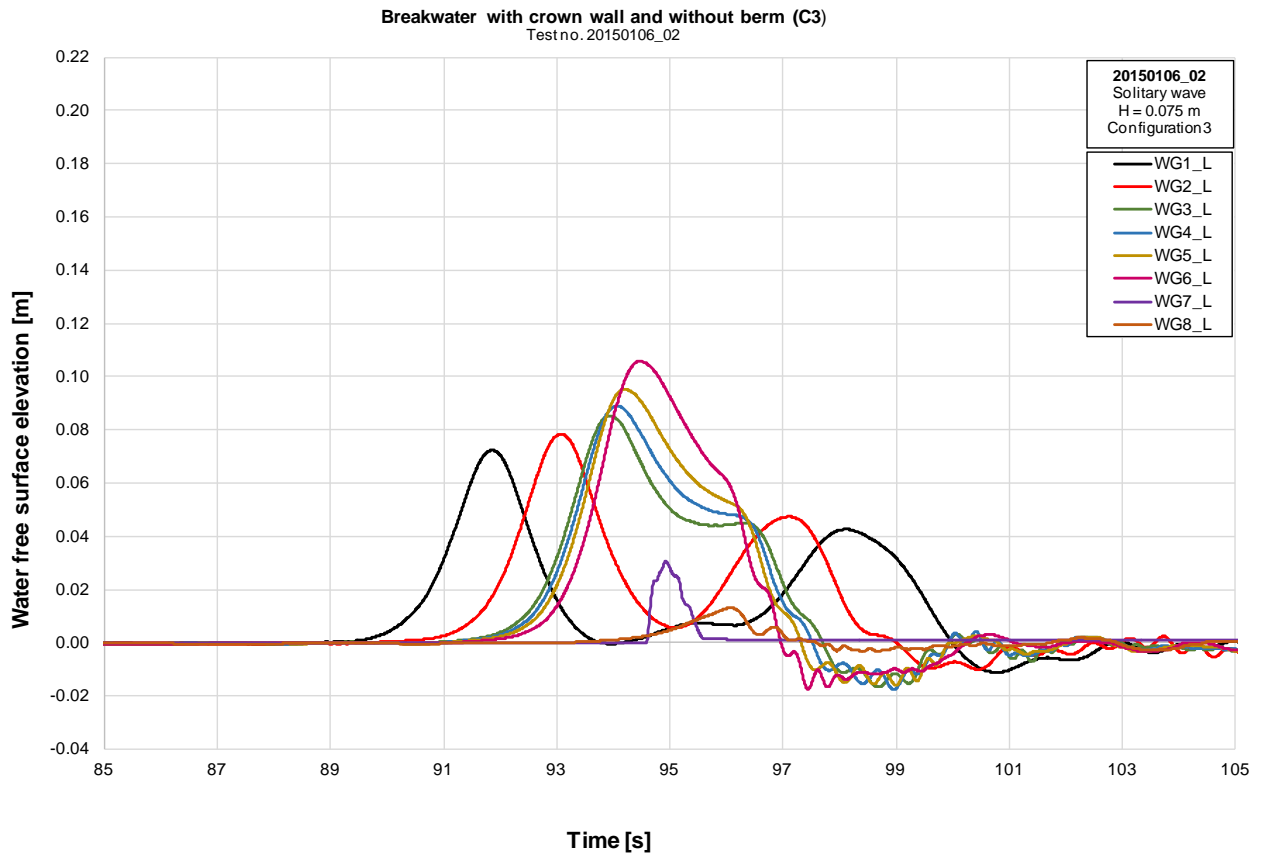


Figure A 23: Solitary profiles for configuration 3 with $H=0.075$ m (Test 20150106_02)



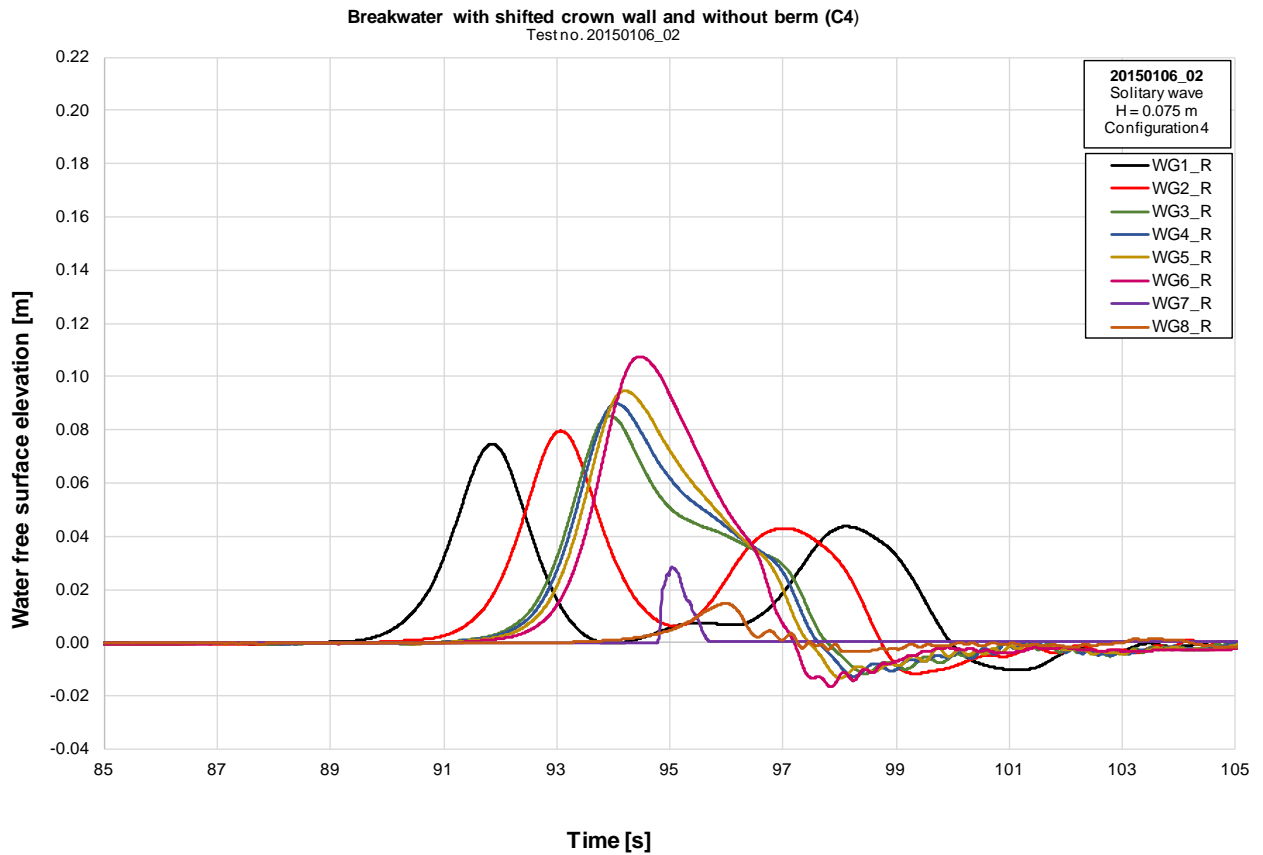


Figure A 24: Solitary profiles for configuration 4 with $H=0.075$ m (Test 20150106_02)



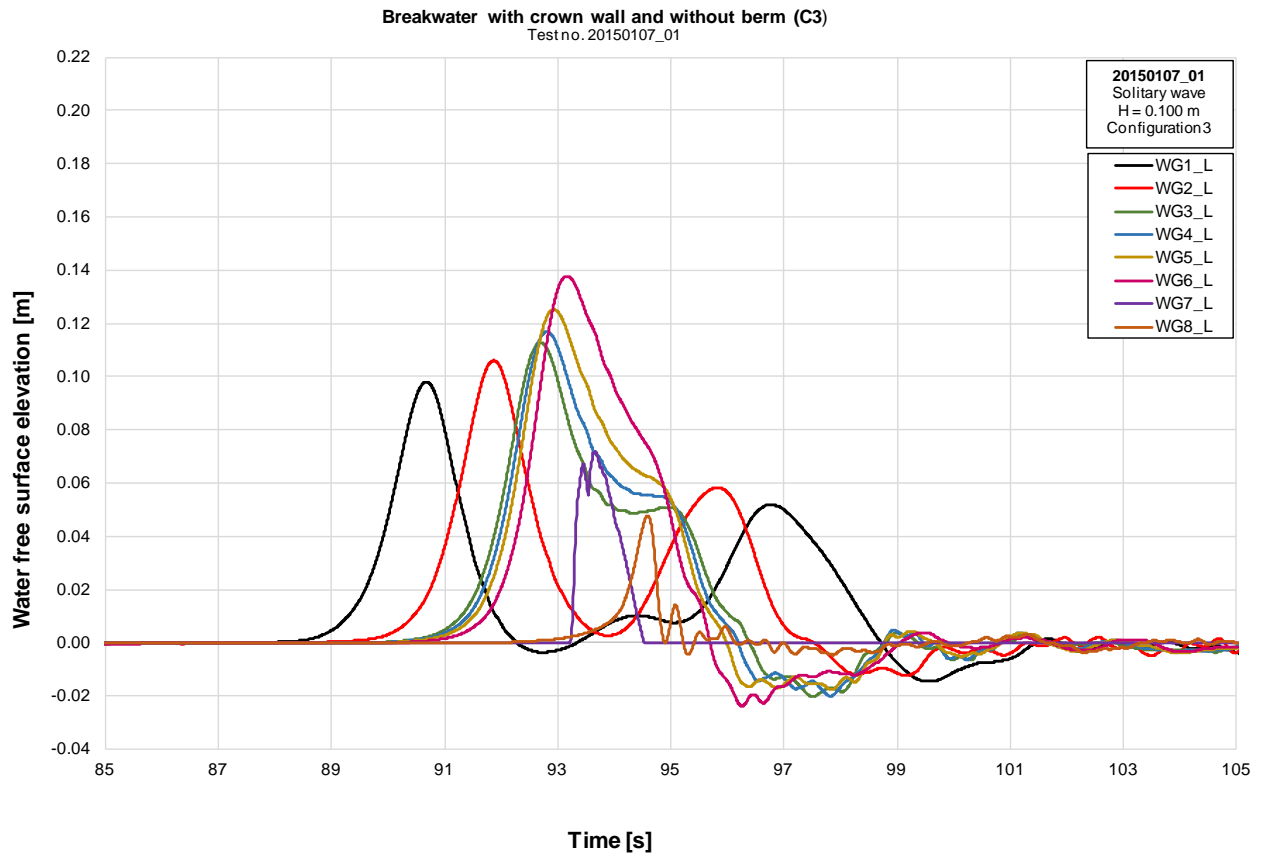


Figure A 25: Solitary profiles for configuration 3 with $H=0.100$ m (Test 20150107_01)



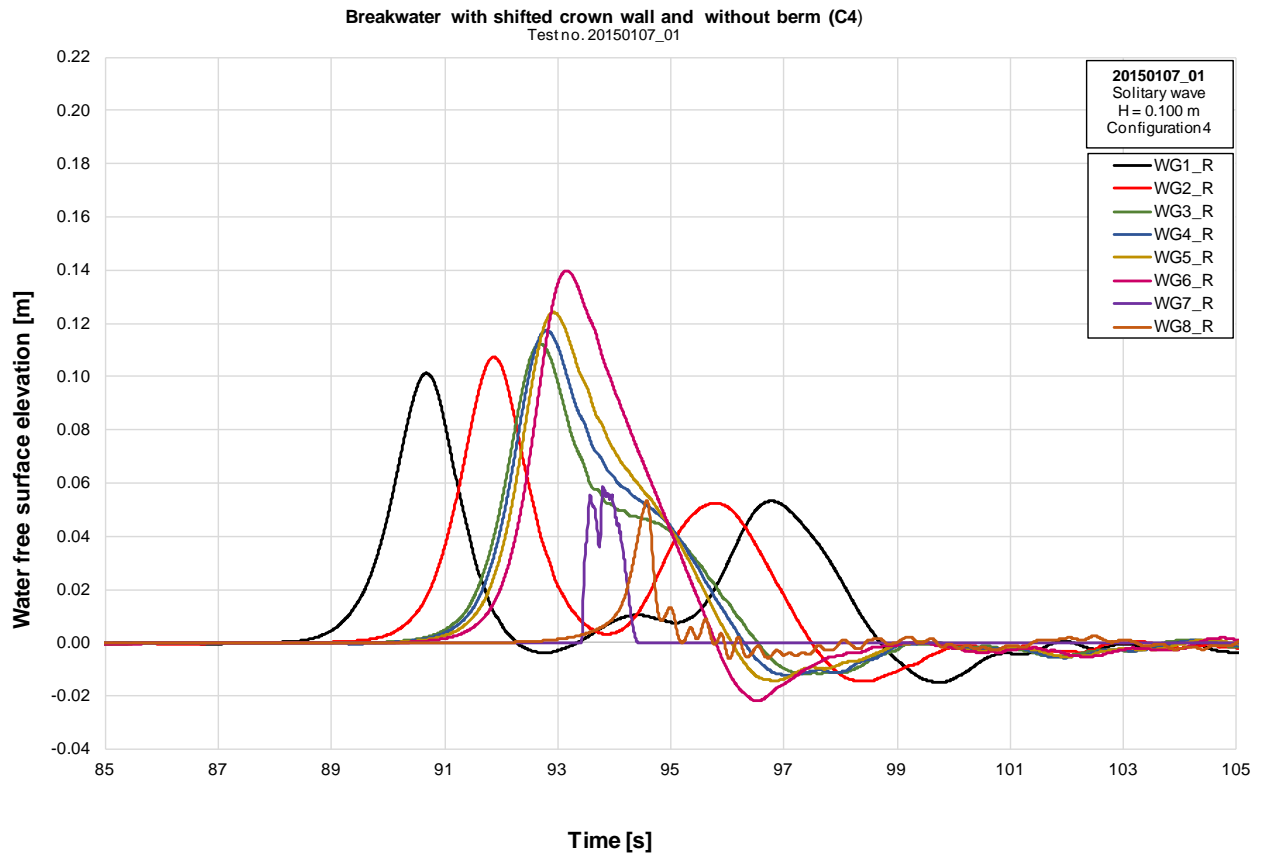


Figure A 26: Solitary profiles for configuration 4 with $H=0.100$ m (Test 20150107_01)



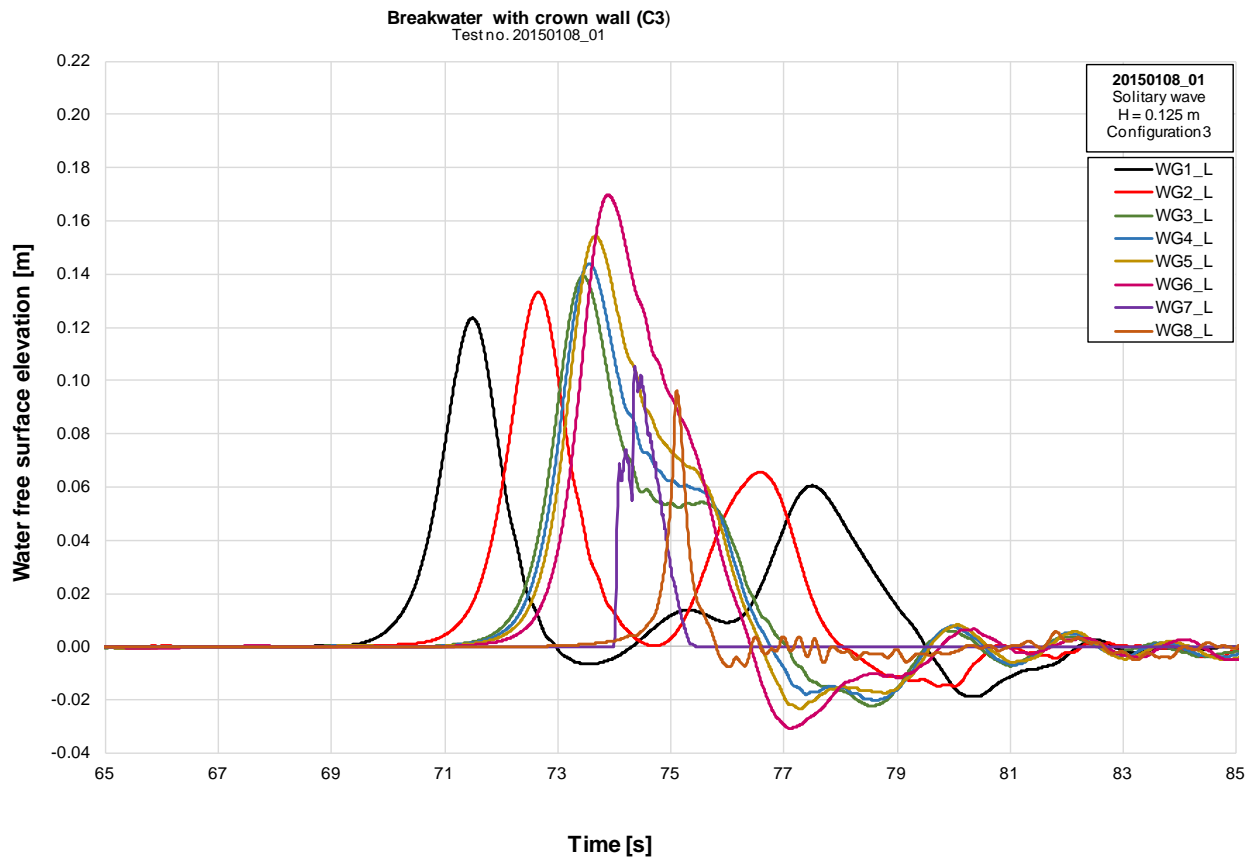


Figure A 27: Solitary profiles for configuration 3 with $H=0.125$ m (Test 20150108_01)



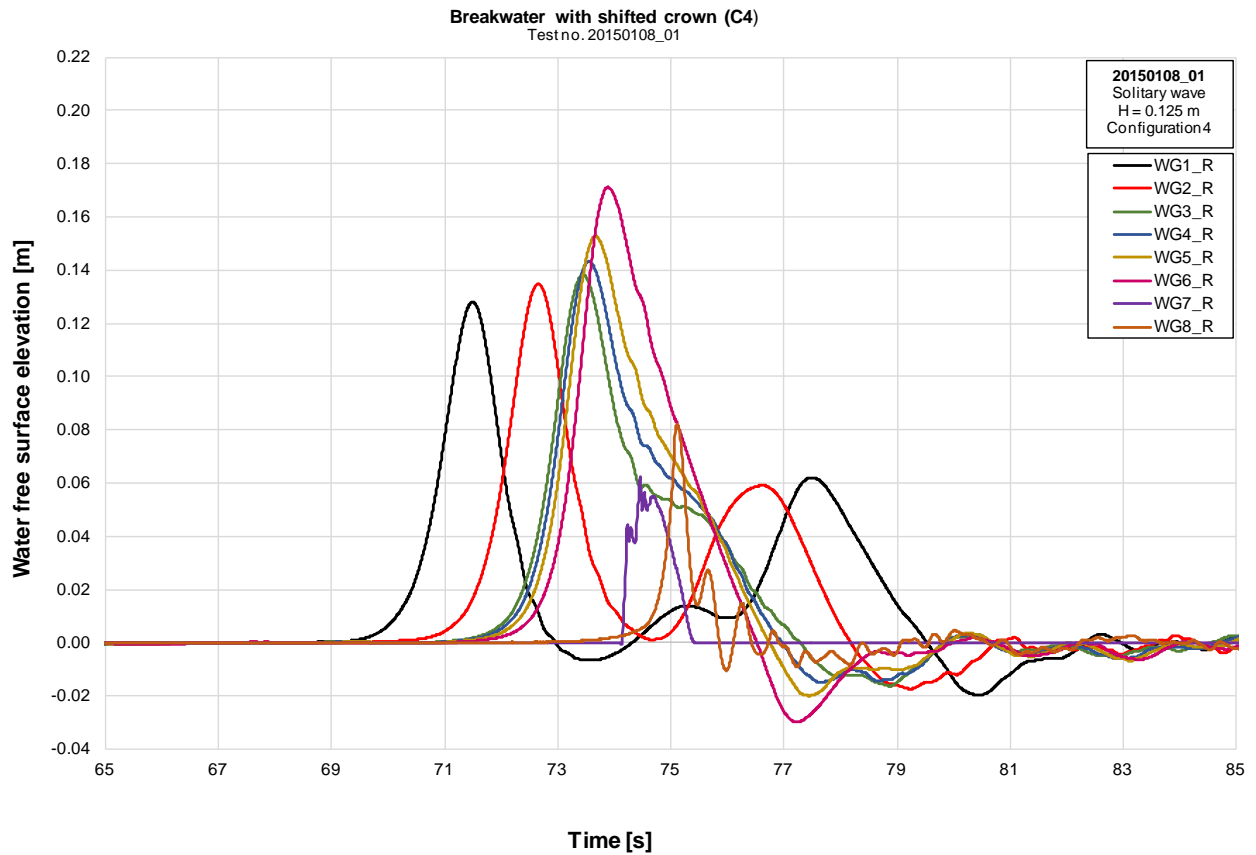


Figure A 28: Solitary profiles for configuration 4 with $H=0.125$ m (Test 20150108_01)



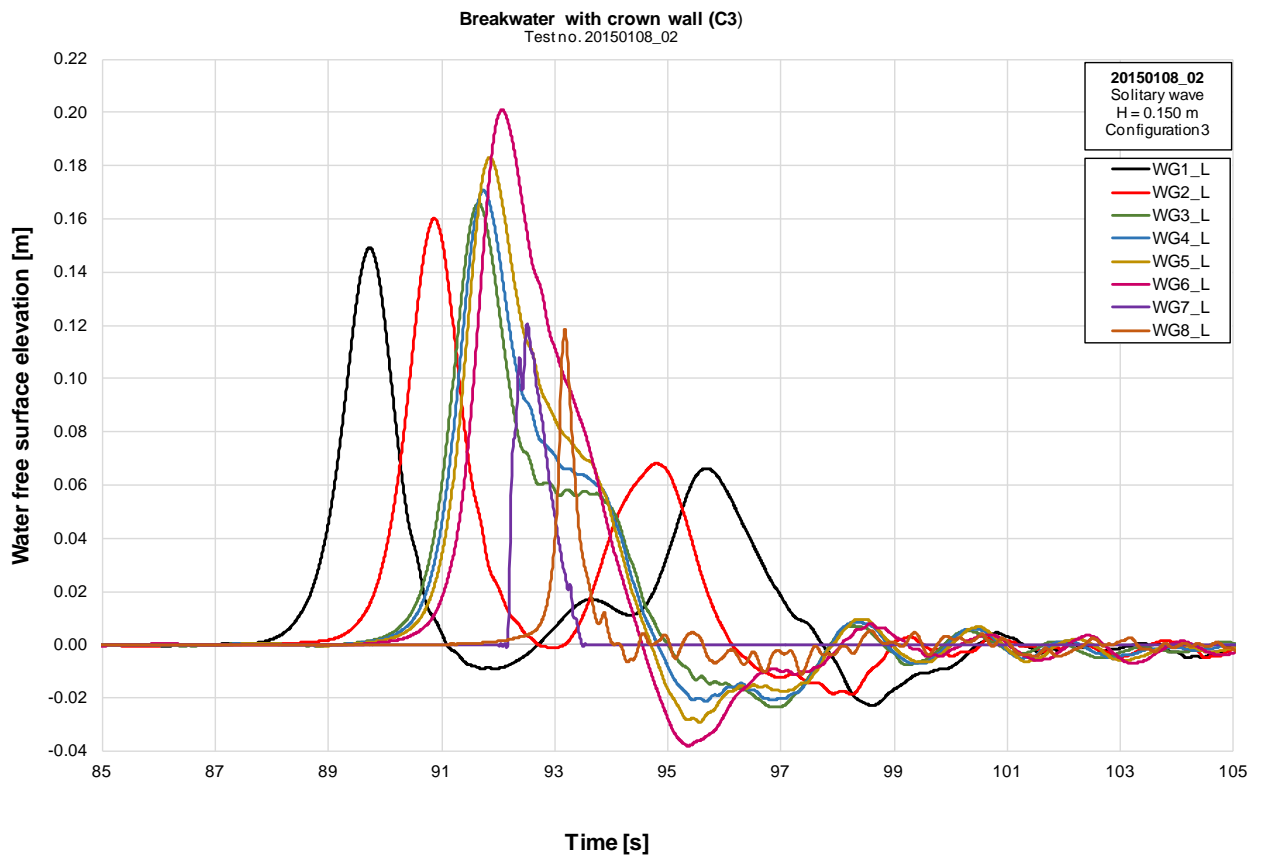


Figure A 29: Solitary profiles for configuration 3 with $H=0.150$ m (Test 20150108_02)



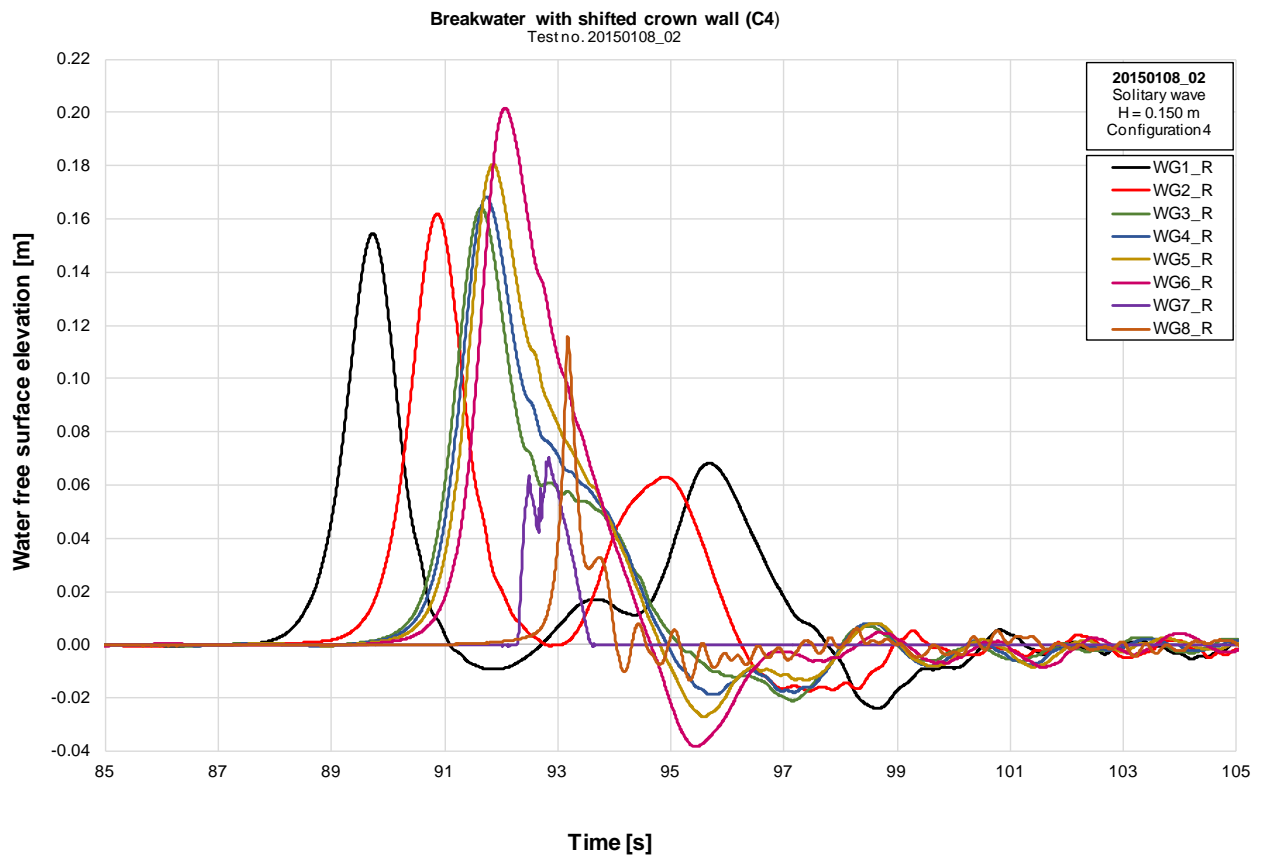


Figure A 30: Solitary profiles for configuration 4 with $H=0.150$ m (Test 20150108_02)



Appendix B

Pressure measurements in experiments at TU-BS



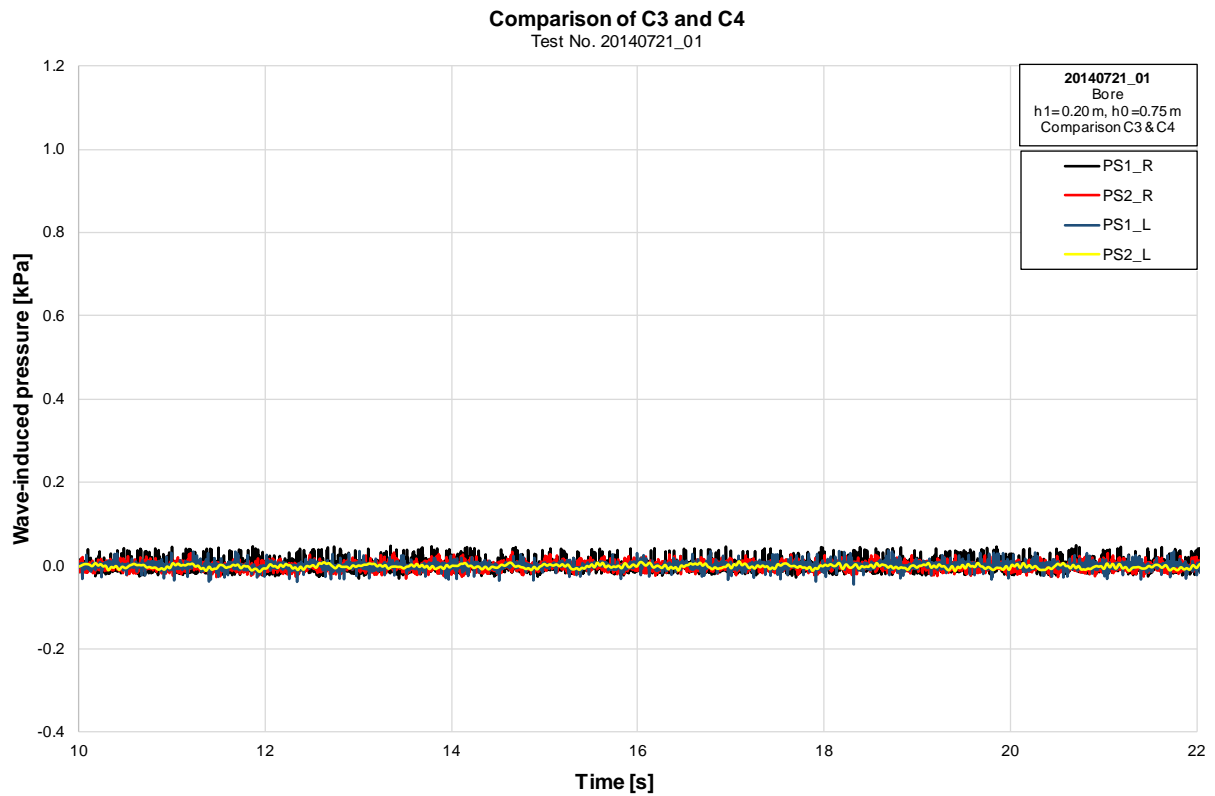


Figure B 1: Comparison of the tsunami bore-induced pressure for configurations 3 and 4 with $h_0=0.75\text{ m}$ and $h_1=0.20\text{ m}$ (Test 20140721_01)



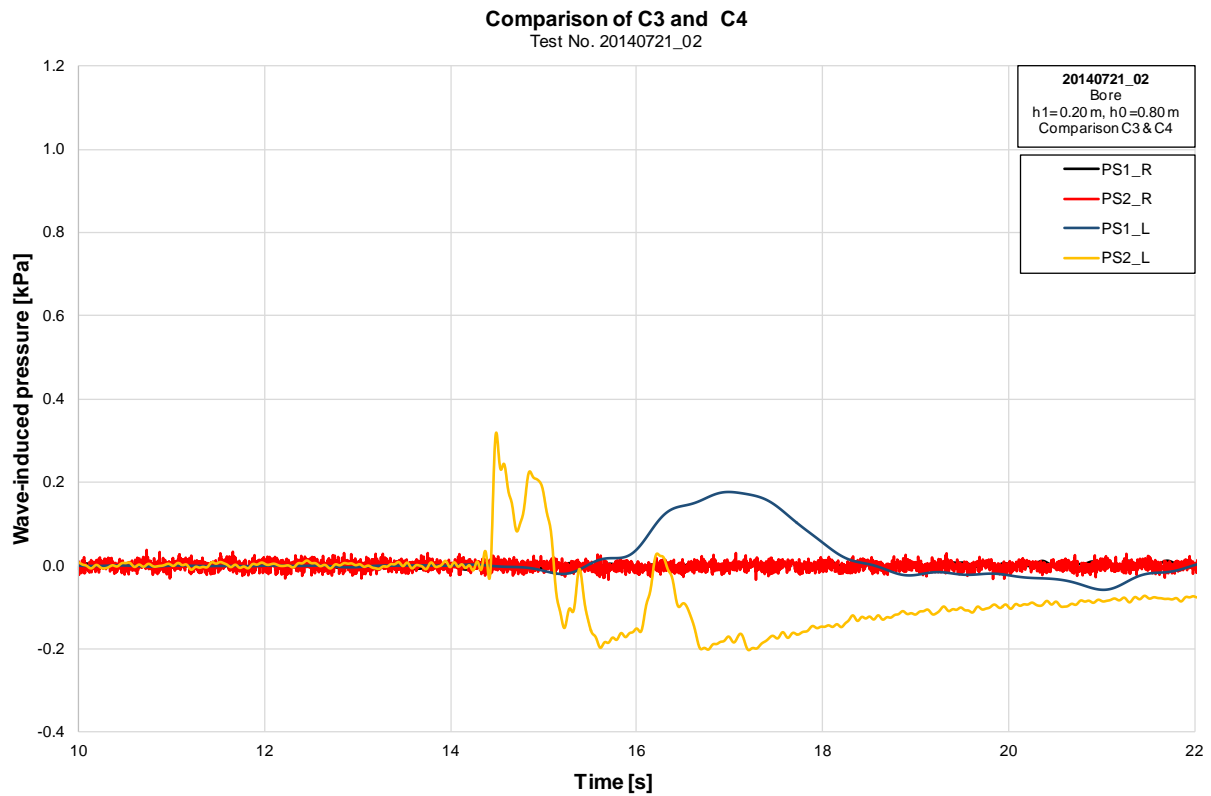


Figure B 2: Comparison of the tsunami bore-induced pressure for configurations 3 and 4 with $h_0=0.80\text{ m}$ and $h_1=0.20\text{ m}$ (Test 20140721_02)



Comparison of C3 and C4
Test No. 20140721_03

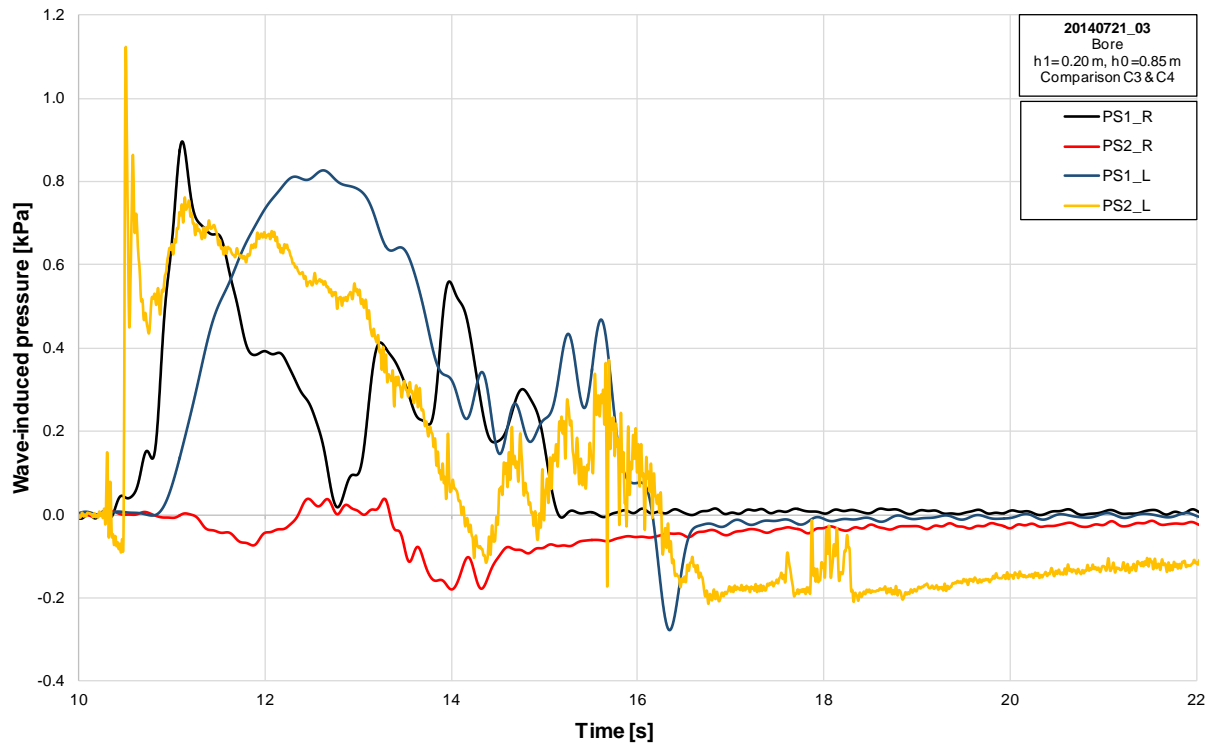


Figure B 3: Comparison of the tsunami bore-induced pressure for configurations 3 and 4 with $h_0=0.85\text{ m}$ and $h_1=0.20\text{ m}$ (Test 20140721_03)



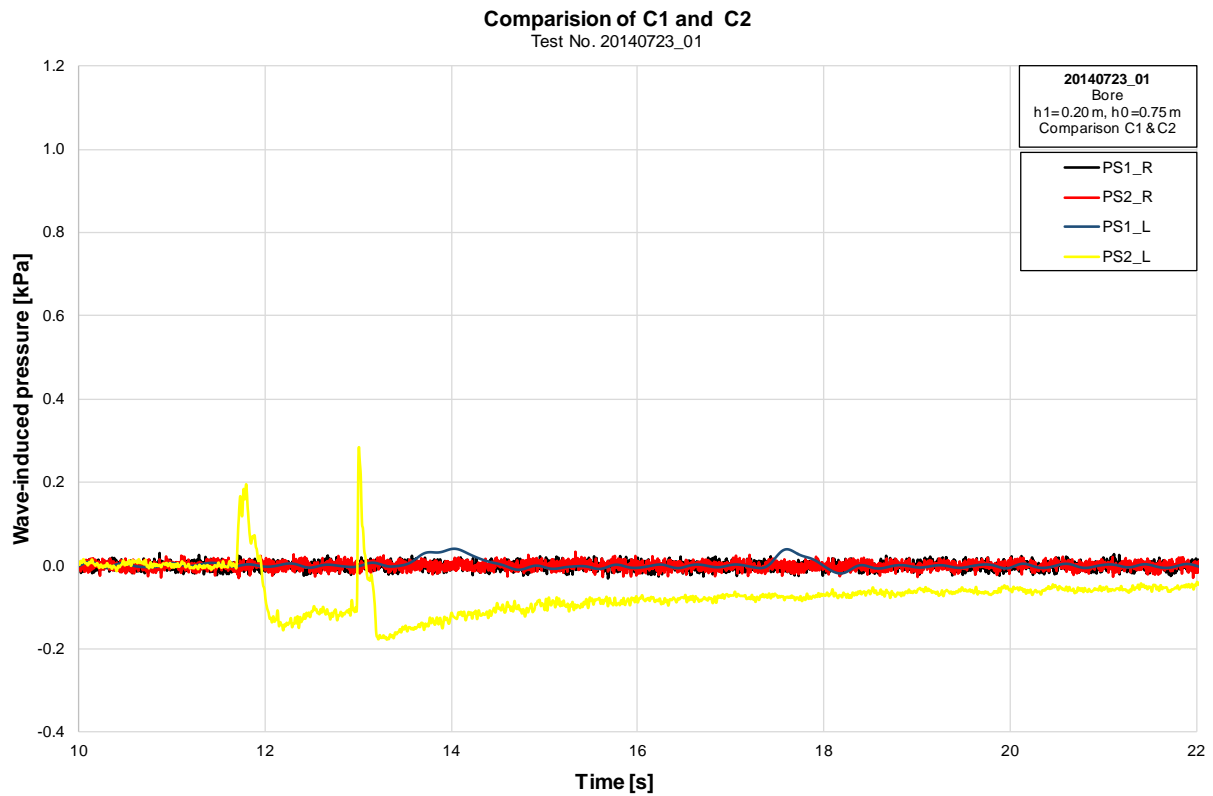


Figure B 4: Comparison of the tsunami bore-induced pressure for configurations 1 and 2 with $h_0=0.75\text{ m}$ and $h_1=0.20\text{ m}$ (Test 20140723_01) (in configuration 2 no pressure sensors were installed)



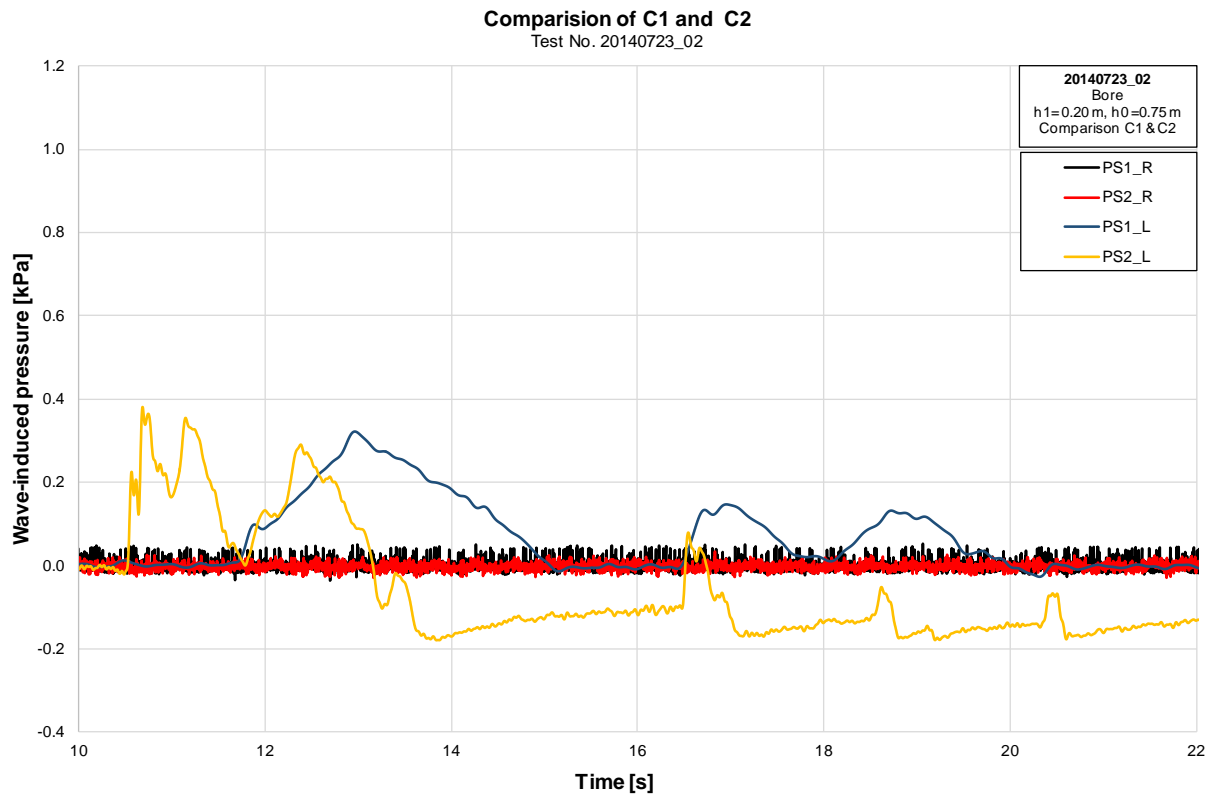


Figure B 5: Comparison of the tsunami bore-induced pressure for configurations 1 and 2 with $h_0=0.80\text{ m}$ and $h_1=0.20\text{ m}$ (Test 20140723_02) (in configuration 2 no pressure sensors were installed)

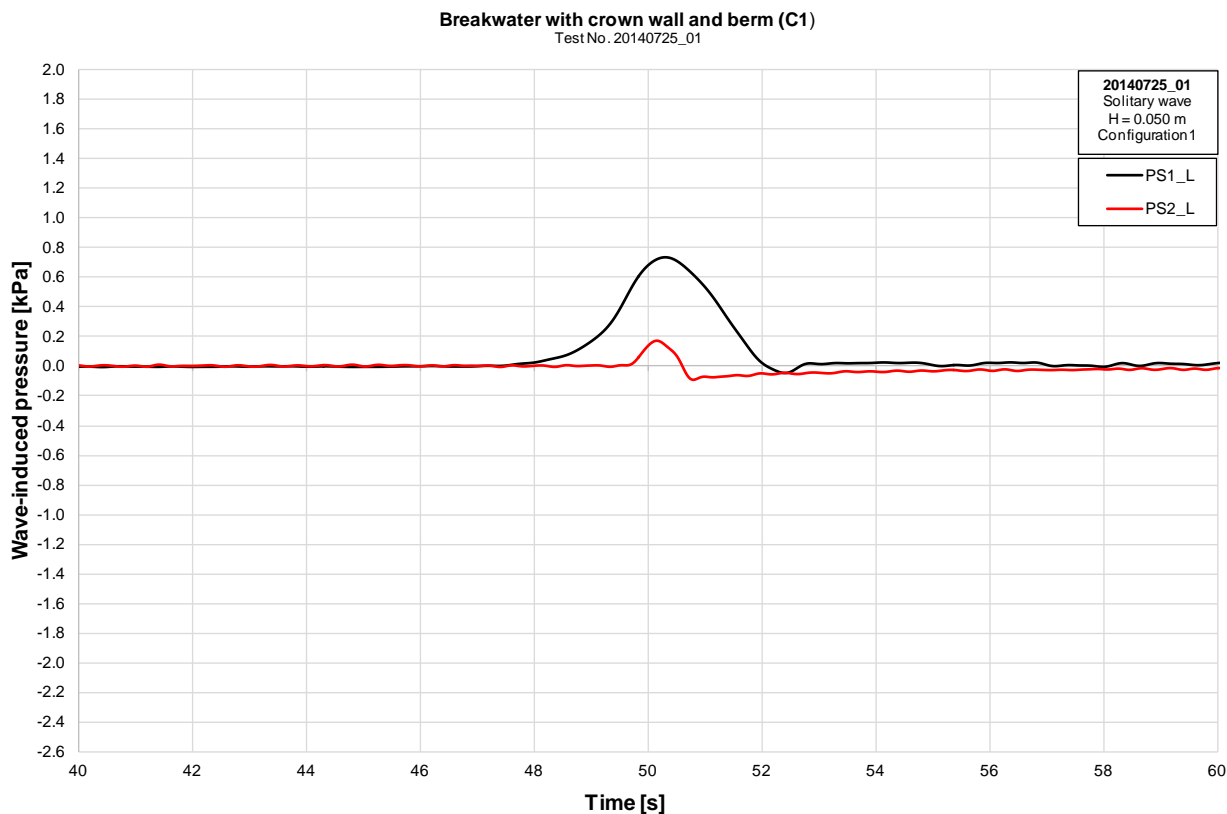


Figure B 6: Comparison of the solitary wave-induced pressure for configurations 1 and 2 with $H=0.050$ m (Test 20140725_01) (in configuration 2 no pressure sensors were installed)



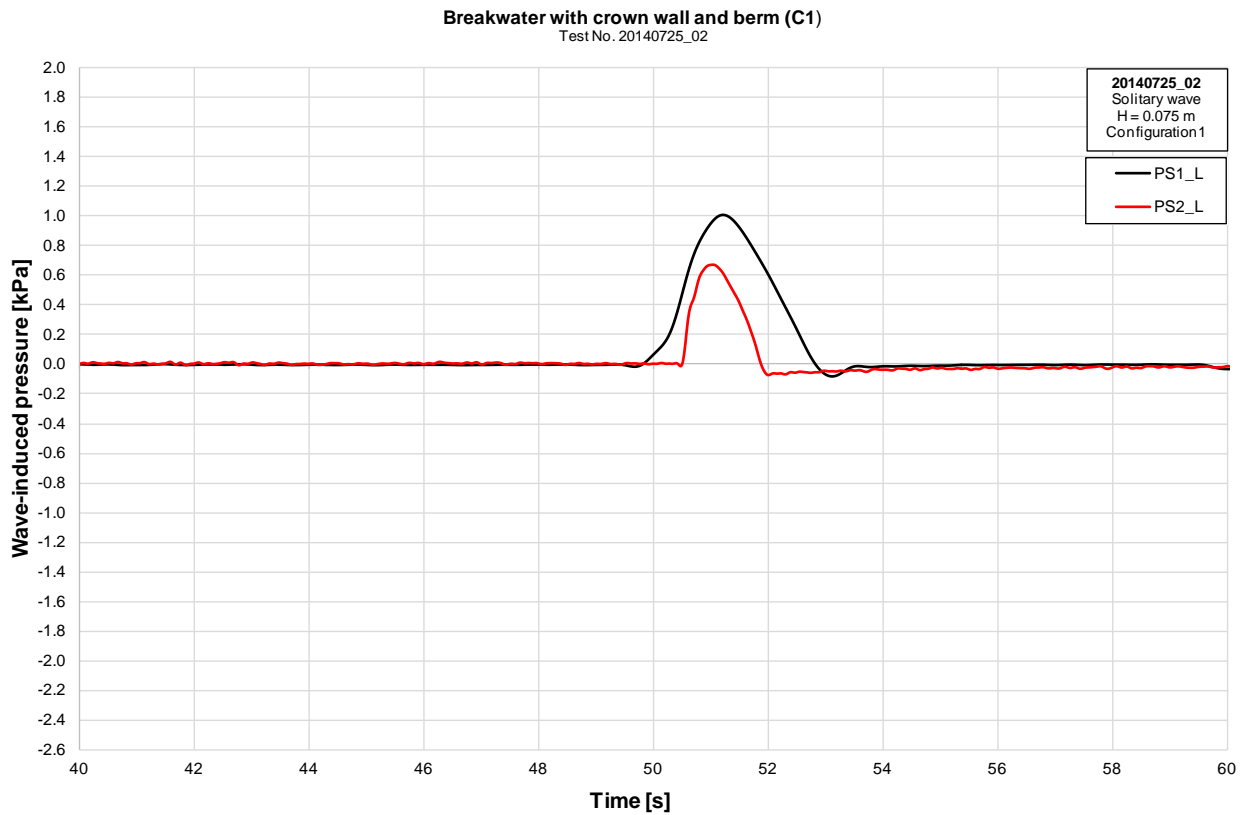


Figure B 7: Comparison of the solitary wave-induced pressure for configurations 1 and 2 with $H=0.075$ m (Test 20140725_02) (in configuration 2 no pressure sensors were installed)



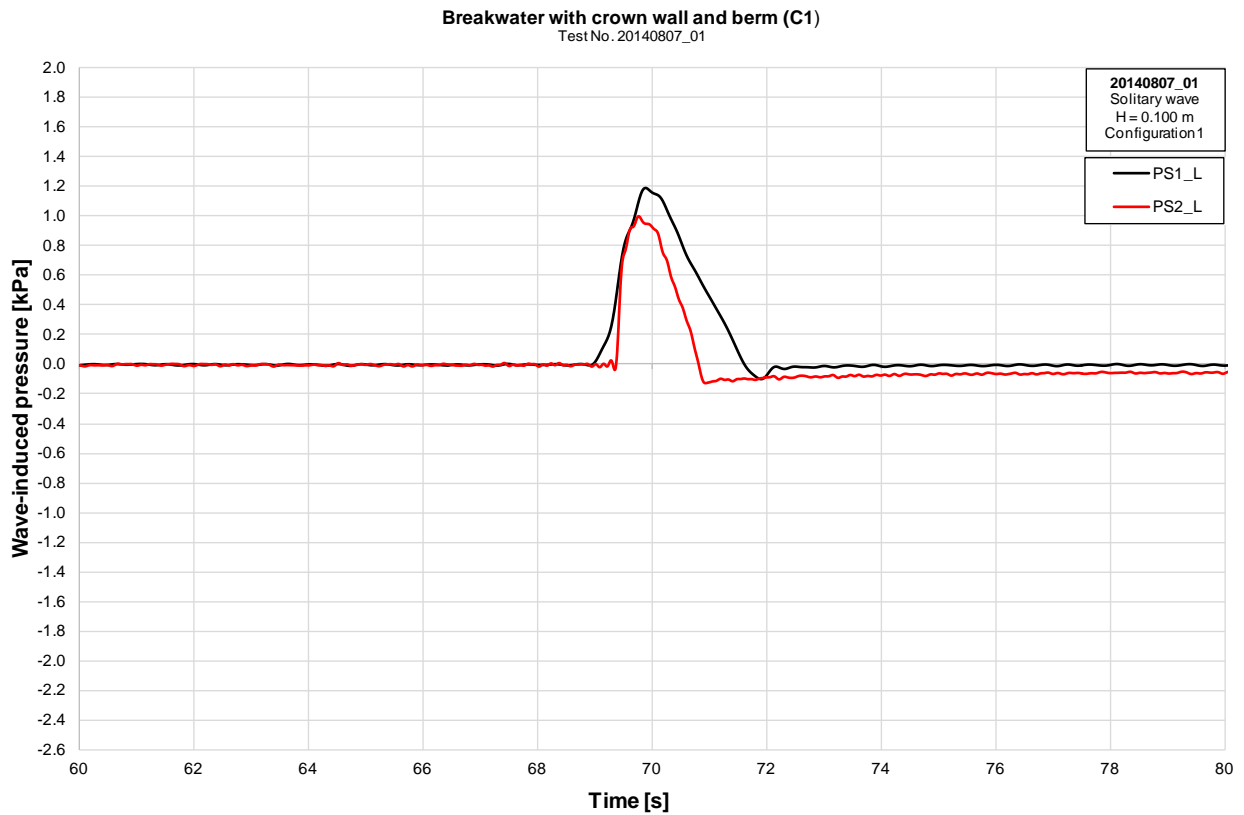


Figure B 8: Comparison of the solitary wave-induced pressure for configurations 1 and 2 with $H=0.100$ m (Test 20140807_01) (in configuration 2 no pressure sensors were installed)



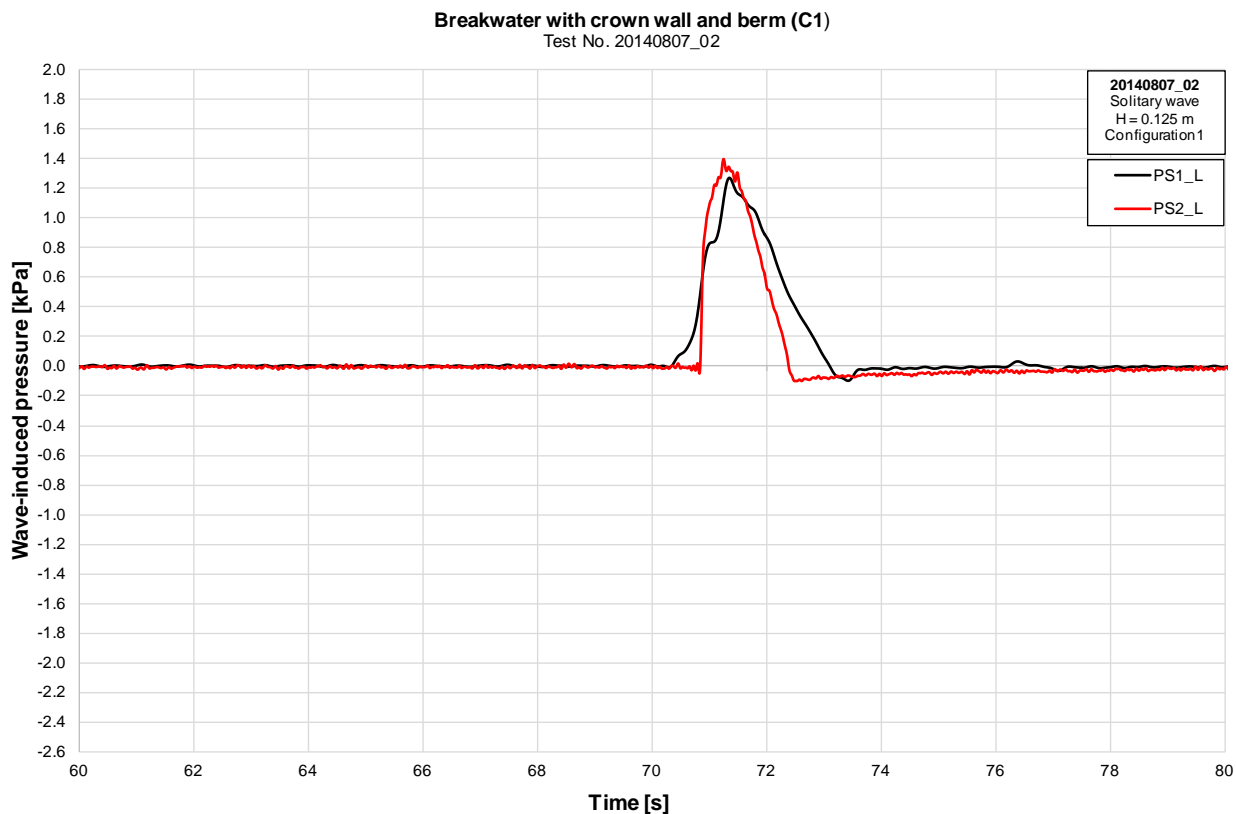


Figure B 9: Comparison of the solitary wave-induced pressure for configurations 1 and 2 with $H=0.125$ m (Test 20140807_02) (in configuration 2 no pressure sensors were installed)

NGI

PARI



CONCERT JAPAN
Connecting and Coordinating
European Research and Technology Development with Japan

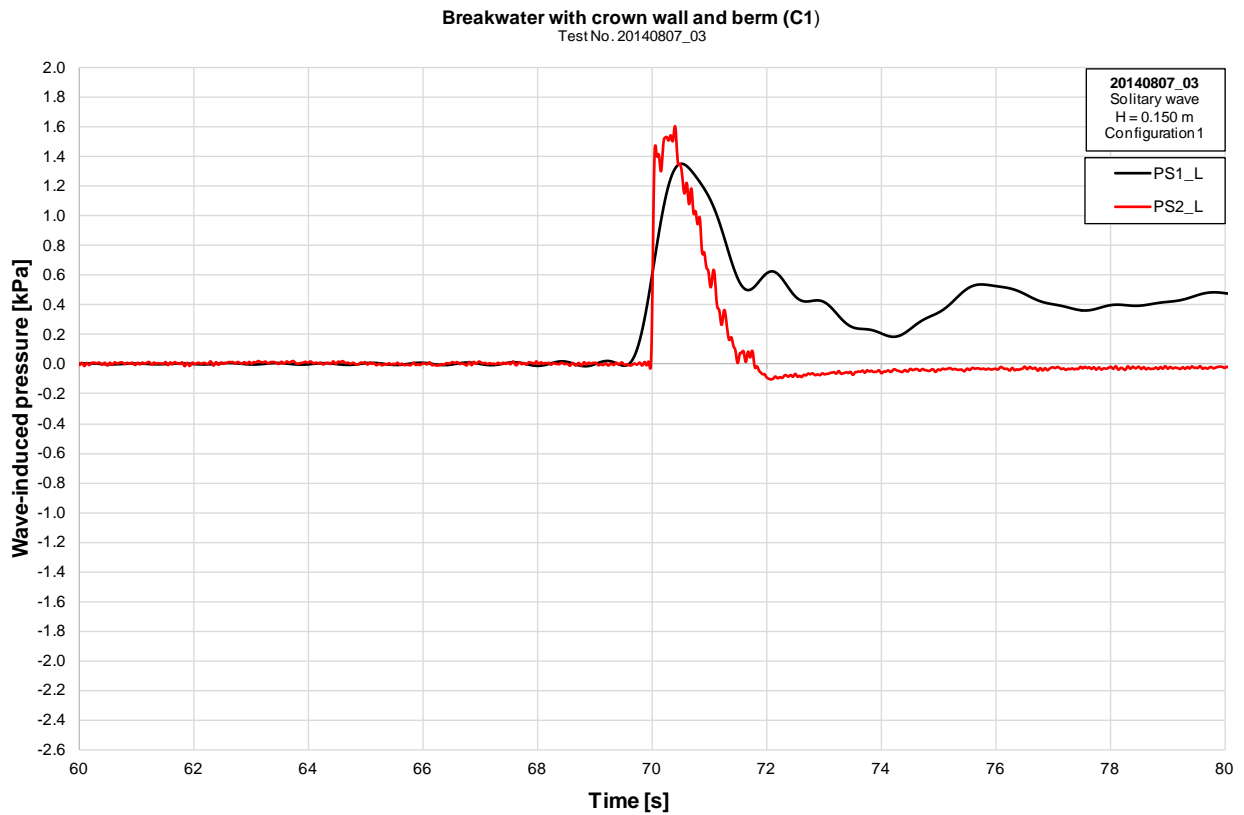


Figure B 10: Comparison of the solitary wave-induced pressure for configurations 1 and 2 with $H=0.150$ m (Test 20140807_03) (in configuration 2 no pressure sensors were installed)



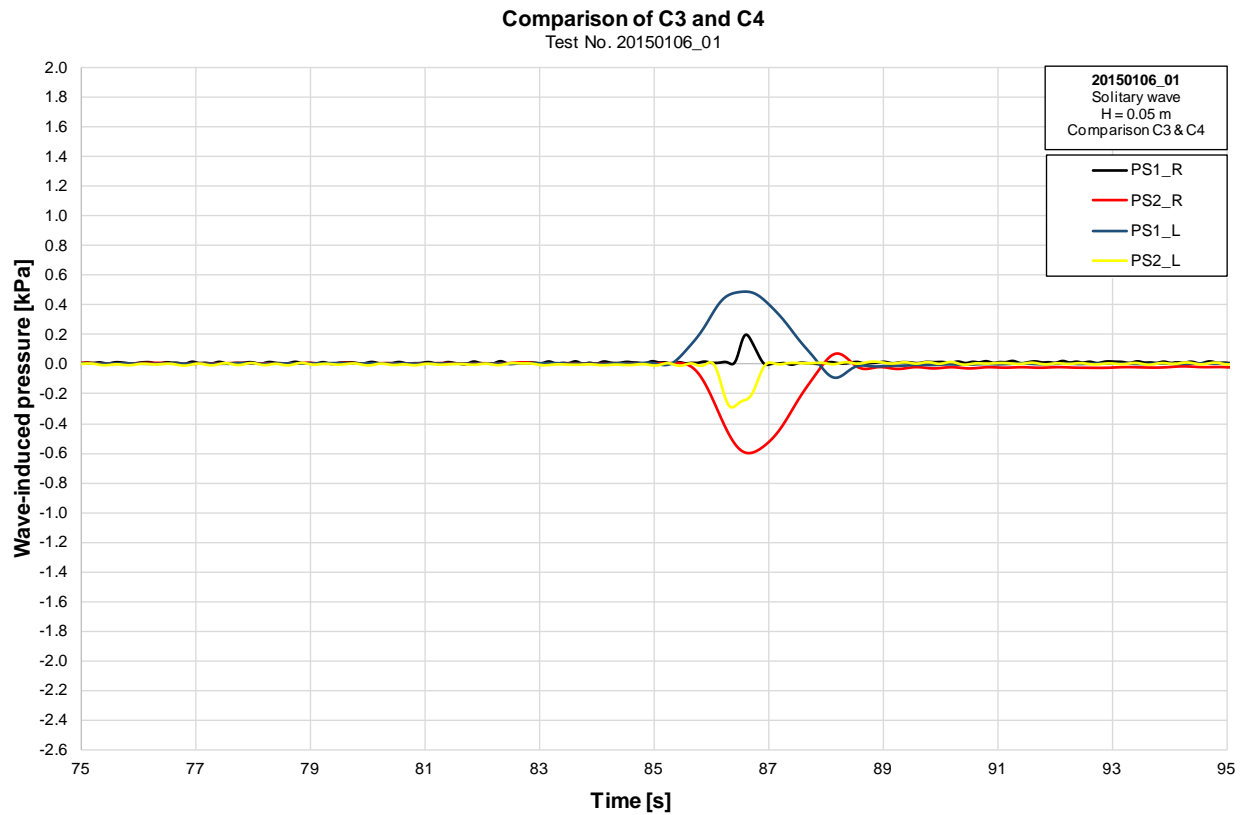


Figure A 31: Comparison of the solitary wave-induced pressure for configurations 3 and 4 with $H=0.050$ m (Test 20150106_01)



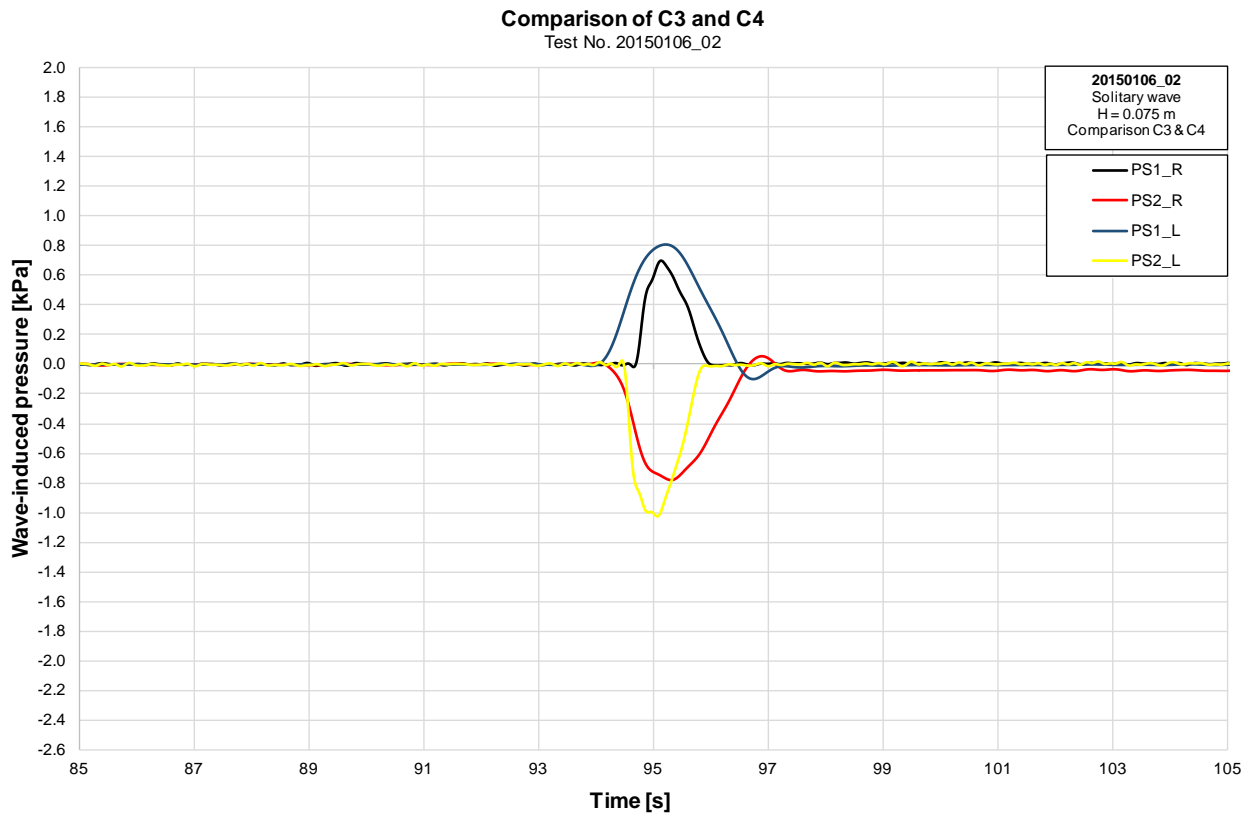


Figure A 32: Comparison of the solitary wave-induced pressure for configurations 3 and 4 with $H=0.075$ m (Test 20150106_02)



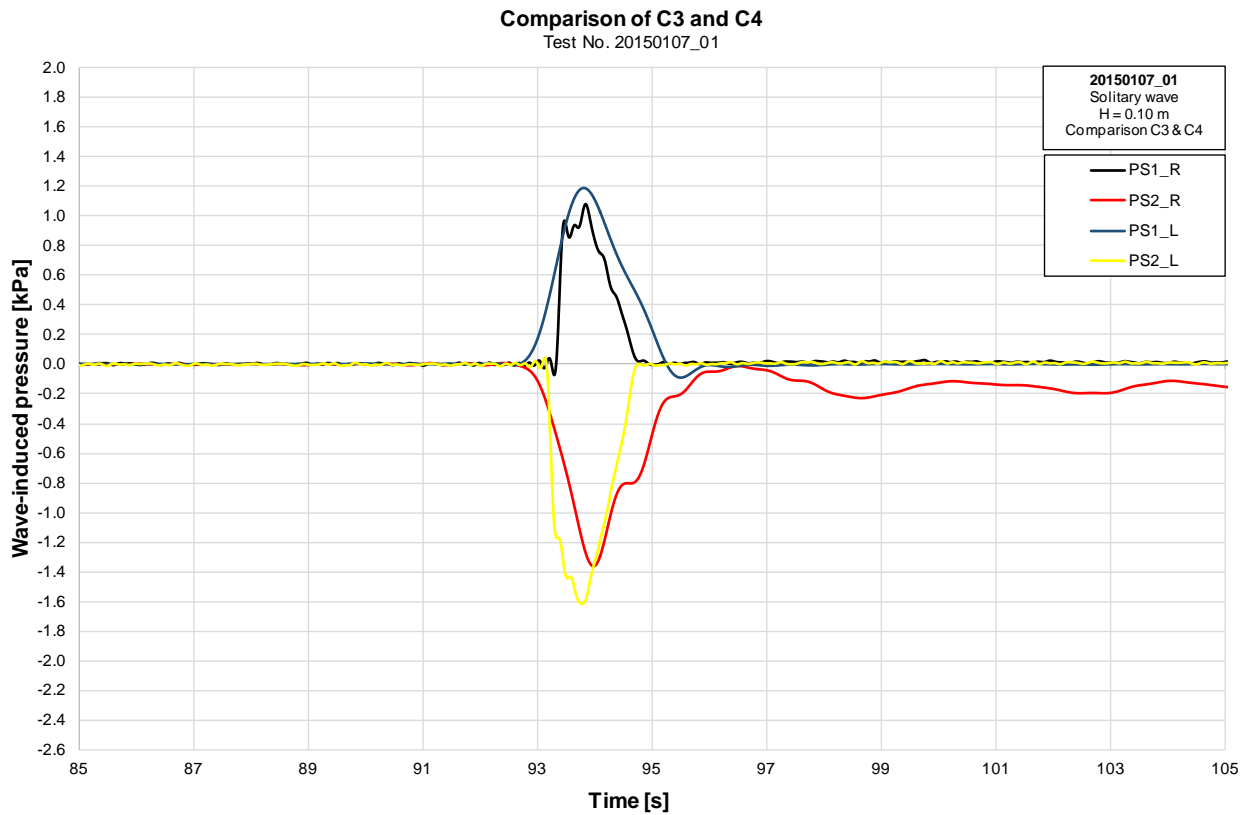


Figure A 33: Comparison of the solitary wave-induced pressure for configurations 3 and 4 with $H=0.100$ m (Test 20150107_01)



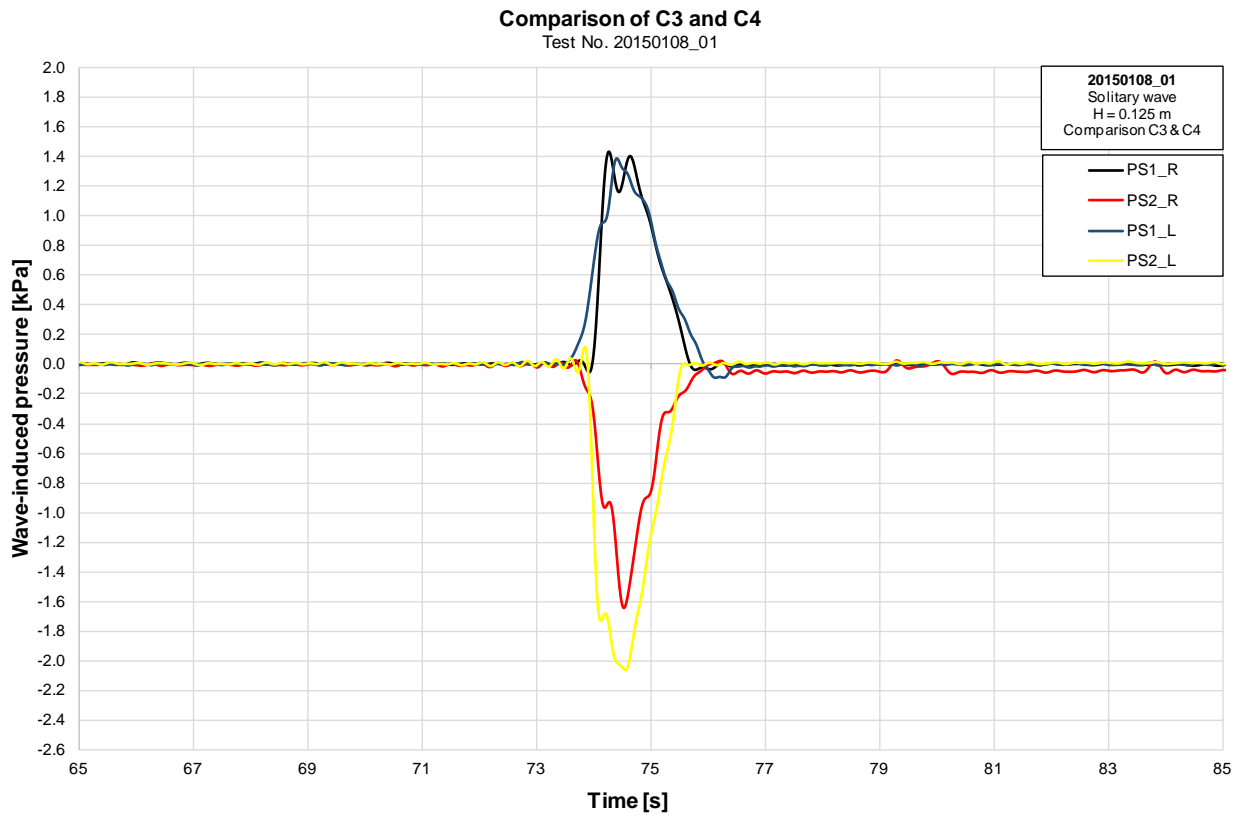


Figure A 34: Comparison of the solitary wave-induced pressure for configurations 3 and 4 with $H=0.125$ m (Test 20150108_01)



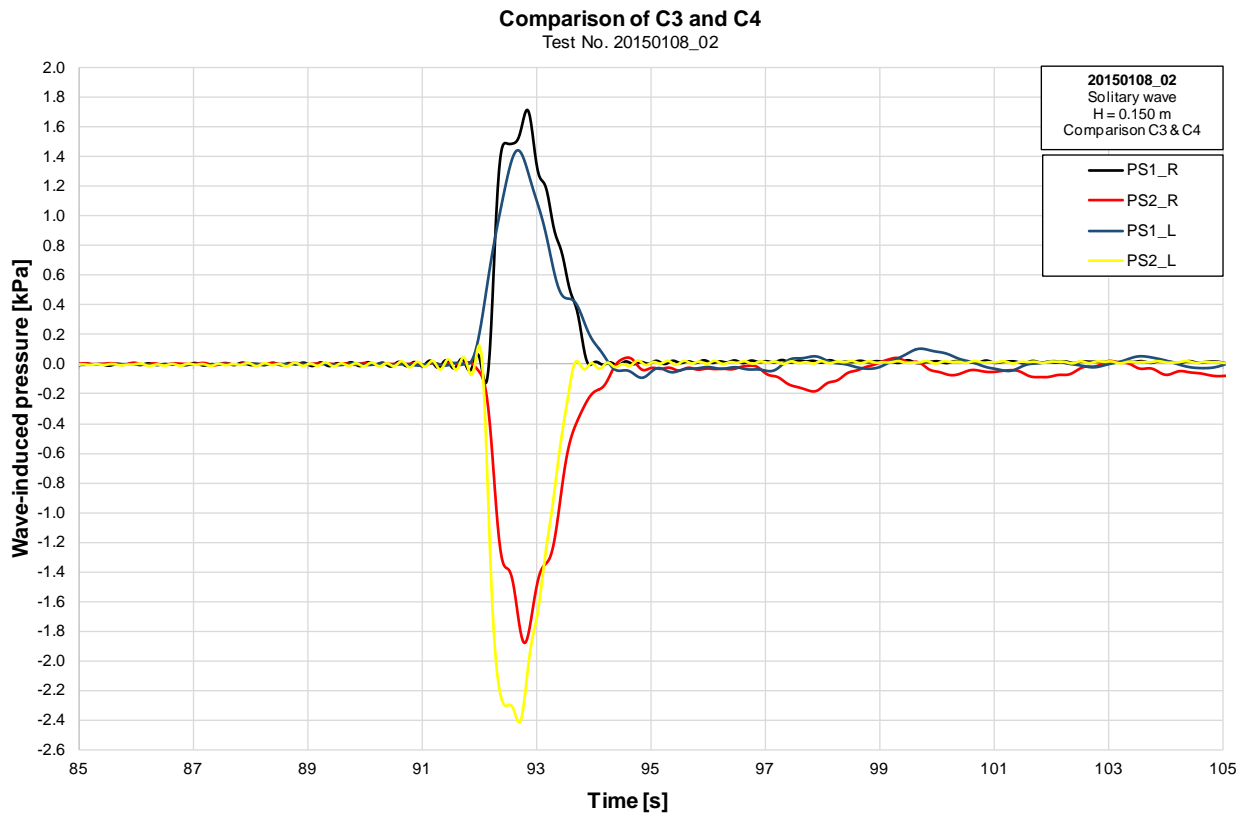


Figure A 35: Comparison of the solitary wave-induced pressure for configurations 3 and 4 with $H=0.150$ m (Test 20150108_02)



Appendix C

Flow velocity measurements in experiments at TU-BS



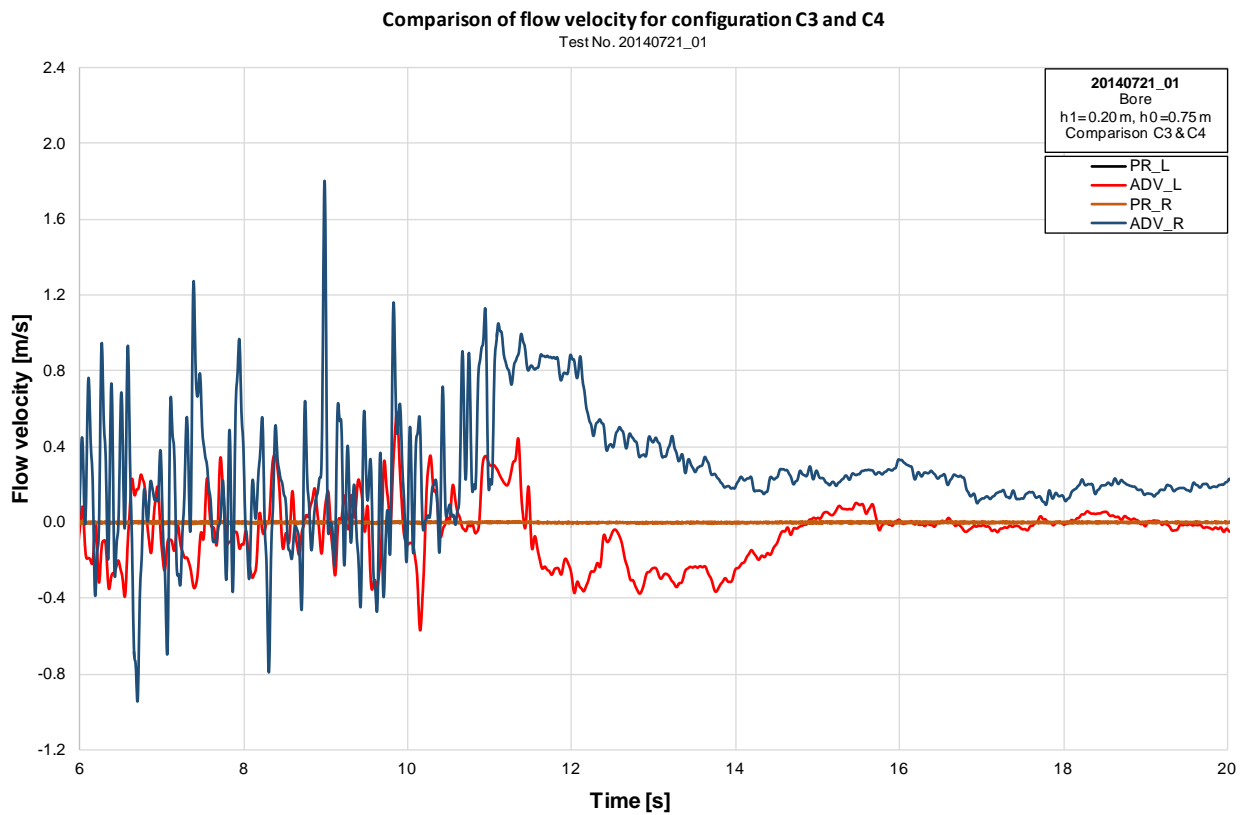


Figure C 1: Flow velocity under tsunami bore with $h_0=0.75\text{ m}$ and $h_1=0.20\text{ m}$ for configurations 3 and 4 (Test 20140721_01)



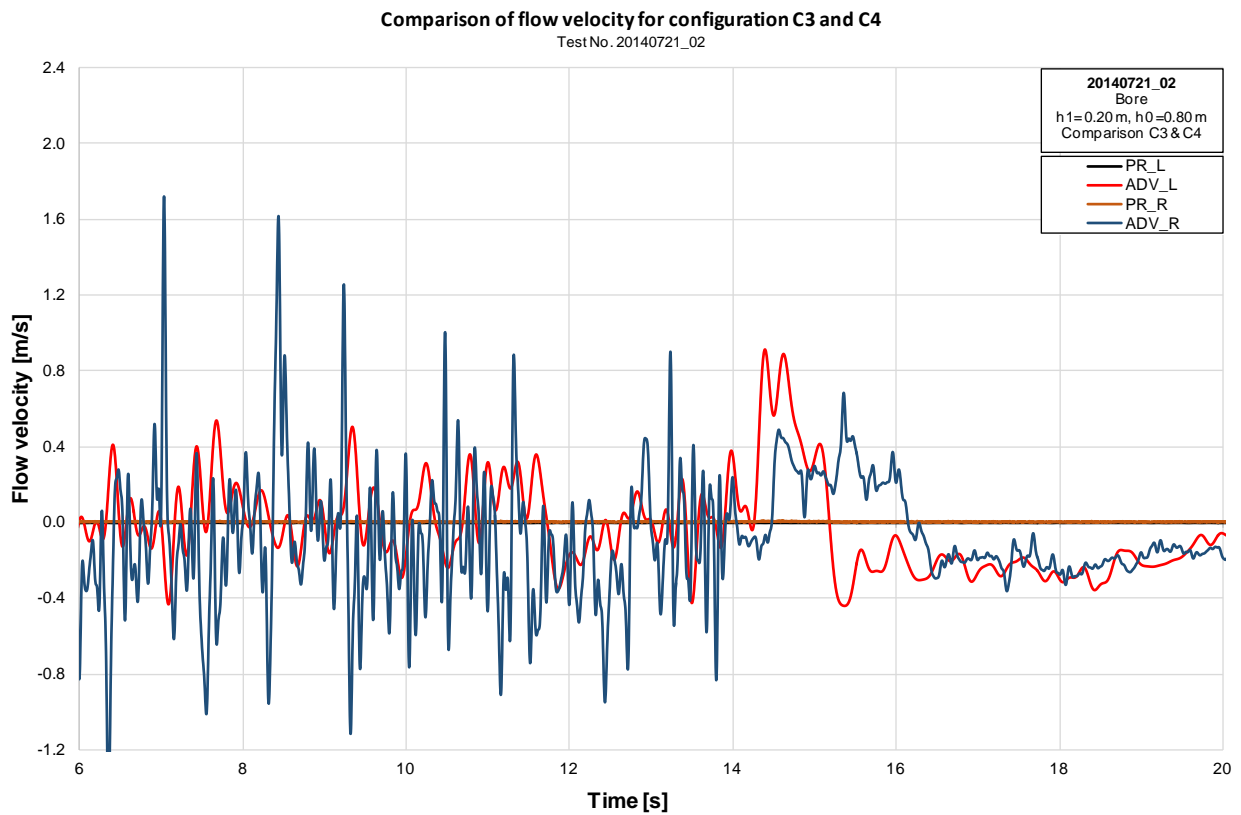


Figure C 2: Flow velocity under tsunami bore with $h_0=0.80\text{ m}$ and $h_1=0.20\text{ m}$ for configurations 3 and 4 (Test 20140721_02)



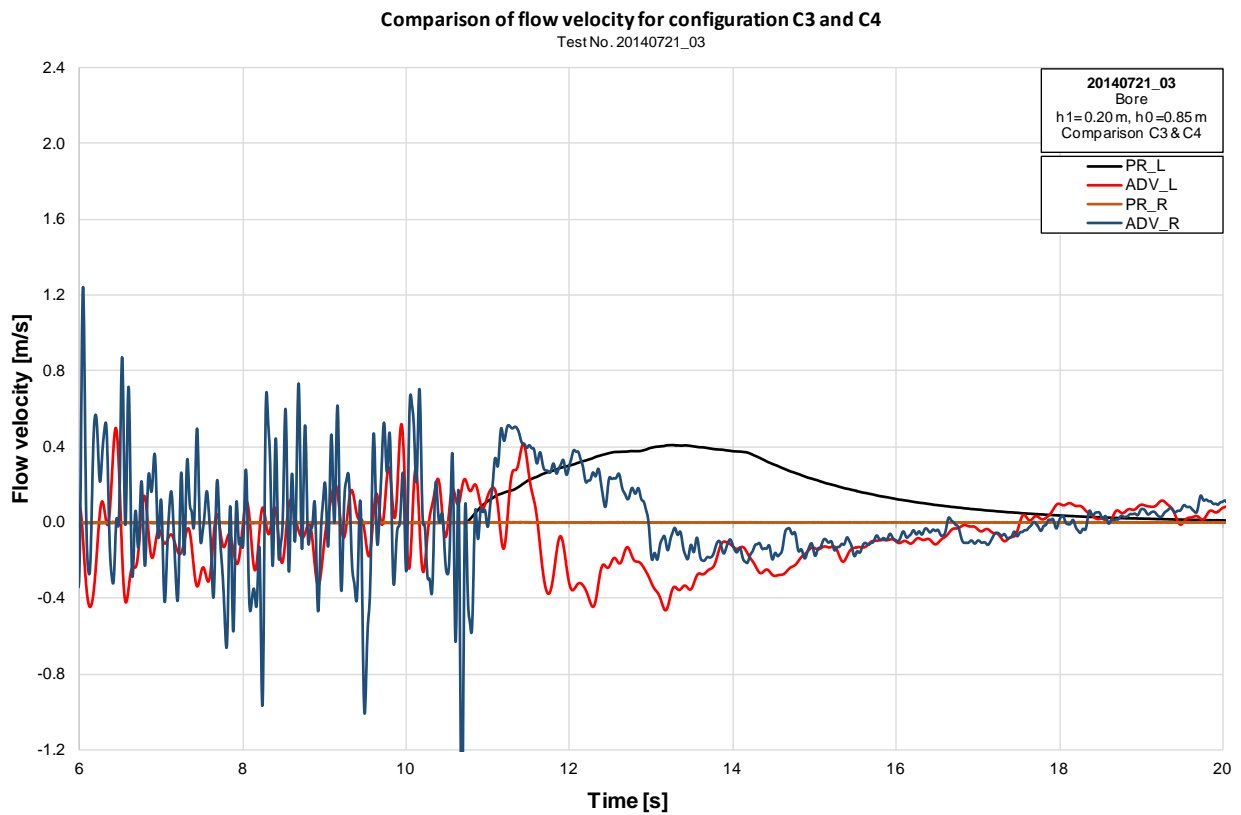


Figure C 3: Flow velocity under tsunami bore with $h_0=0.85\text{ m}$ and $h_1=0.20\text{ m}$ for configurations 3 and 4 (Test 20140721_03)



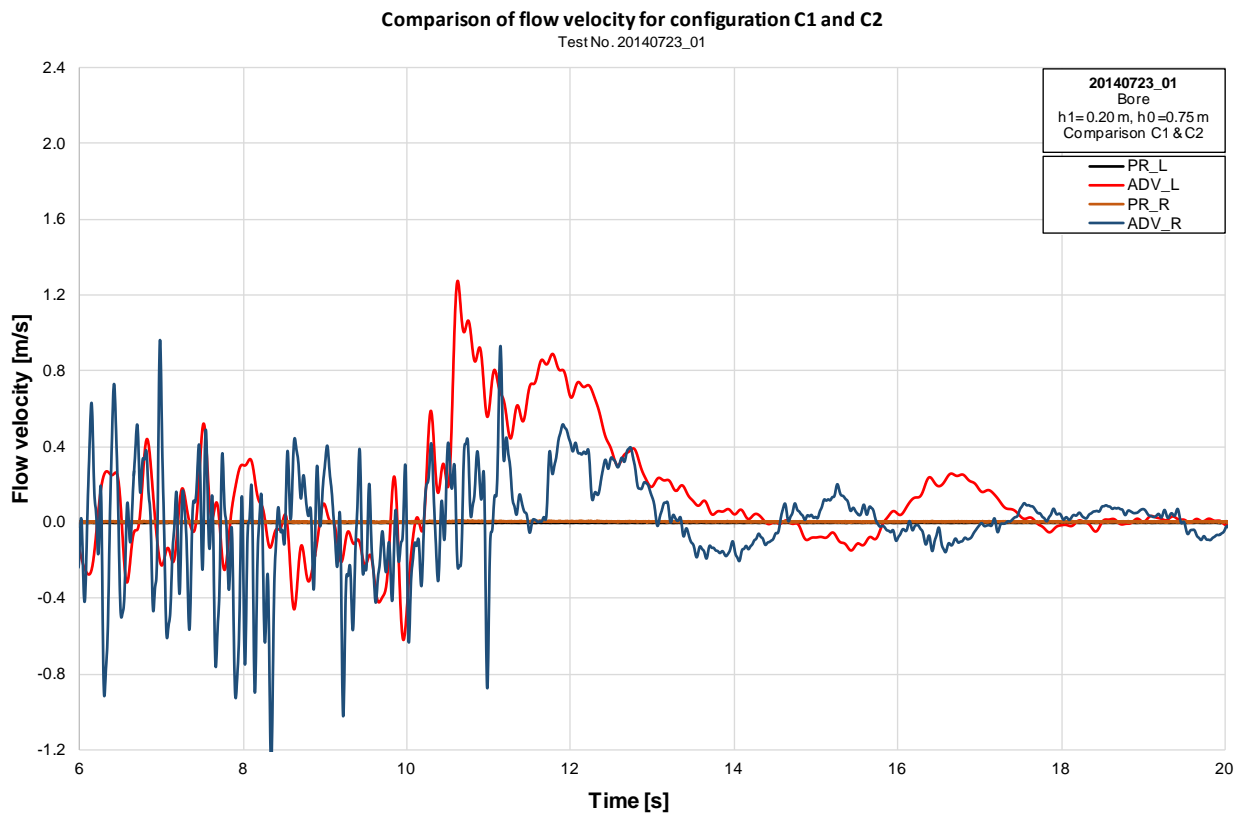


Figure C 4: Flow velocity under tsunami bore with $h_0=0.75\text{ m}$ and $h_1=0.20\text{ m}$ for configurations 1 and 2 (Test 20140723_01)



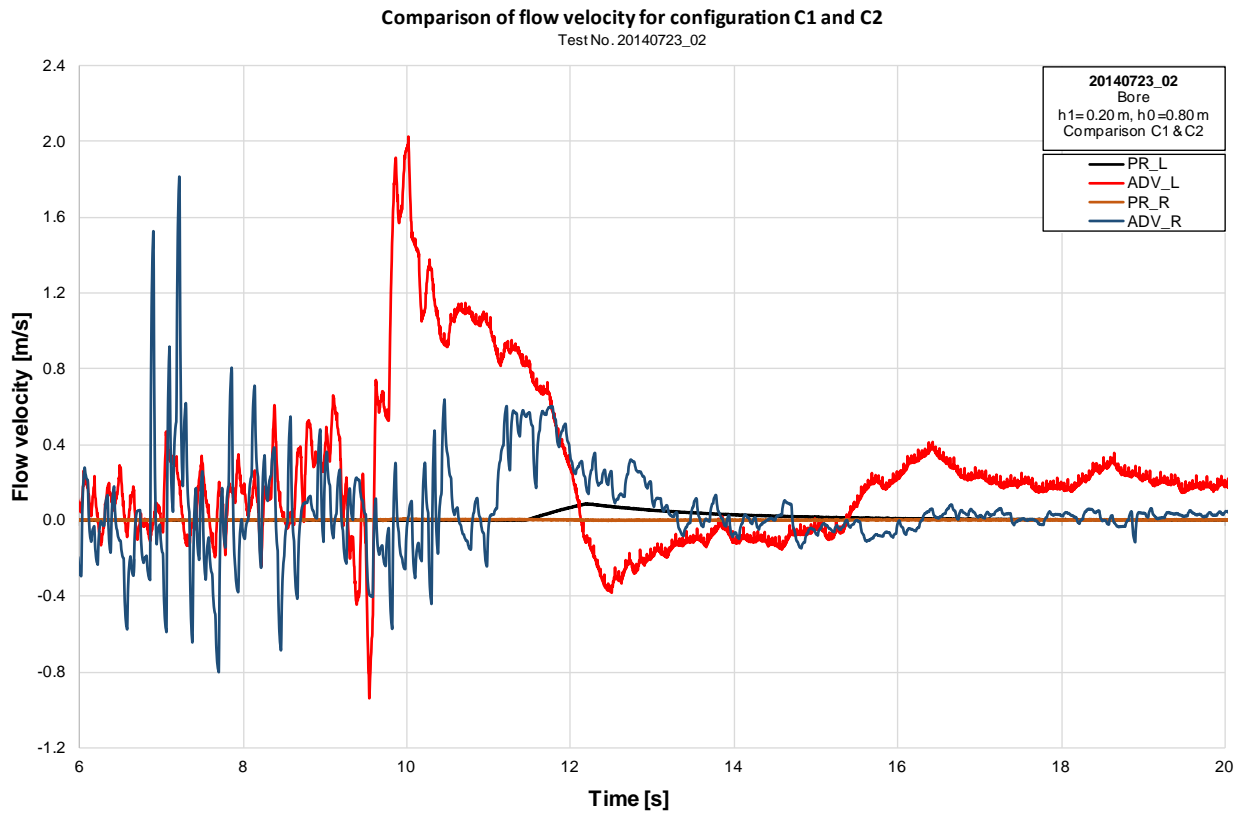


Figure C 5: Flow velocity under tsunami bore with $h_0=0.80$ m and $h_1=0.20$ m for configurations 1 and 2 (Test 20140723_02)



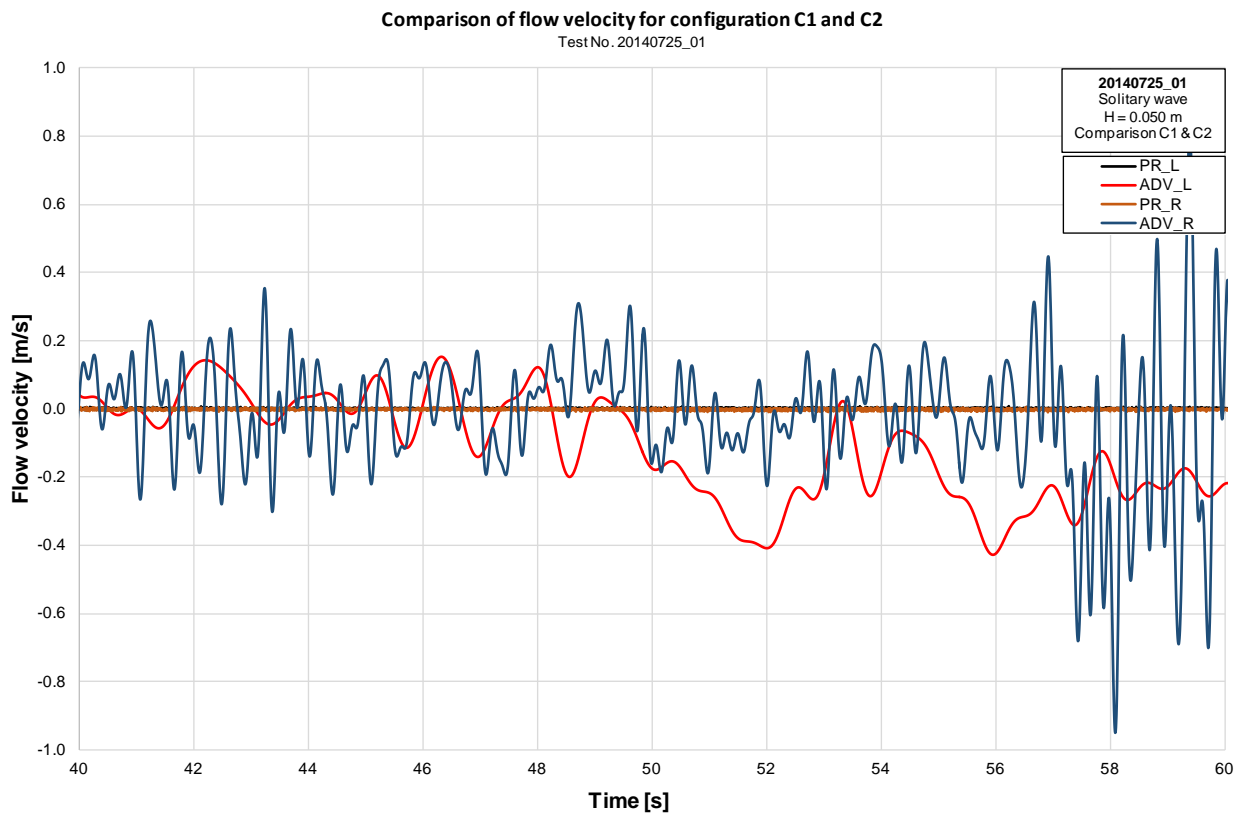


Figure C 6: Flow velocity under solitary wave with $H=0.050$ m for configurations 1 and 2 (Test 20140725_01)



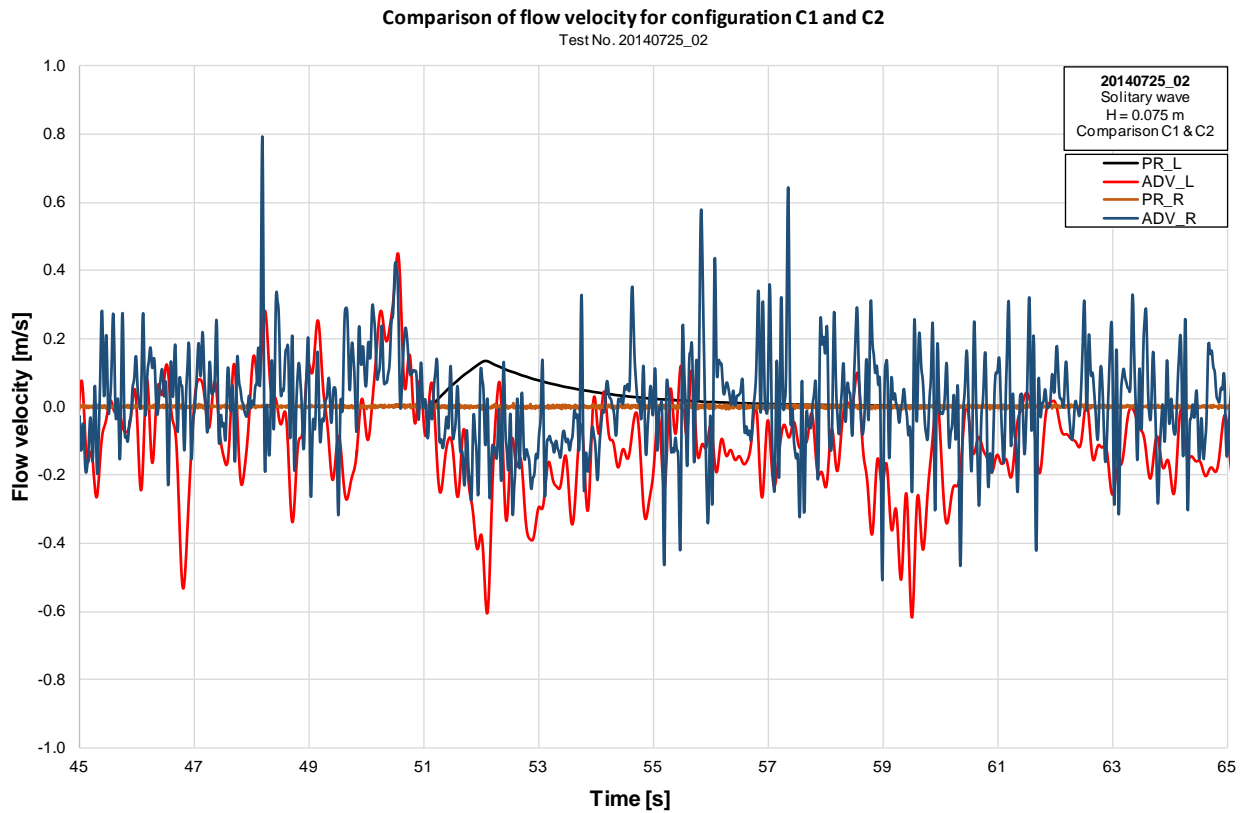


Figure C 7: Flow velocity under solitary wave with $H=0.075$ m for configurations 1 and 2 (Test 20140725_02)



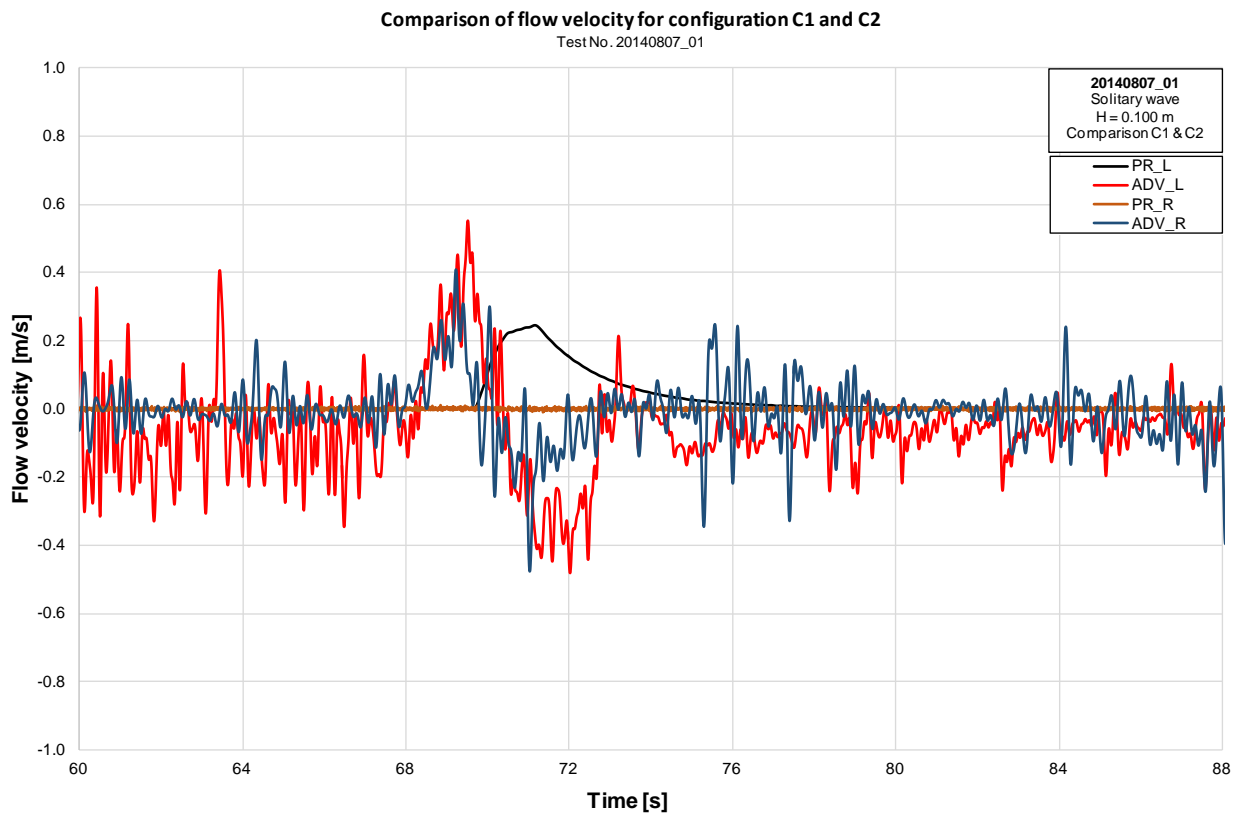


Figure C 8: Flow velocity under solitary wave with $H=0.100$ m for configurations 1 and 2 (Test 20140807_01)



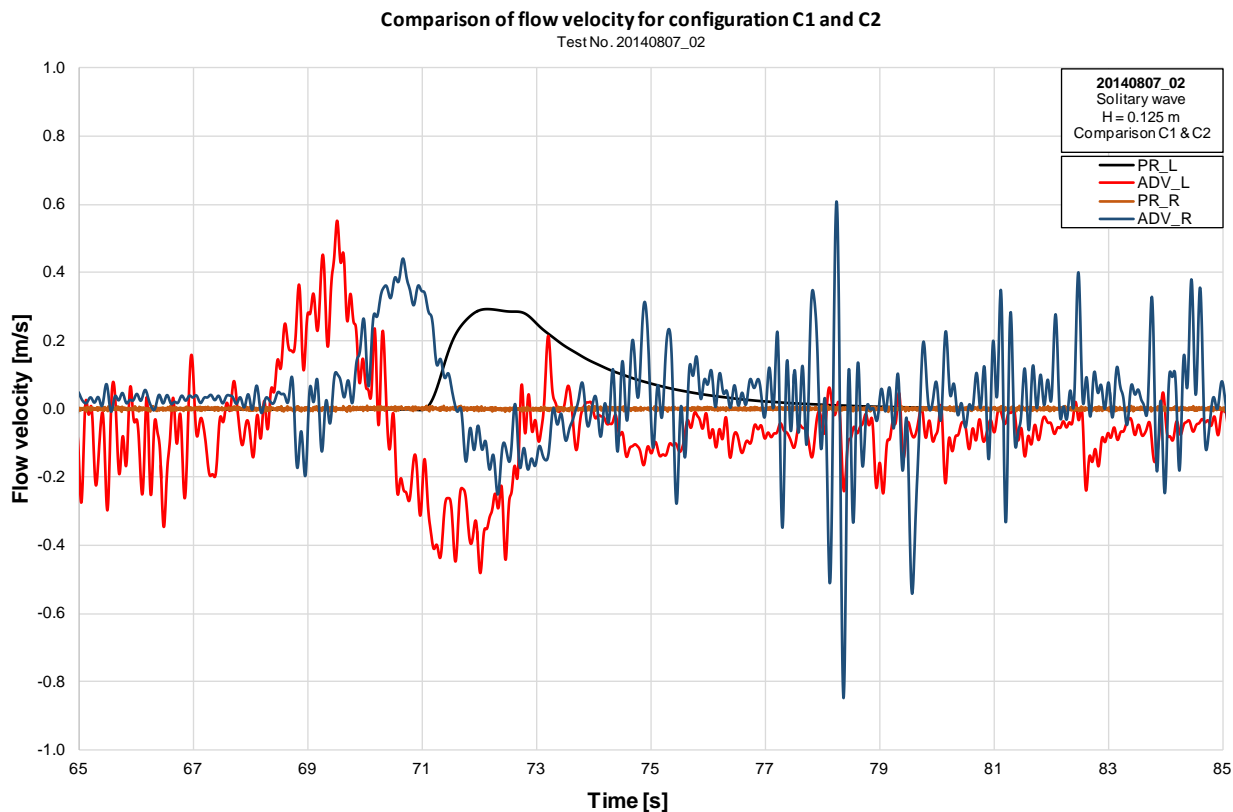


Figure C 9: Flow velocity under solitary wave with $H=0.125$ m for configurations 1 and 2 (Test 20140807_02)



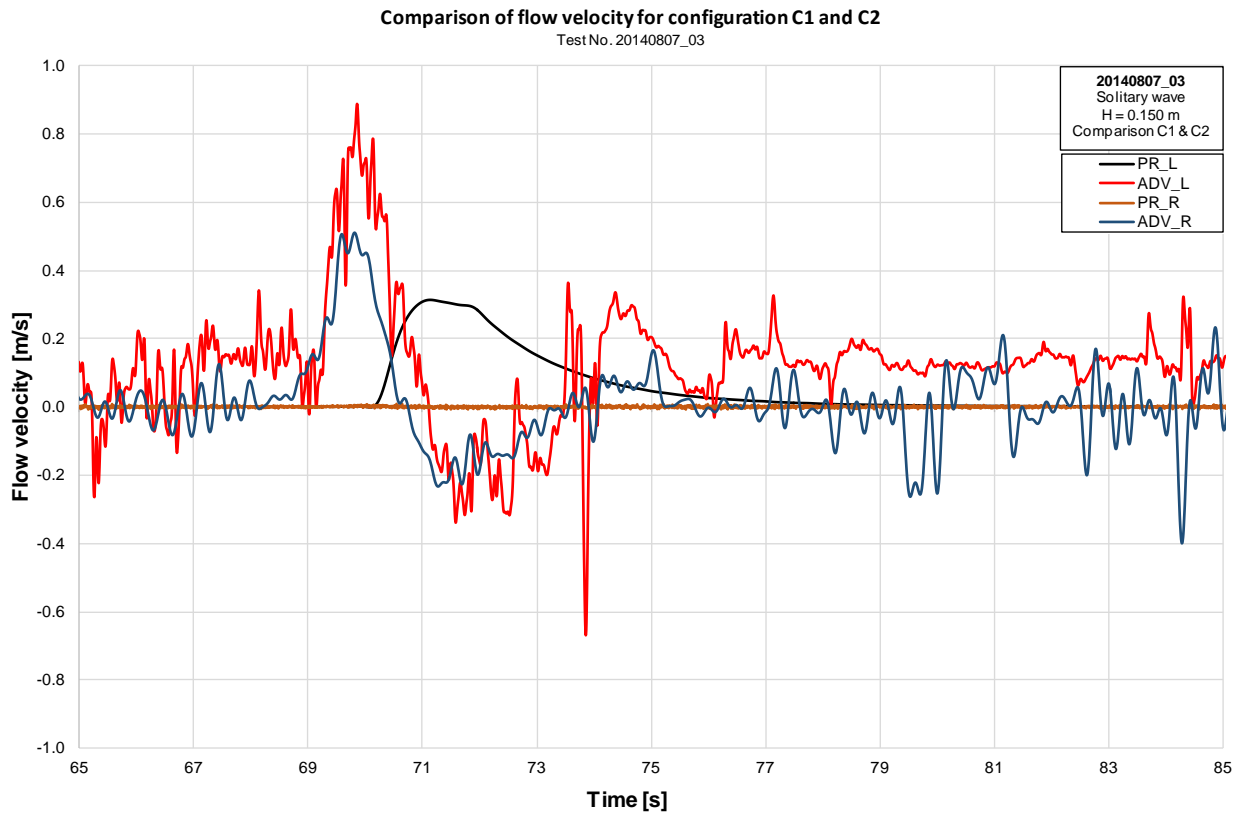


Figure C 10: Flow velocity under solitary wave with $H=0.125$ m for configurations 1 and 2 (Test 20140807_03)



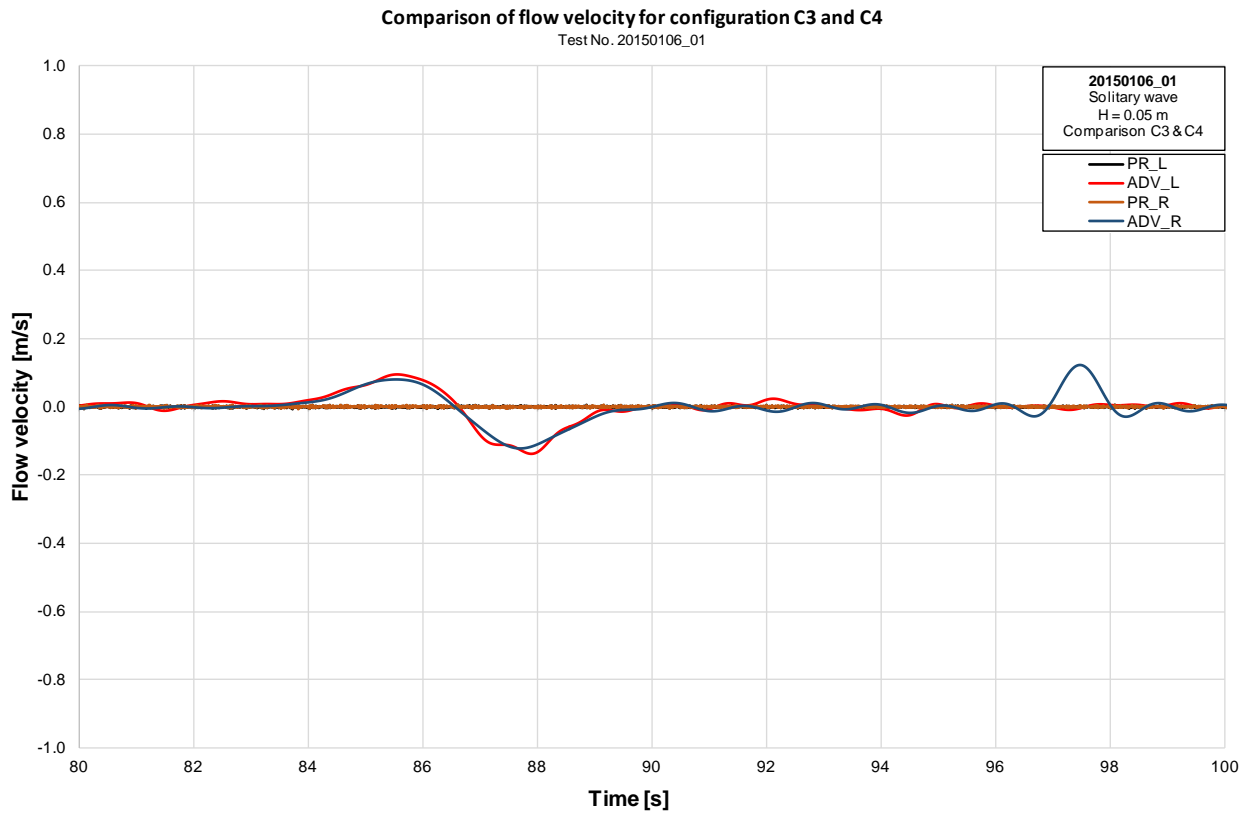


Figure C 11: Flow velocity under solitary wave with $H=0.050$ m for configurations 3 and 4 (Test 20150106_01)



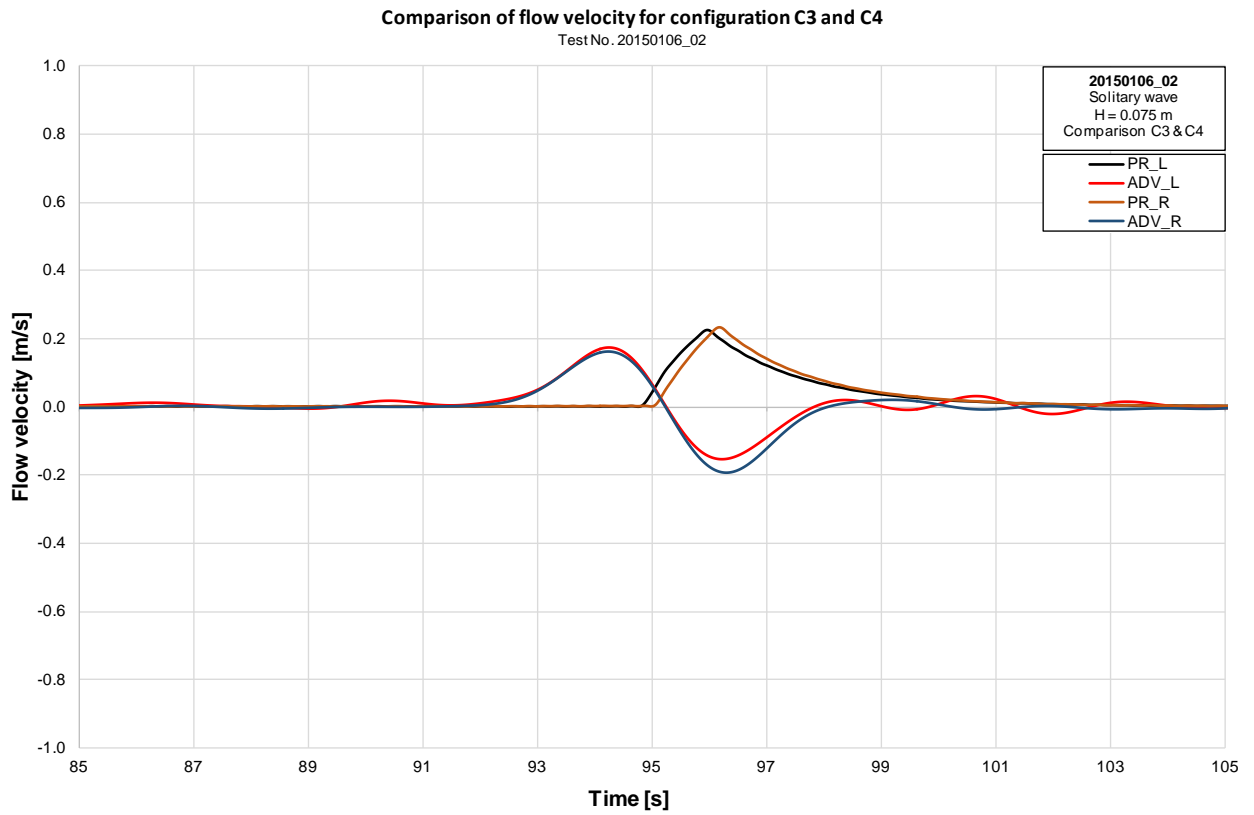


Figure C 12: Flow velocity under solitary wave with $H=0.075$ m for configurations 3 and 4 (Test 20150106_02)



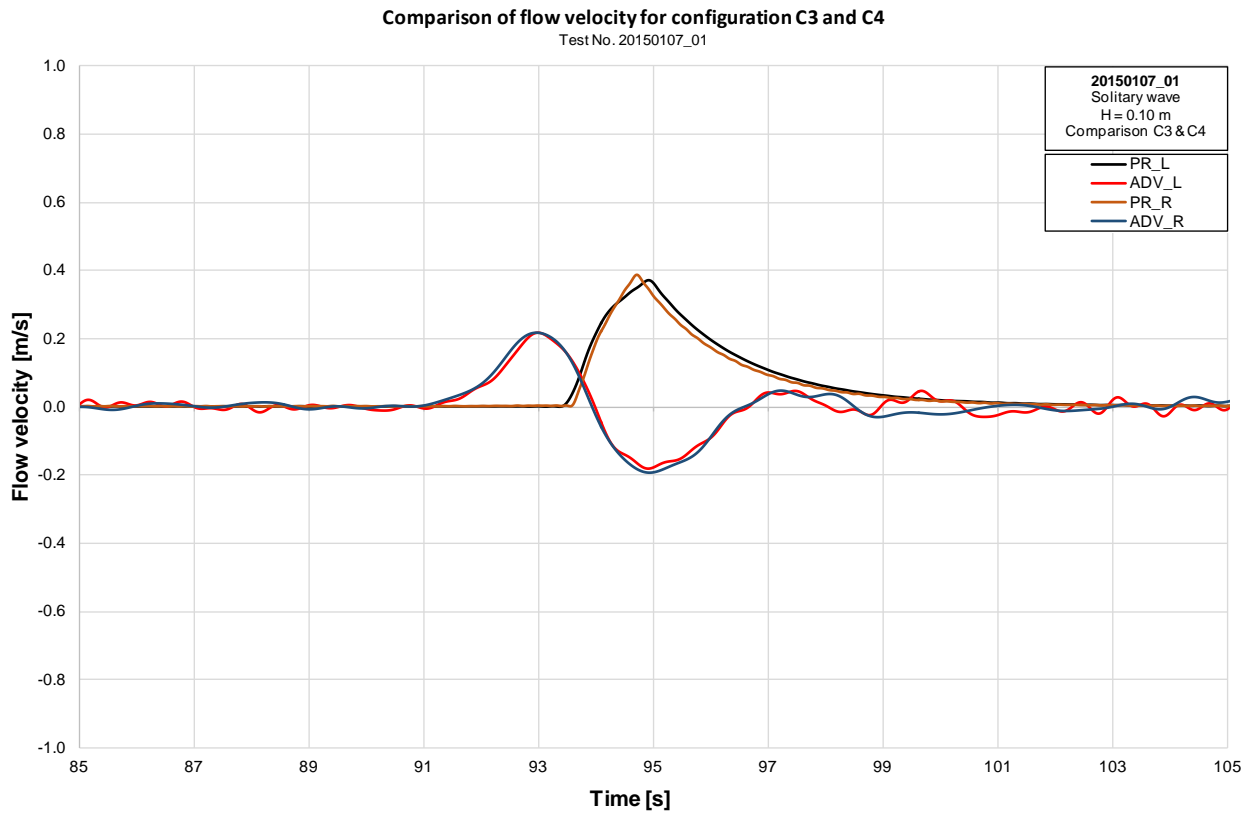


Figure C 13: Flow velocity under solitary wave with $H=0.100$ m for configurations 3 and 4 (Test 20150107_01)



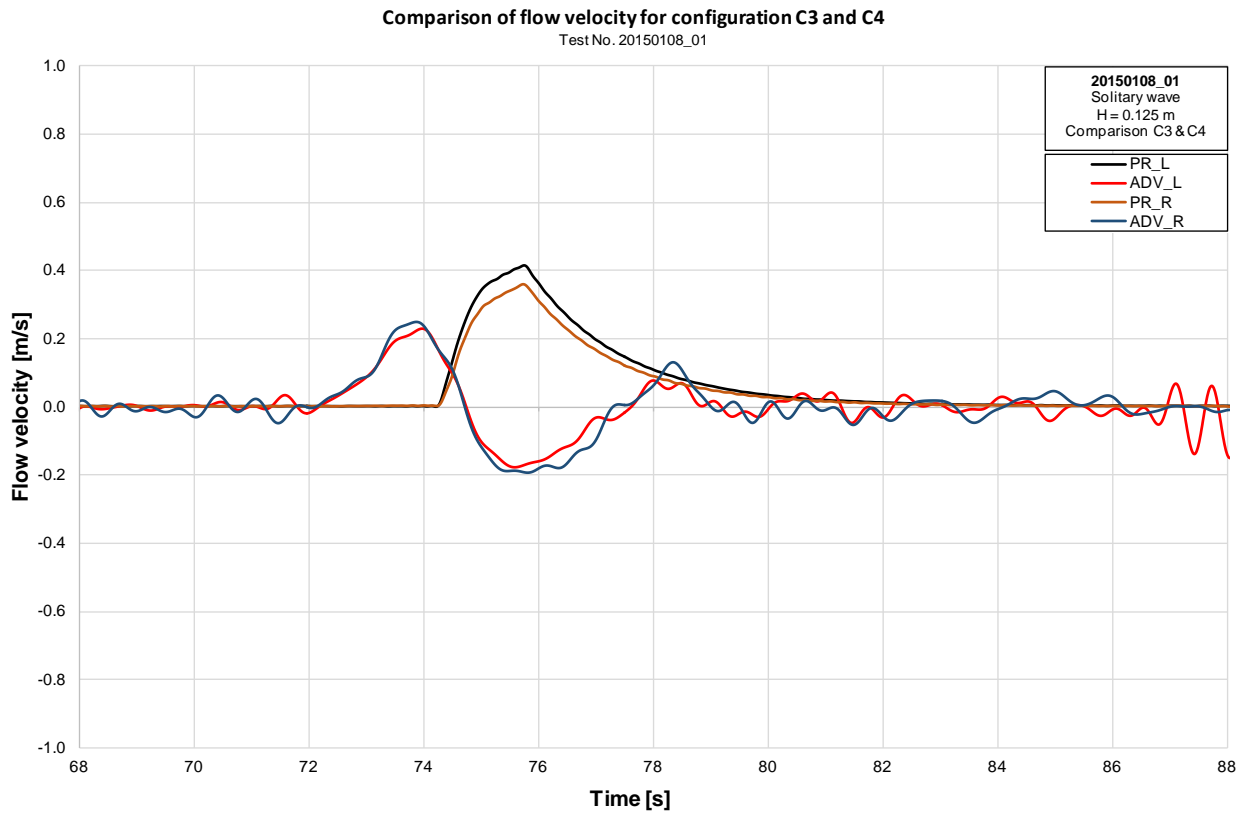


Figure C 14: Flow velocity under solitary wave with $H=0.125$ m for configurations 3 and 4 (Test 20150108_01)



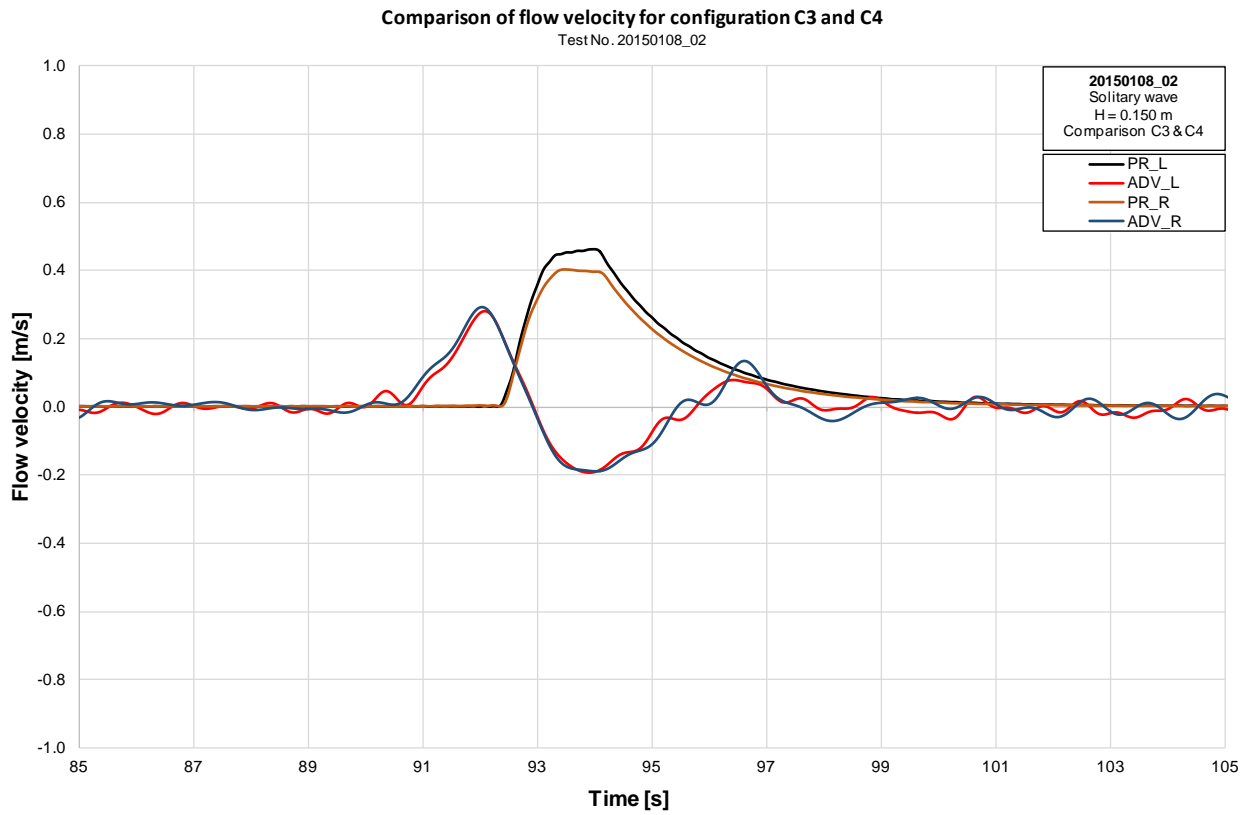


Figure C 15: Flow velocity under solitary wave with $H=0.150$ m for configurations 3 and 4 (Test 20150108_02)



Appendix D

Breakwater damage profiles in experiments at TU-BS



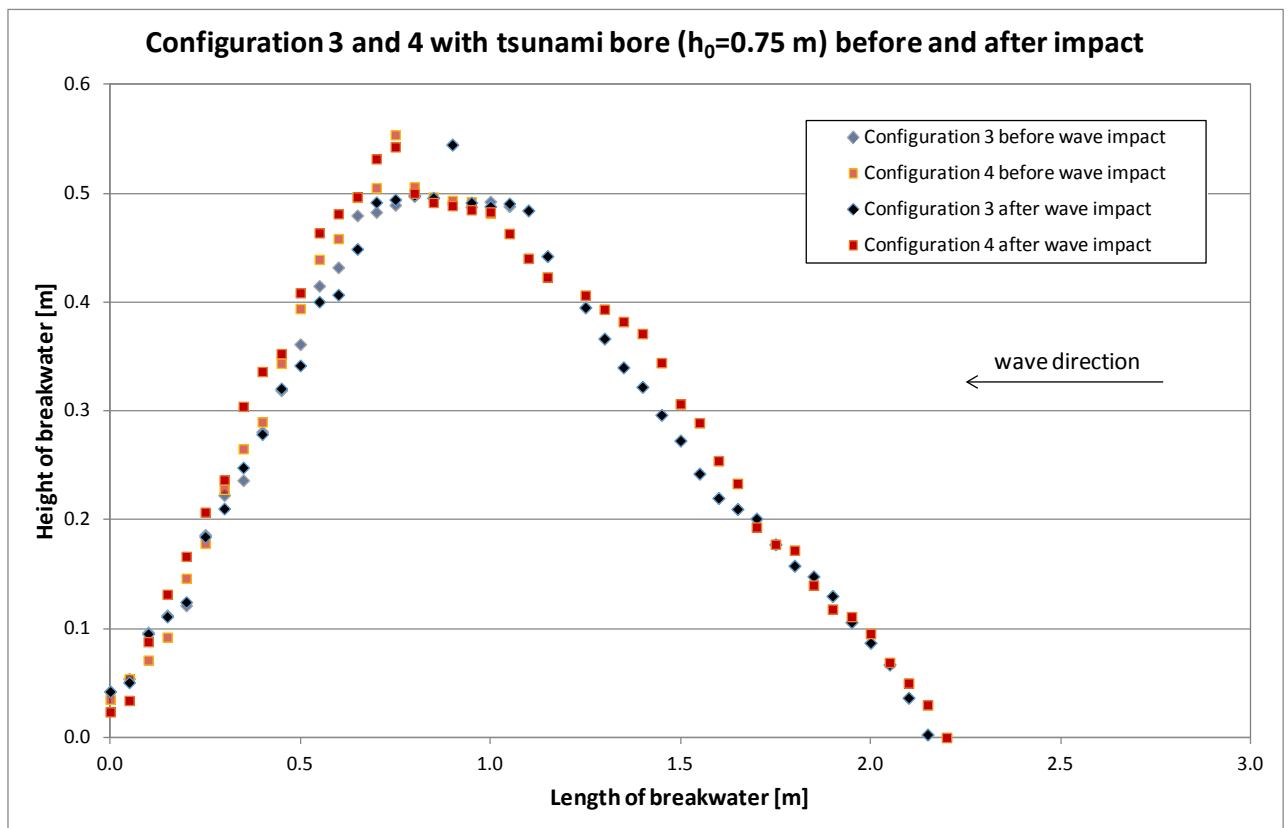


Figure D 1: Configurations 3 and 4 with tsunami bore ($h_0=0.75$ m and $h_1=0.20$ m) before and after impact (Test 20140721_1)



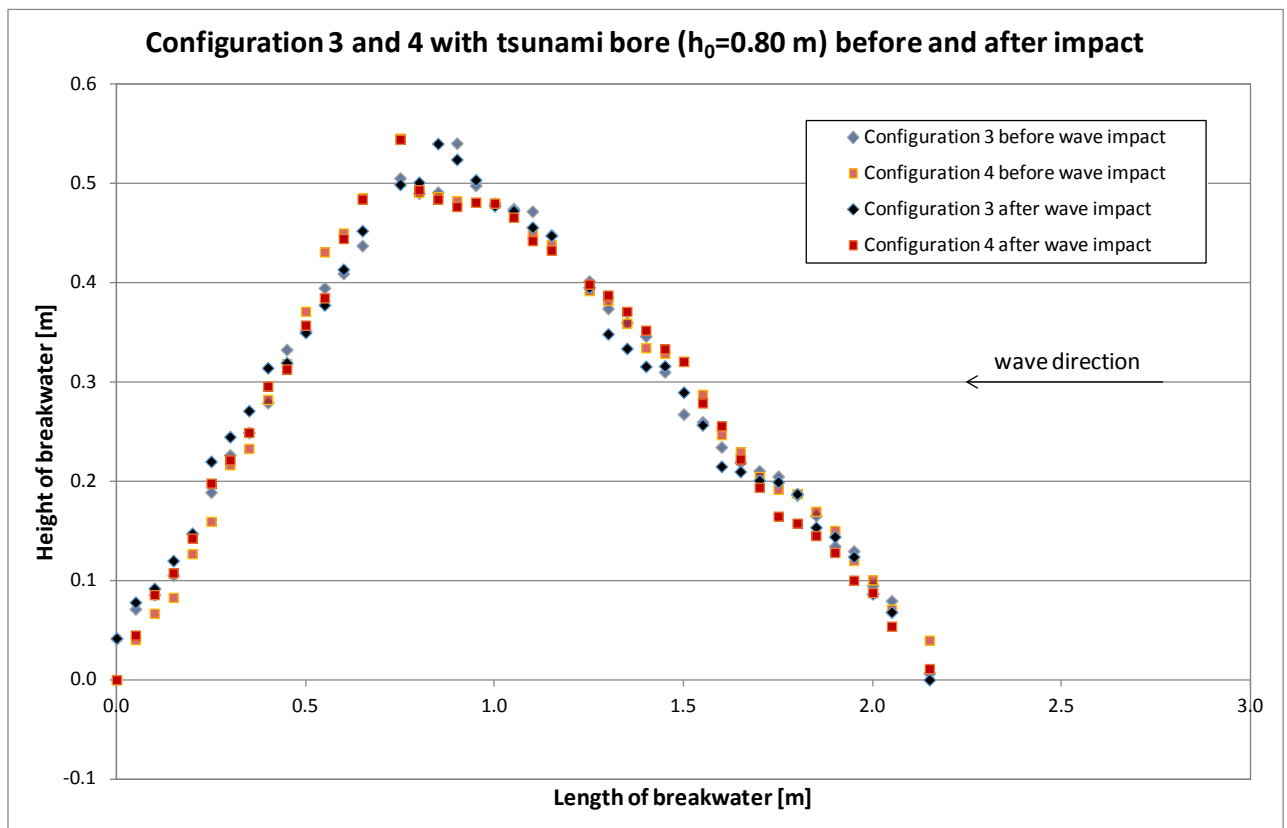


Figure D 2: Configurations 3 and 4 with tsunami bore ($h_0=0.80$ m and $h_1=0.20$ m) before and after impact (Test 20140721_2)



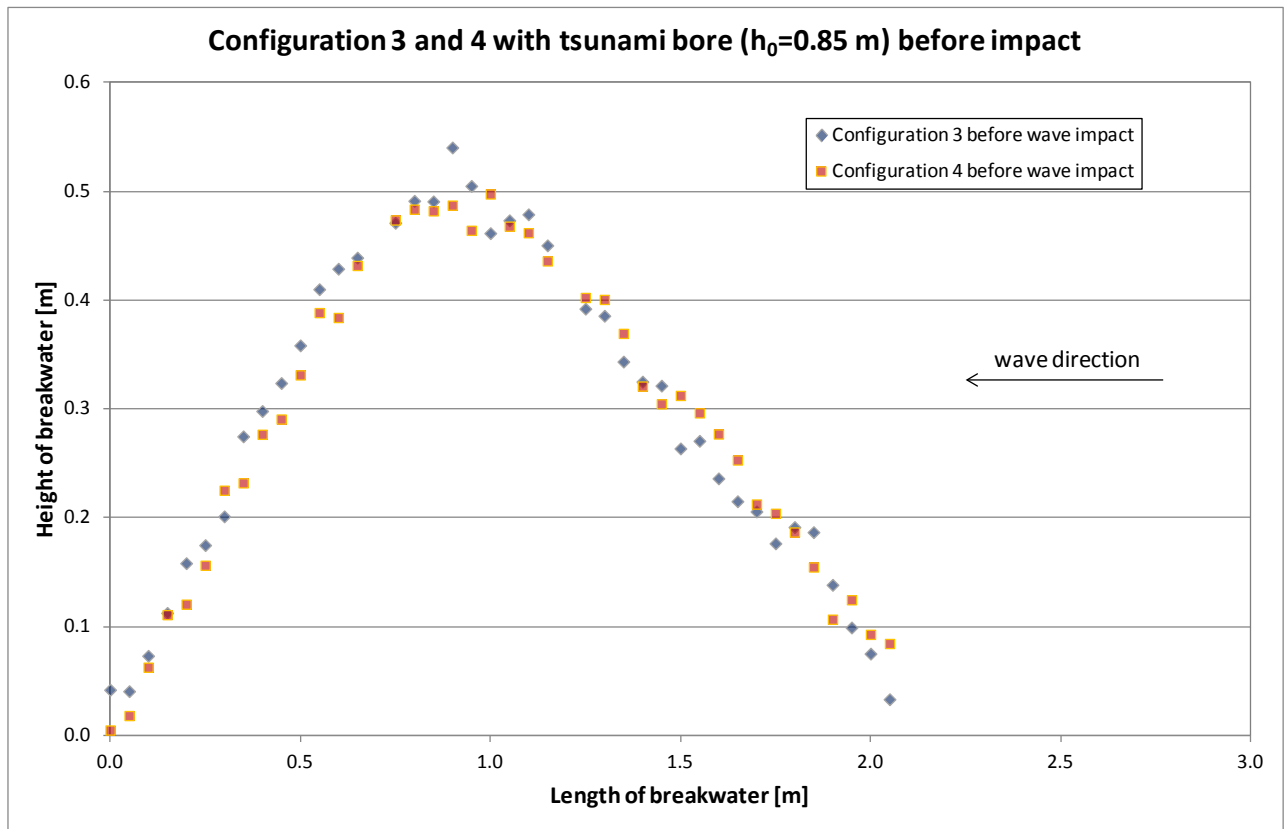


Figure D 3: Configurations 3 and 4 with tsunami bore ($h_0=0.85$ m and $h_1=0.20$ m) before impact; after impact were not measured (Test 20140721_3)



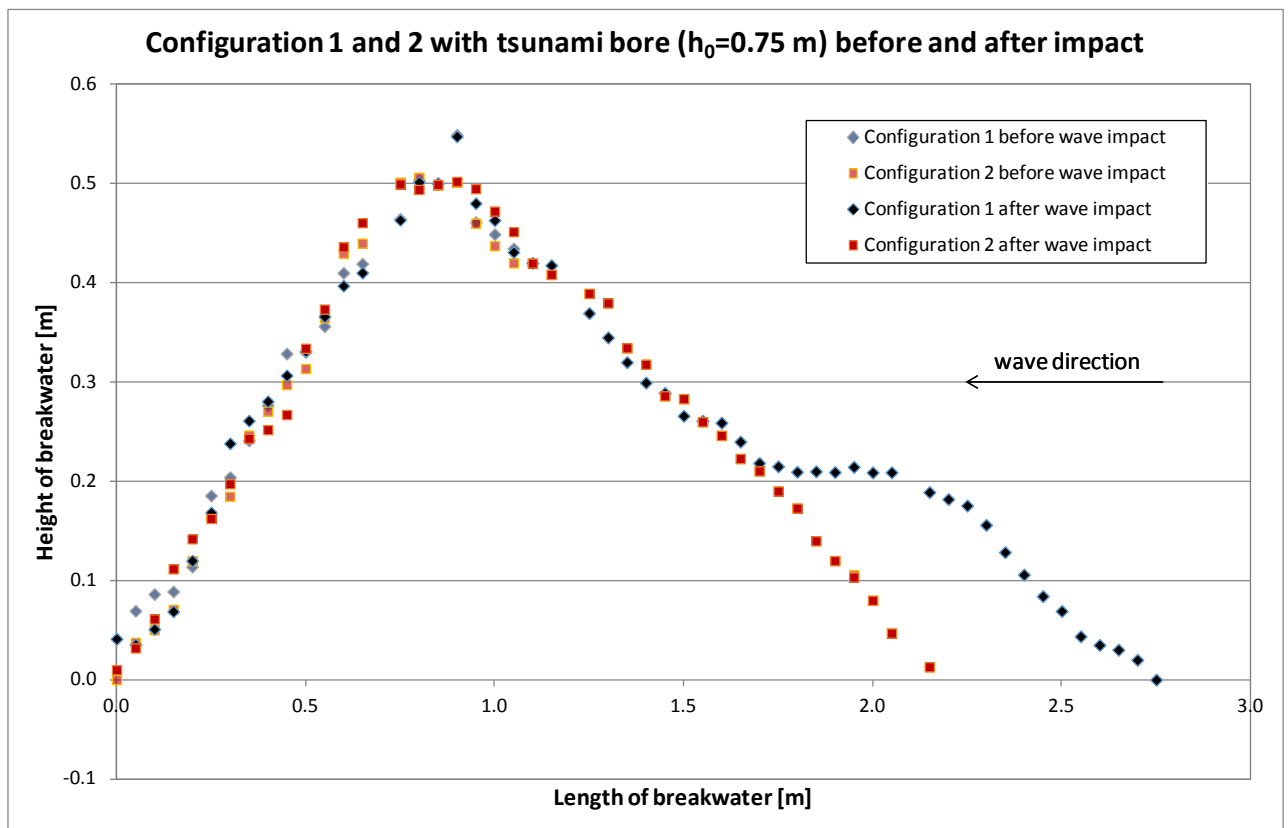


Figure D 4: Configurations 1 and 2 with tsunami bore ($h_0=0.75$ m and $h_1=0.20$ m) before and after impact (Test 20140723_1)



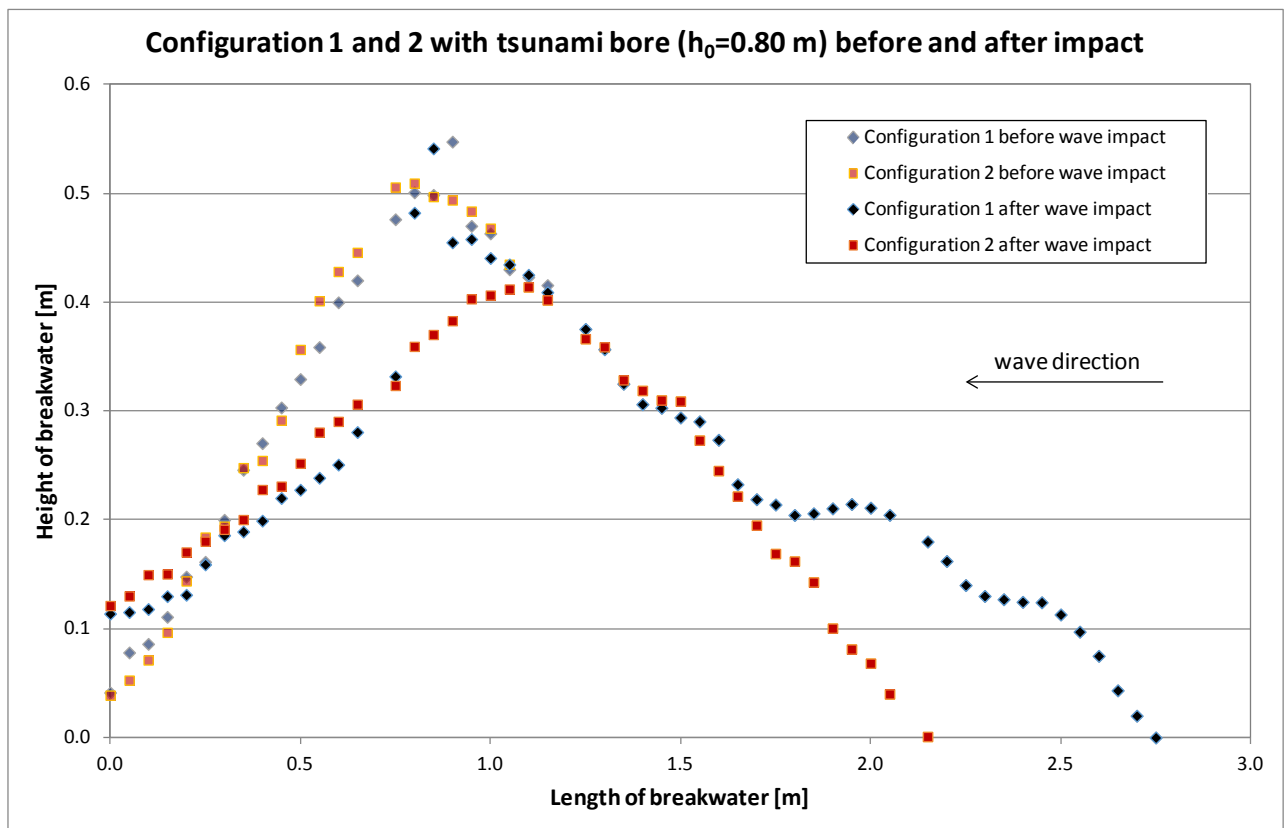


Figure D 5: Configurations 1 and 2 with tsunami bore ($h_0=0.80$ m and $h_1=0.20$ m) before and after impact (Test 20140723_2)



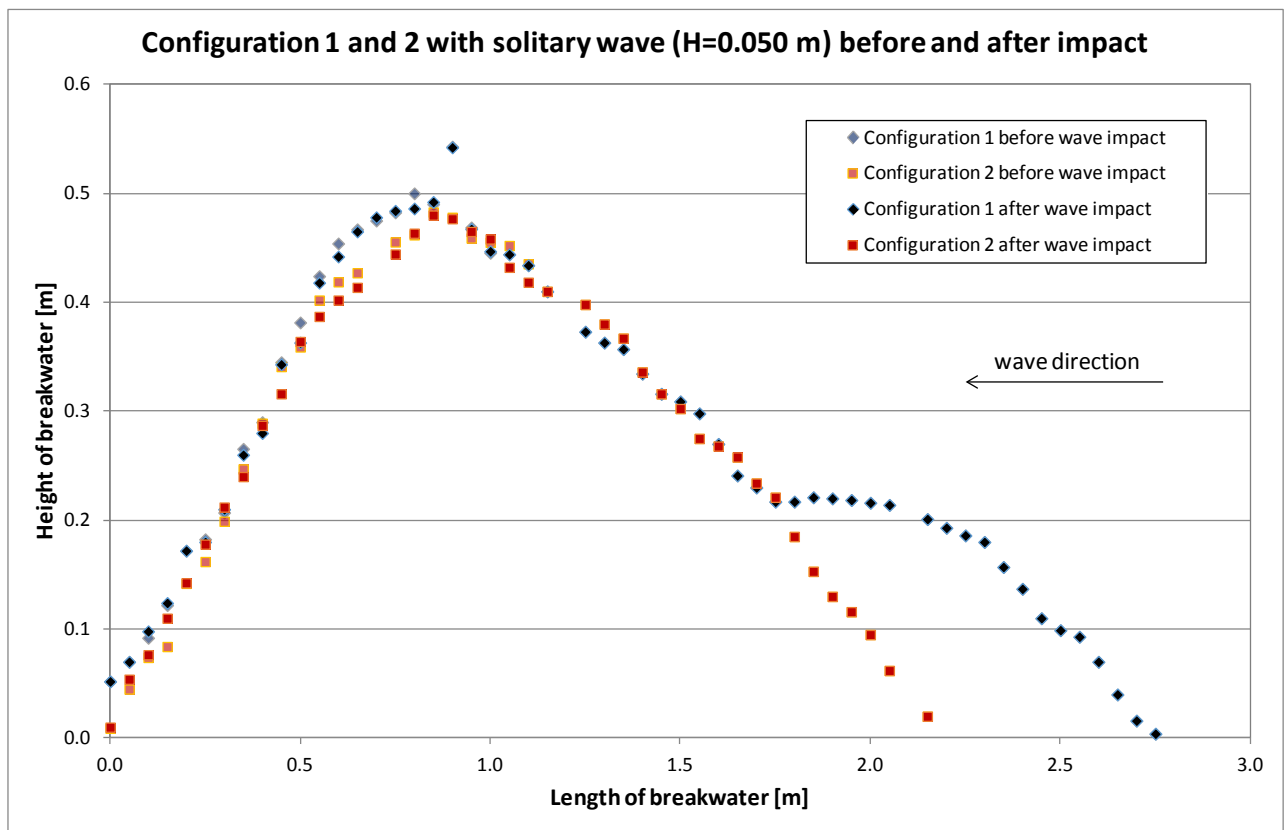


Figure D 6: Configurations 1 and 2 with solitary wave ($H=0.050$ m) before and after impact (Test 20140725_1)



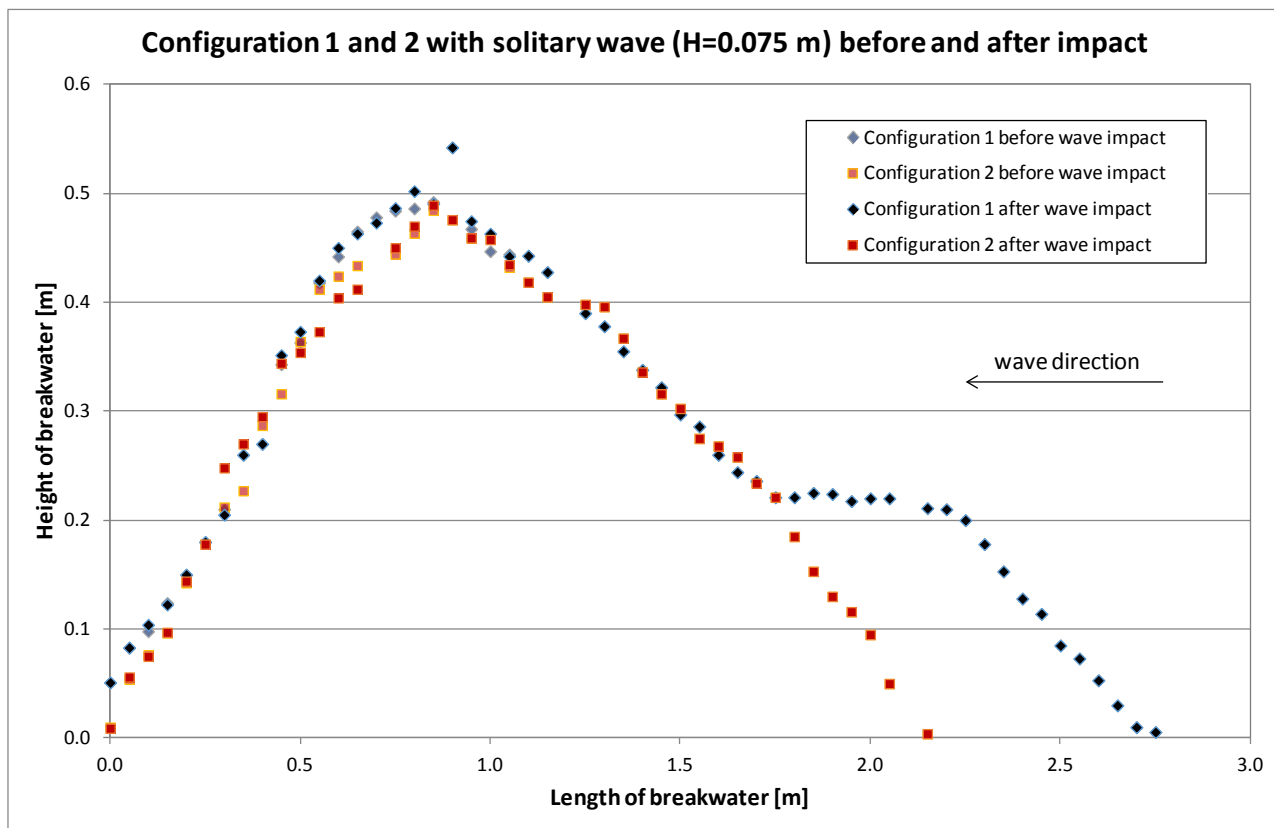


Figure D 7: Configurations 1 and 2 with solitary wave ($H=0.075$ m) before and after impact (Test 20140725_2)



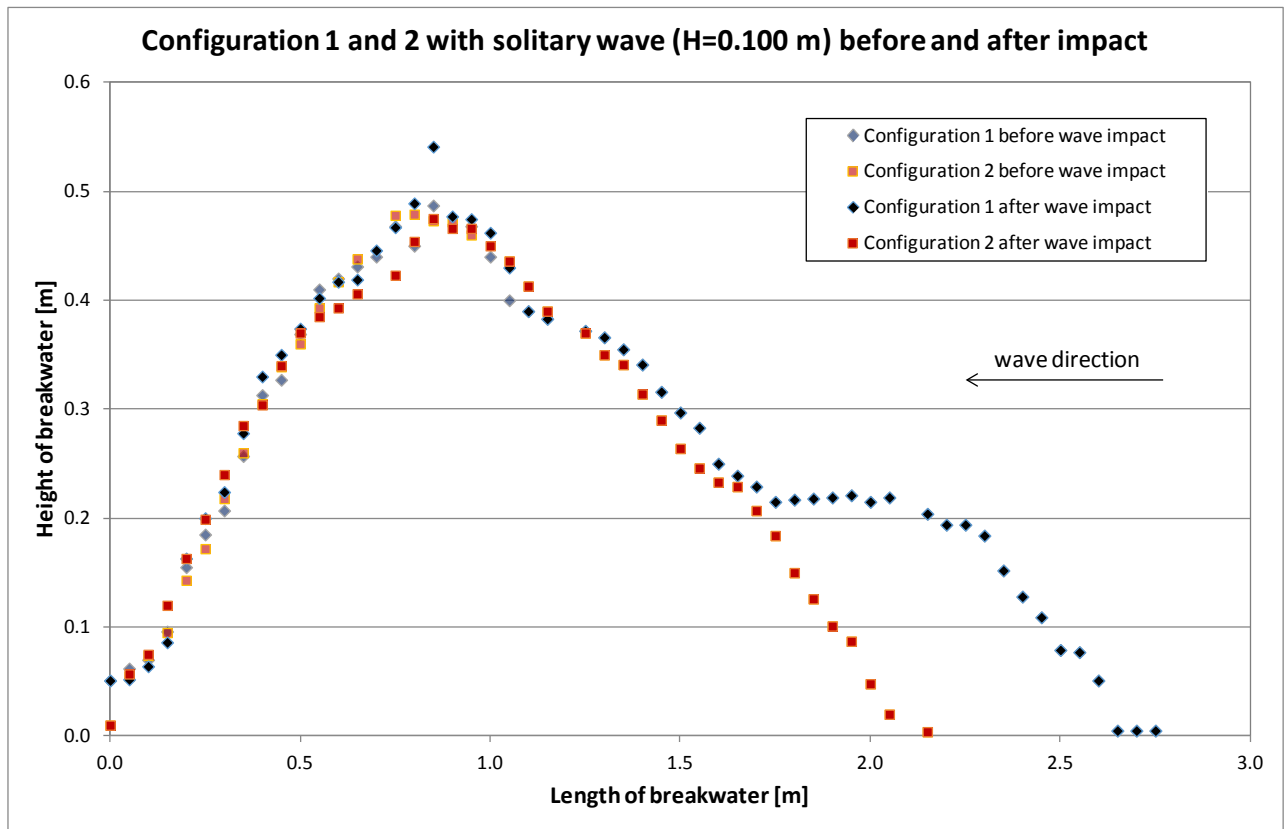


Figure D 8: Configurations 1 and 2 with solitary wave ($H=0.100$ m) before and after impact (Test 20140807_1)



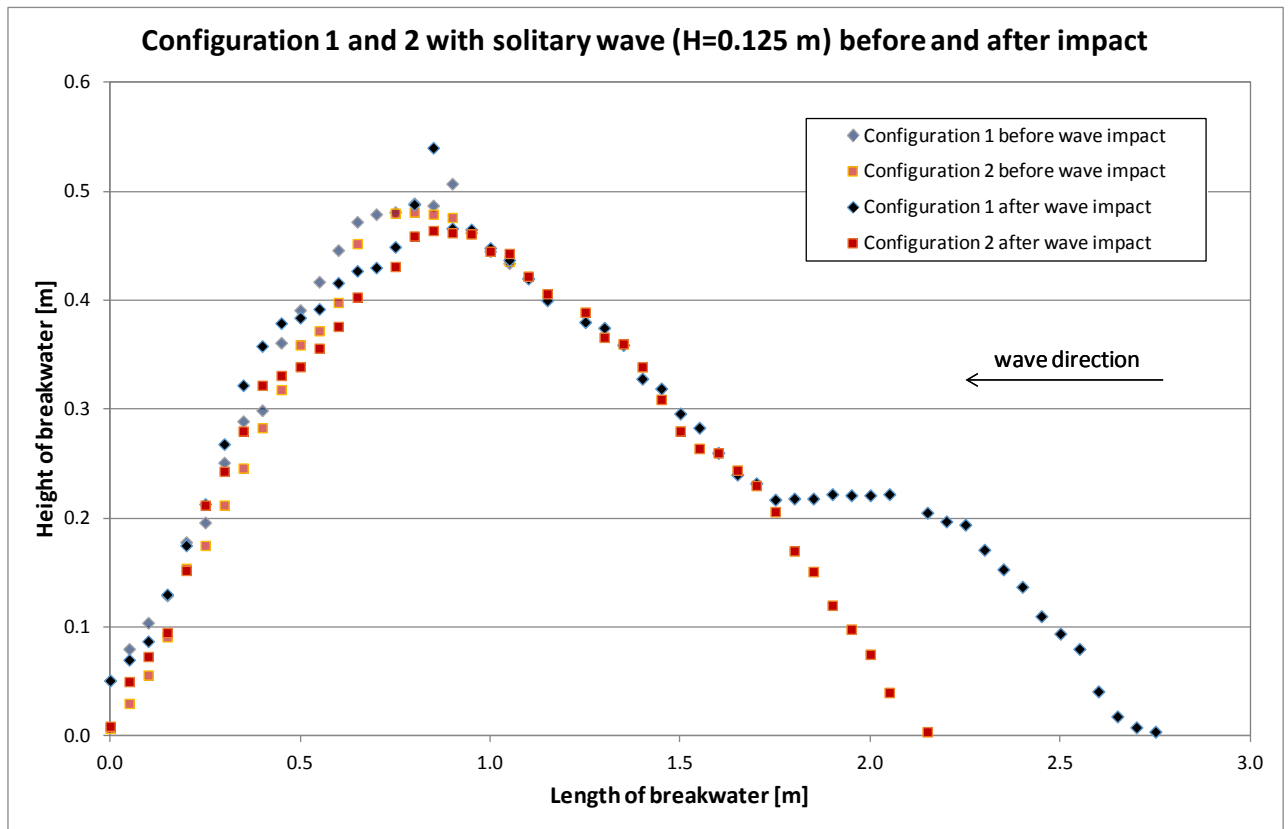


Figure D 9: Configurations 1 and 2 with solitary wave ($H=0.125$ m) before and after impact (Test 20140807_2)



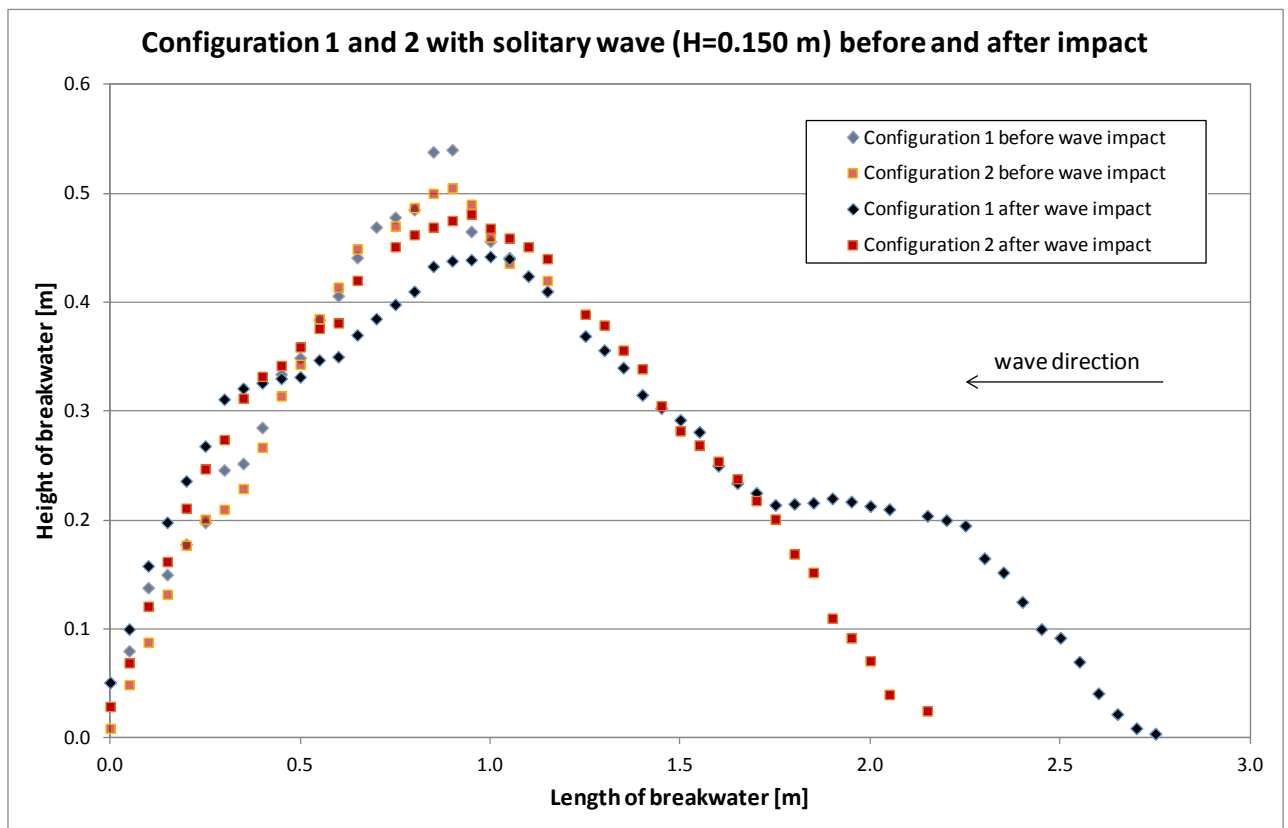


Figure D 10: Configurations 1 and 2 with solitary wave ($H=0.150$ m) before and after impact (Test 20140807_3)



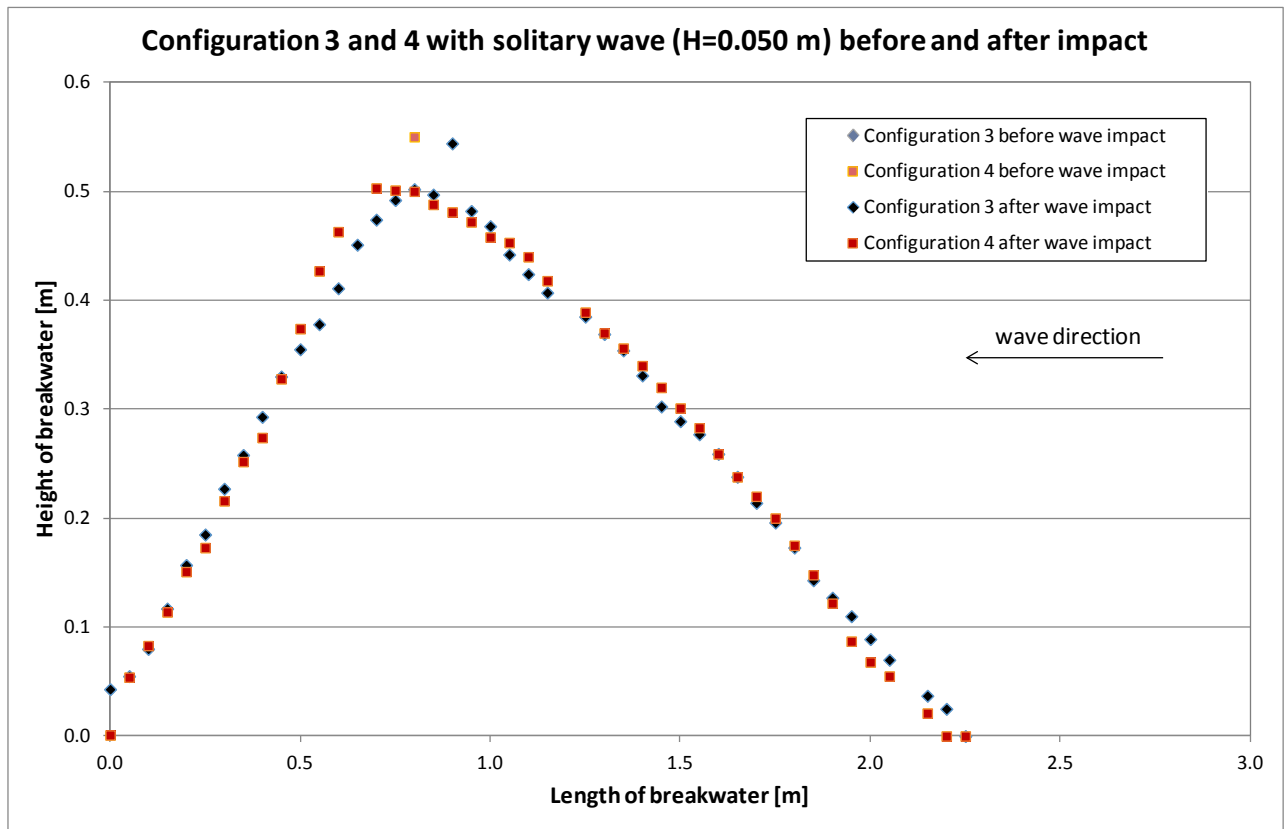


Figure D 11: Configurations 3 and 4 with solitary wave ($H=0.050$ m) before and after impact (Test 20150106_1)



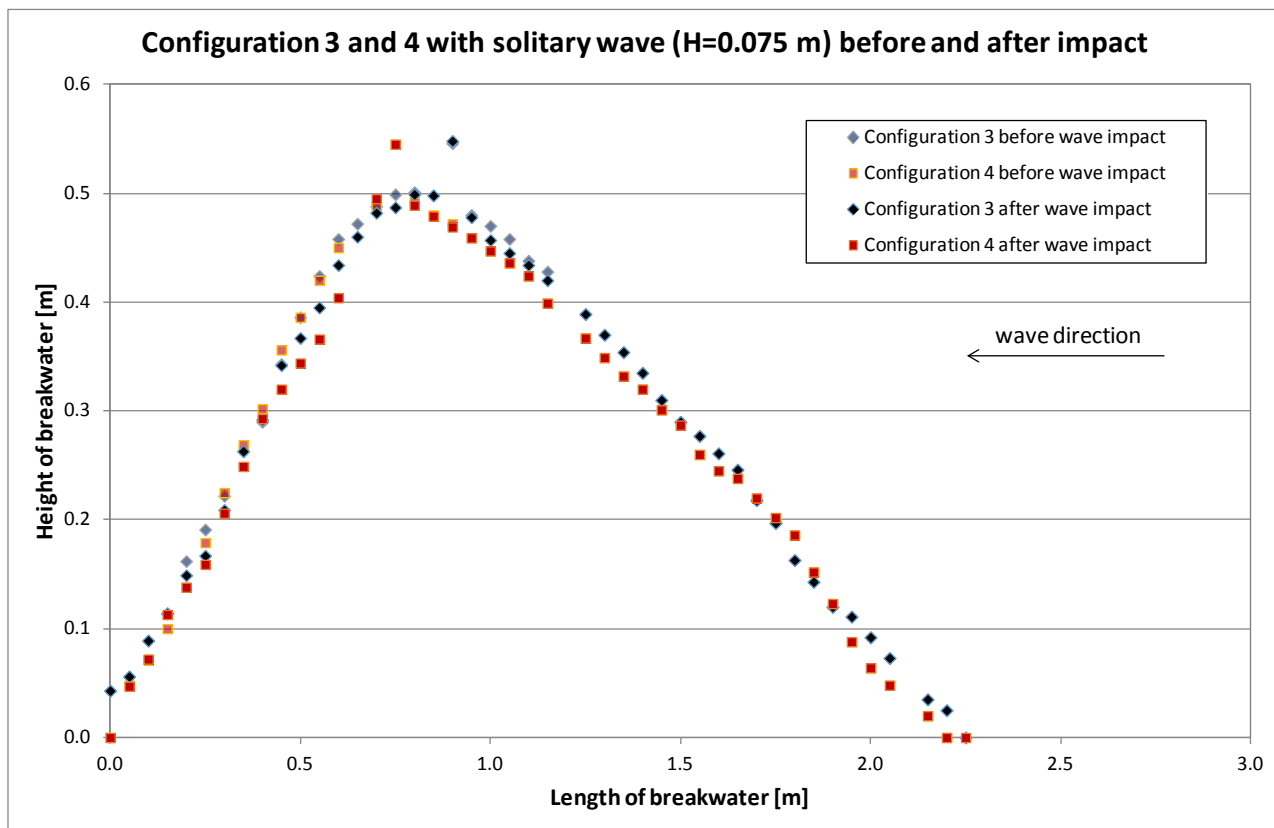


Figure D 12: Configurations 3 and 4 with solitary wave ($H=0.075$ m) before and after impact (Test 20150106_2)



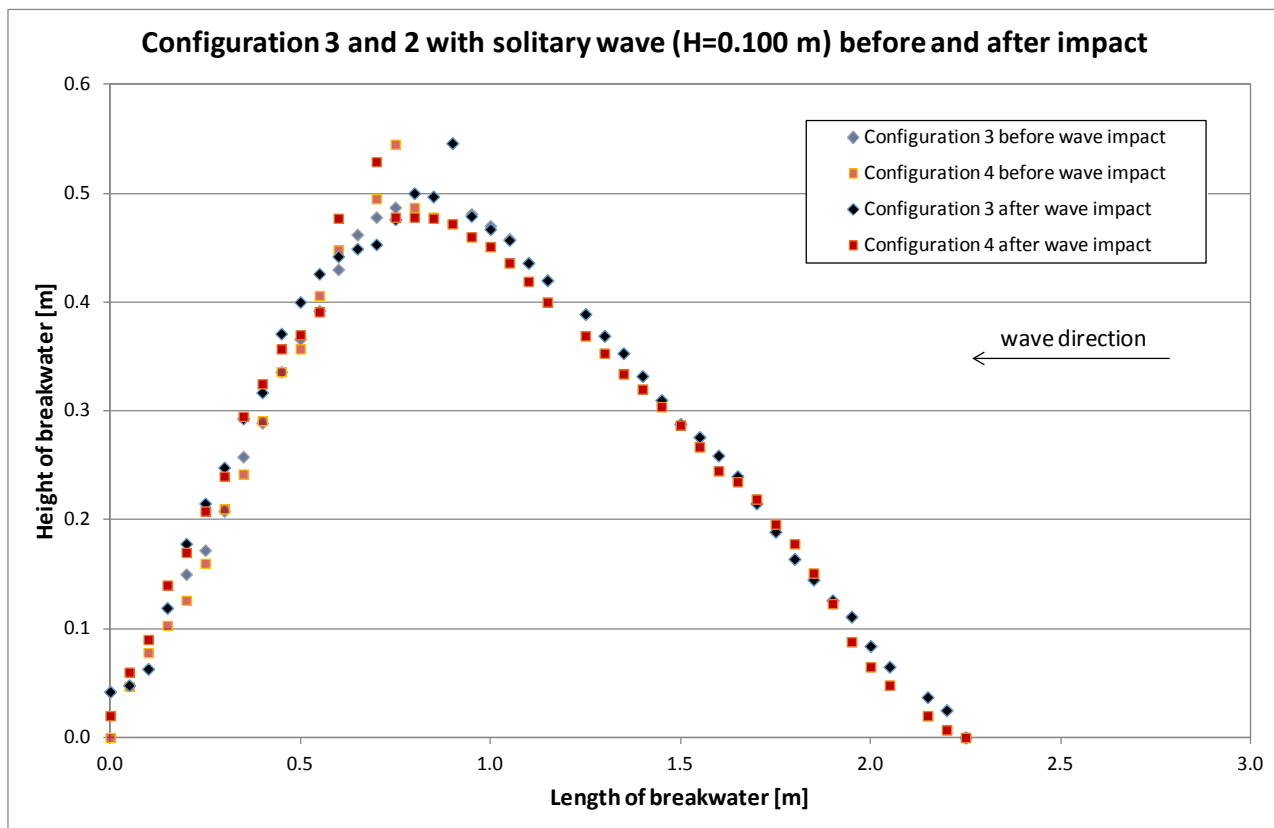


Figure D 13: Configurations 3 and 4 with solitary wave ($H=0.100$ m) before and after impact (Test 20150107_1)



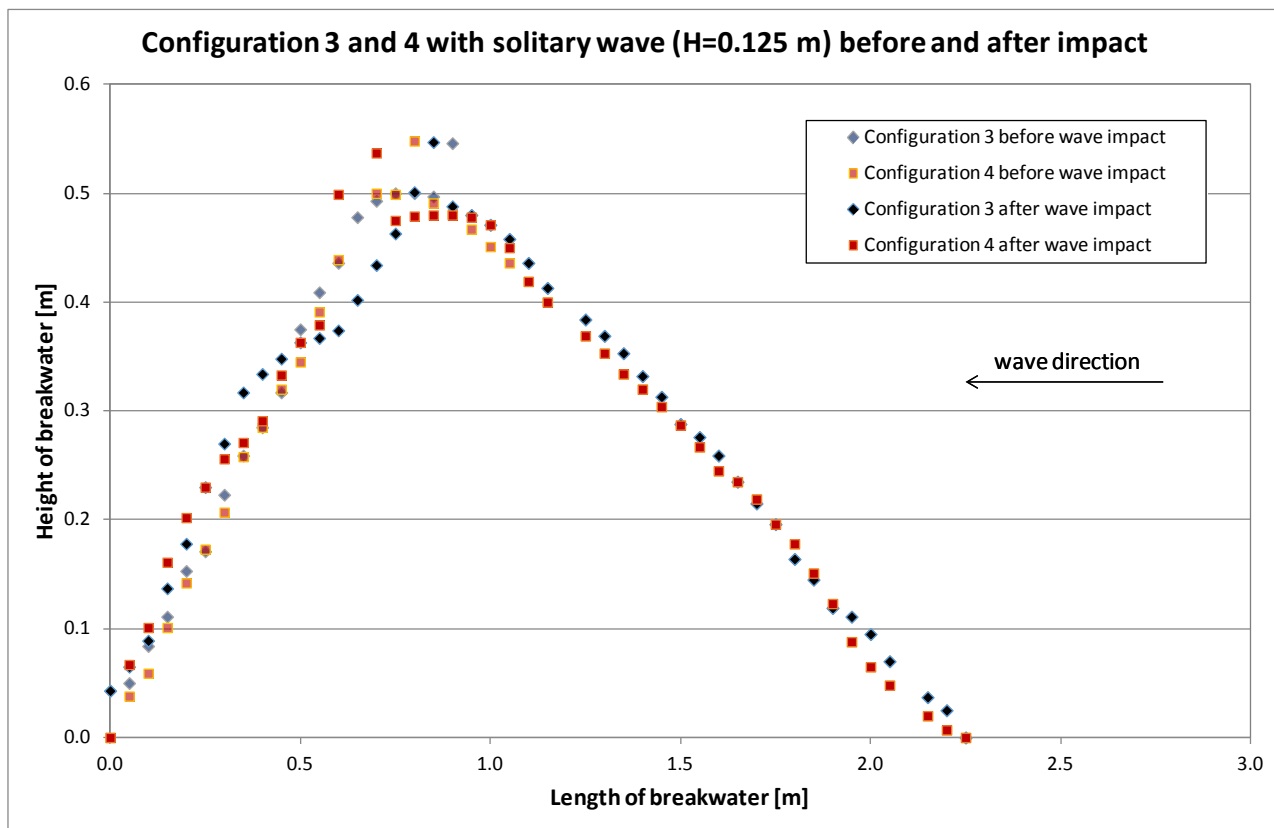


Figure D 14: Configurations 3 and 4 with solitary wave ($H=0.125$ m) before and after impact (Test 20150108_1)



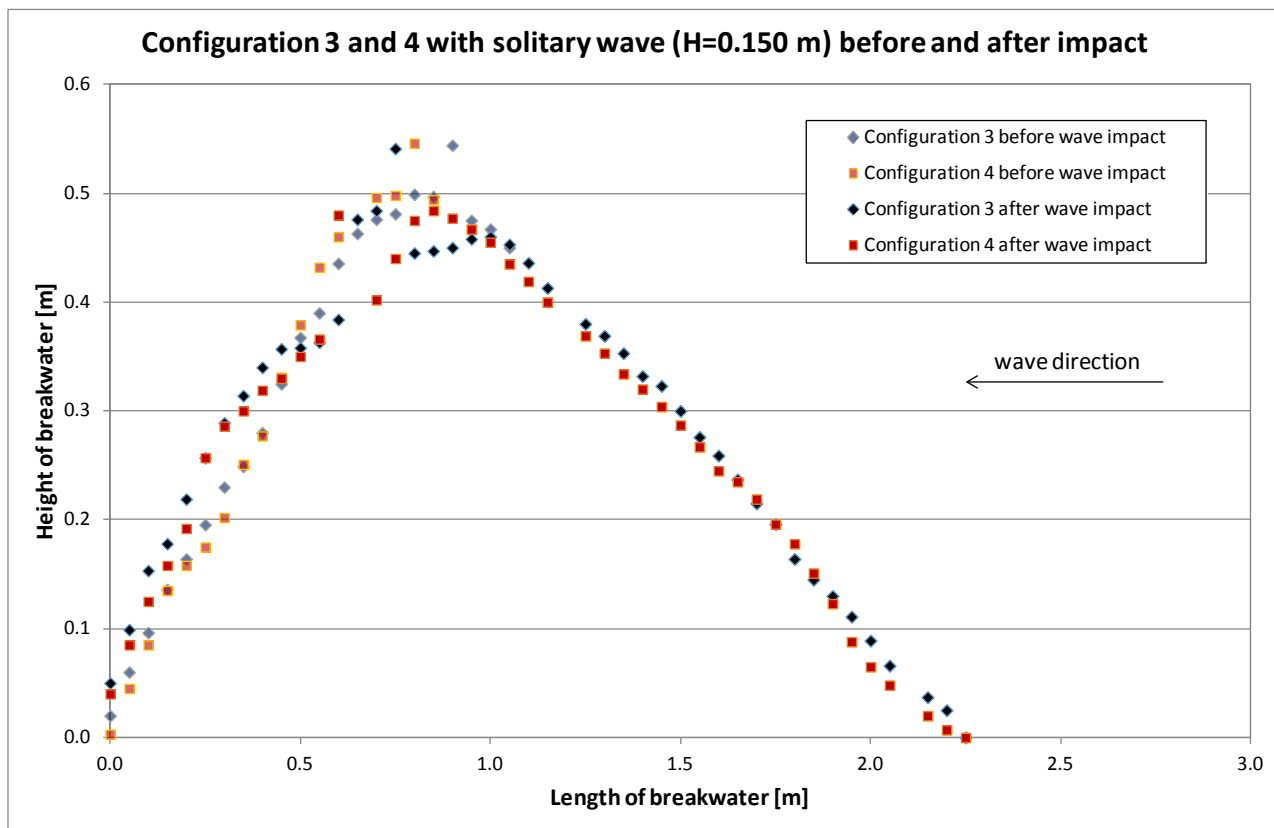


Figure D 15: Configurations 3 and 4 with solitary wave ($H=0.150$ m) before and after impact (Test 20150108_2)



Appendix E

Photo documentation of breakwater damage in experiments at TU-BS

NGI



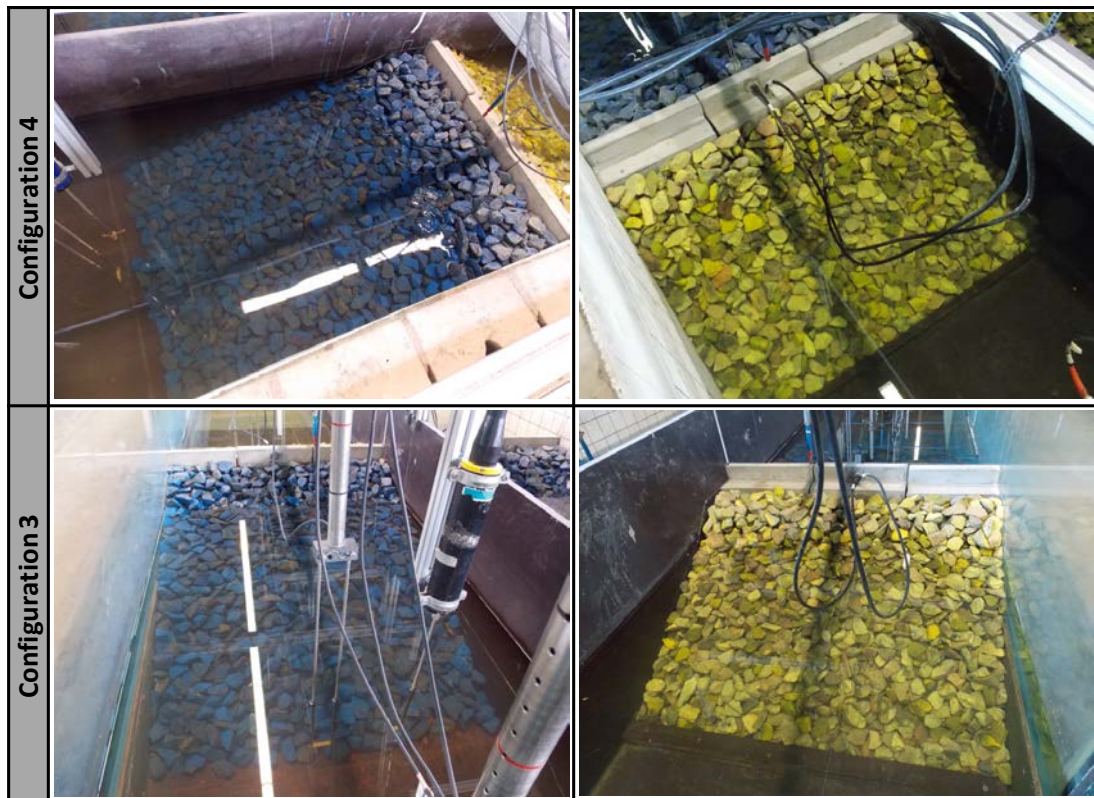


Figure E 1: Damage of configurations 3 and 4 due to tsunami bore with $h_0=0.75$ m and $h_1=0.20$ m (Test 20140721_01)



Figure E 2: Damage of configurations 3 and 4 due to tsunami bore with $h_0=0.80$ m and $h_1=0.20$ m (Test 20140721_02)



Figure E 3: Damage of configurations 3 and 4 due to tsunami bore with $h_0=0.85$ m and $h_1=0.20$ m (Test 20140721_03)



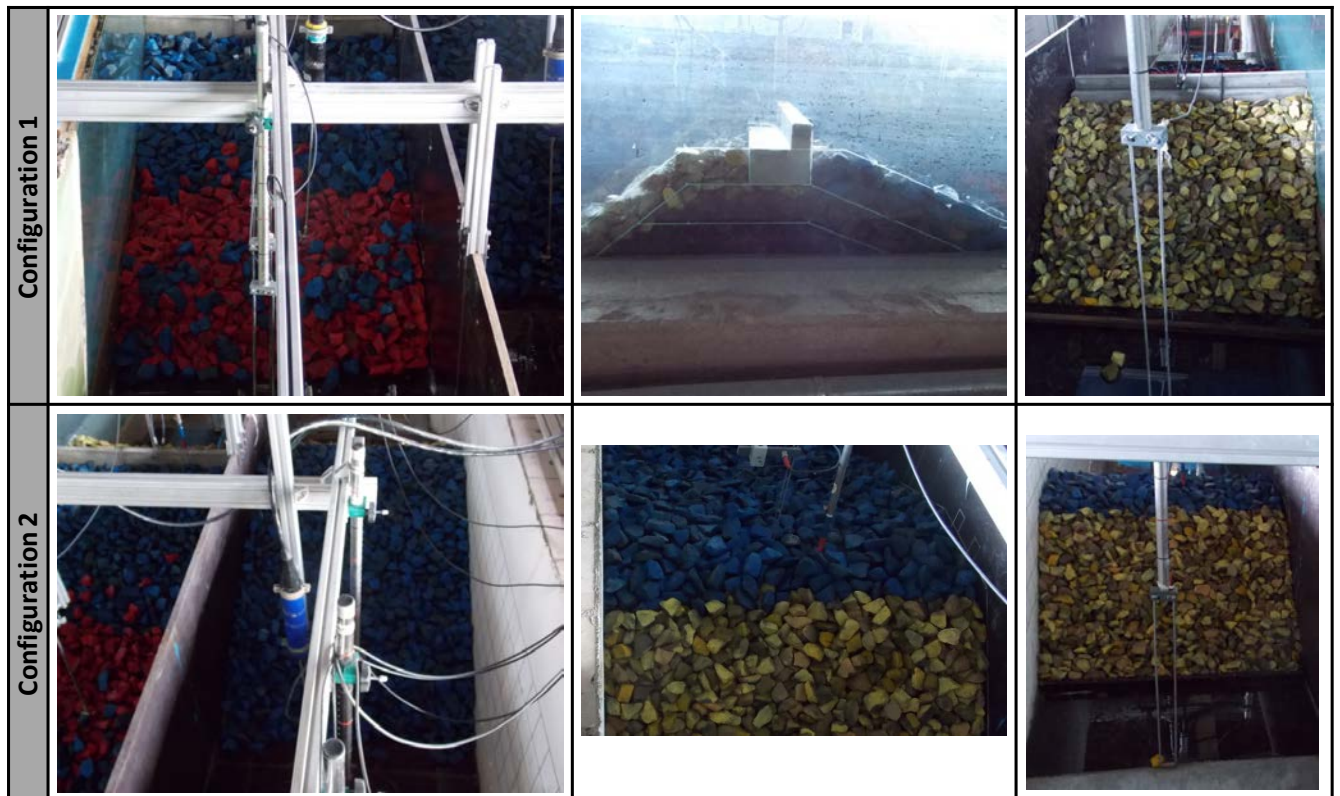


Figure E 4: Damage of configurations 1 and 2 due to tsunami bore with $h_0=0.75$ m and $h_1=0.20$ m (Test 20140723_01)

NGI

PARI



CONCERT JAPAN
Connecting and Coordinating
European Research and Technology Development with Japan

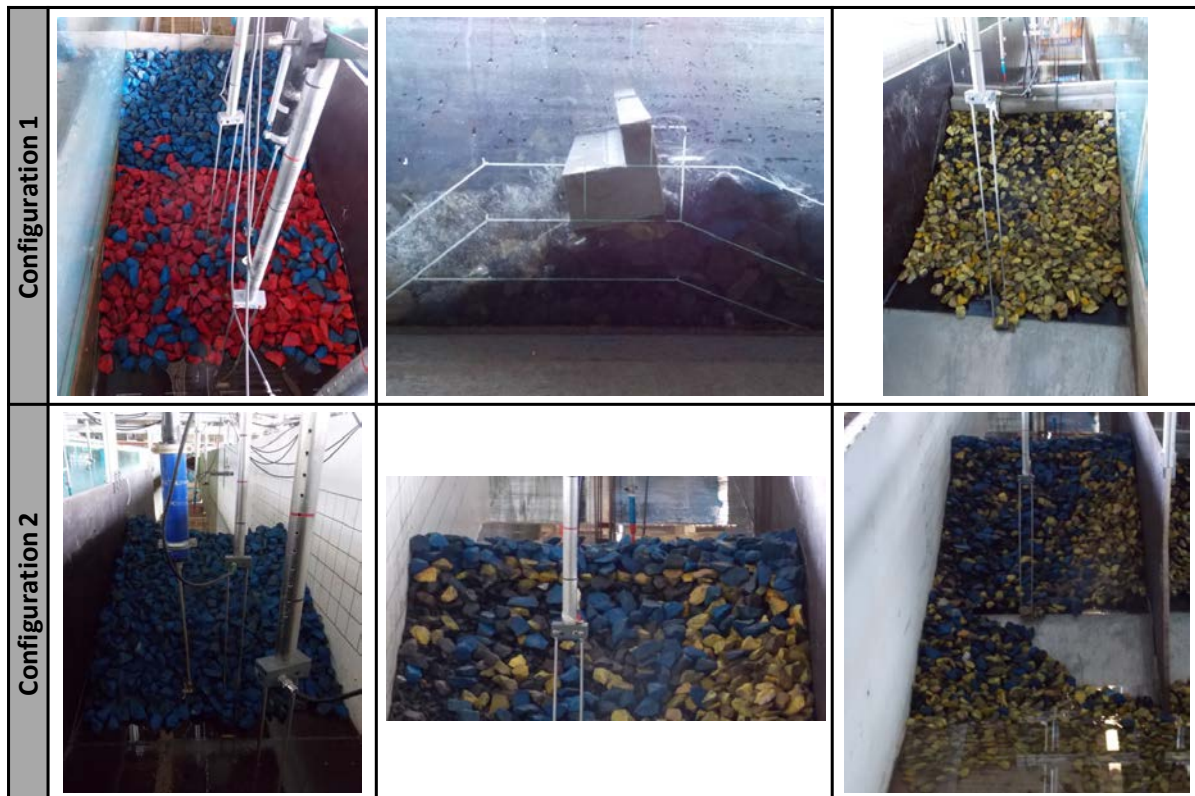


Figure E 5: Damage of configurations 1 and 2 due to tsunami bore with $h_0=0.80$ m and $h_1=0.20$ m (Test 20140723_02)

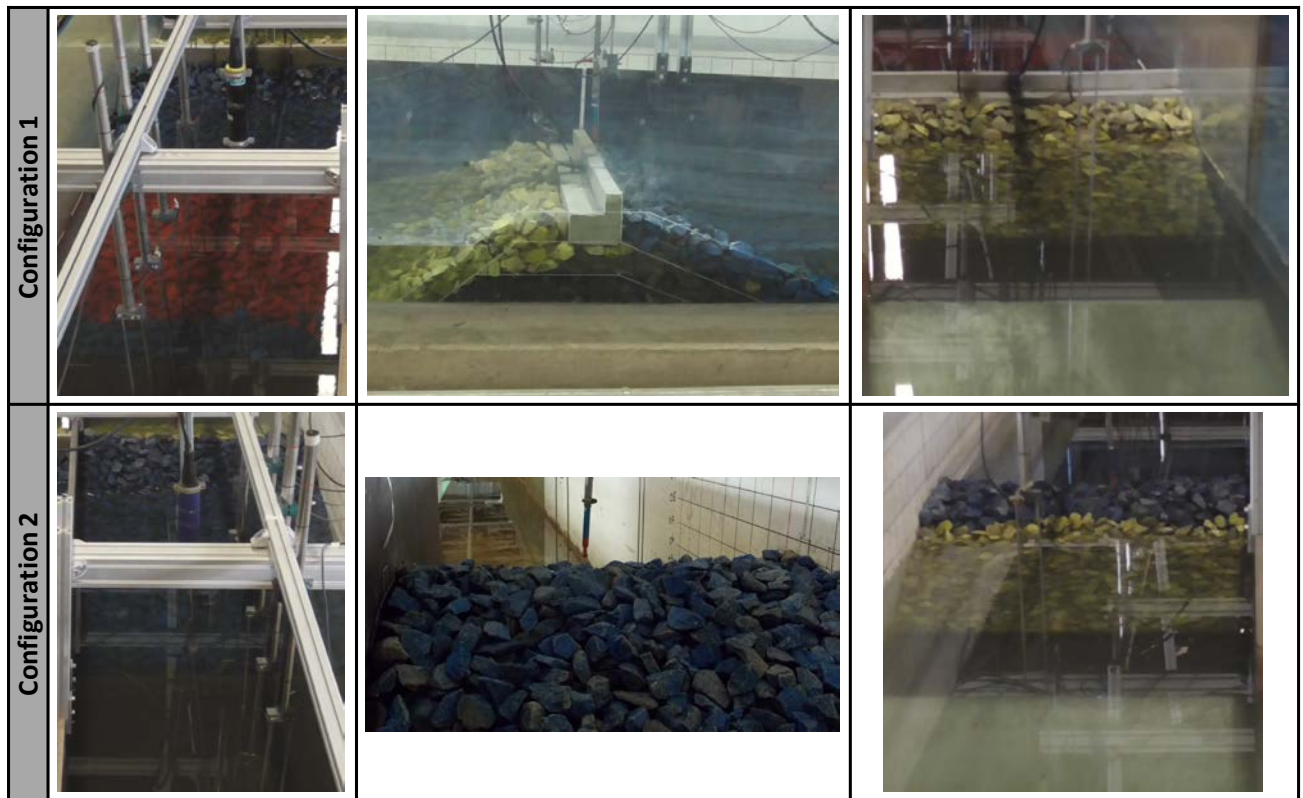


Figure E 6: Damage of configurations 1 and 2 due to solitary wave with $H=0.050$ m (Test 20140725_01)

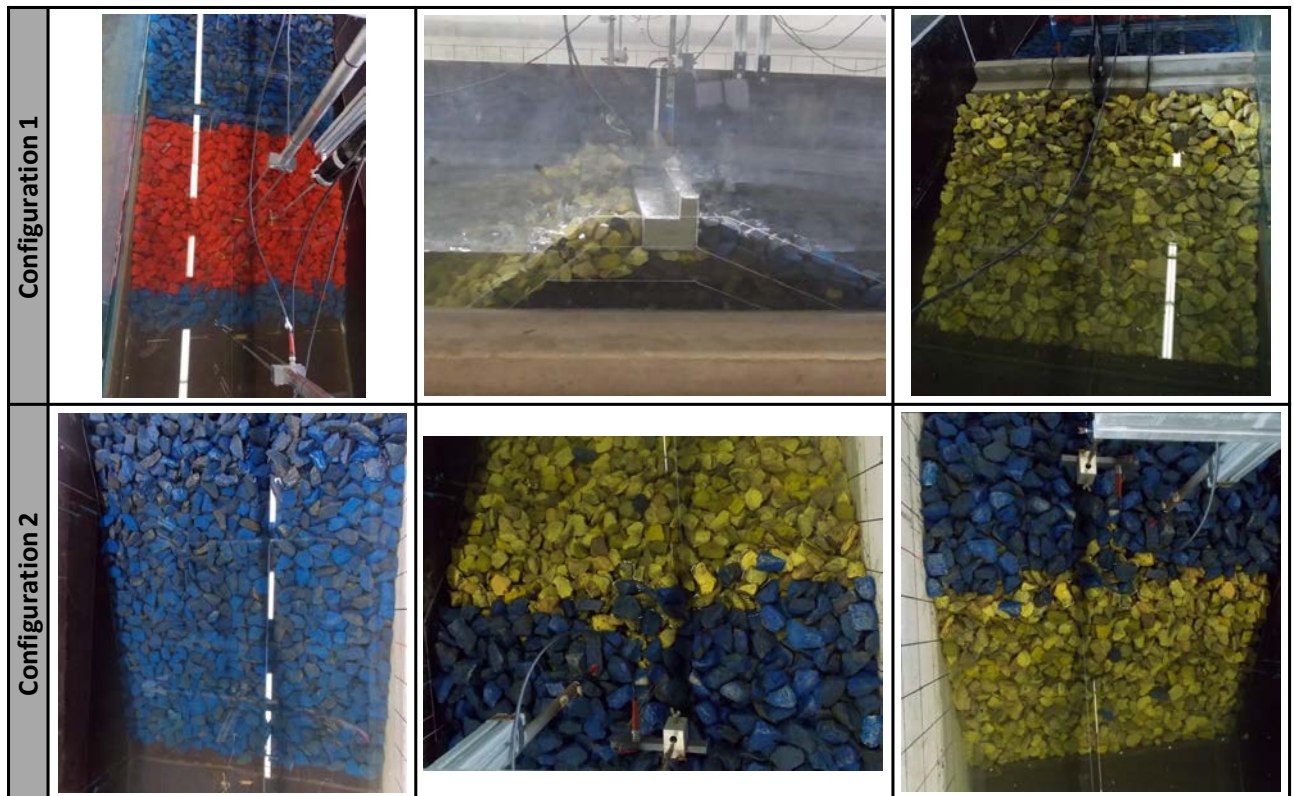


Figure E 7: Damage of configurations 1 and 2 due to solitary wave with $H=0.075$ m (Test 20140725_02)

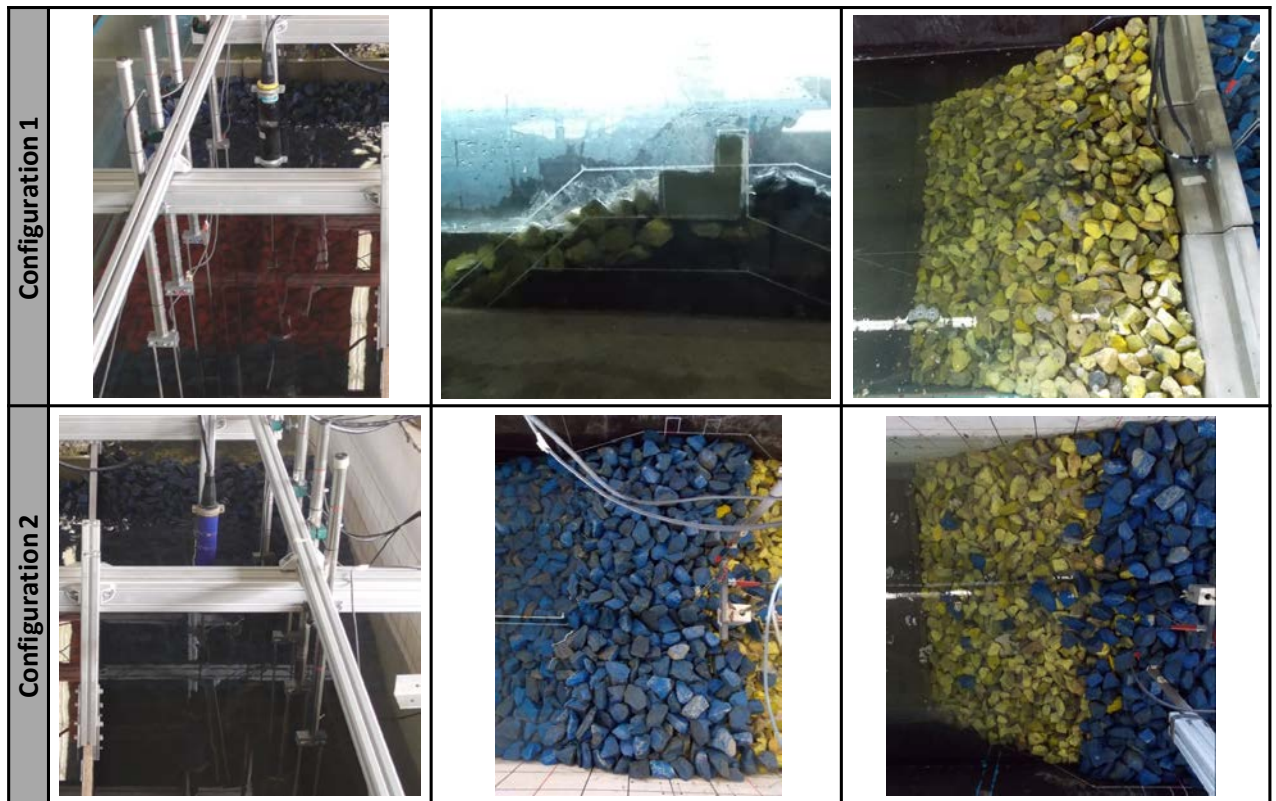


Figure E 8: Damage of configurations 1 and 2 due to solitary wave with $H=0.100$ m (Test 20140807_01)

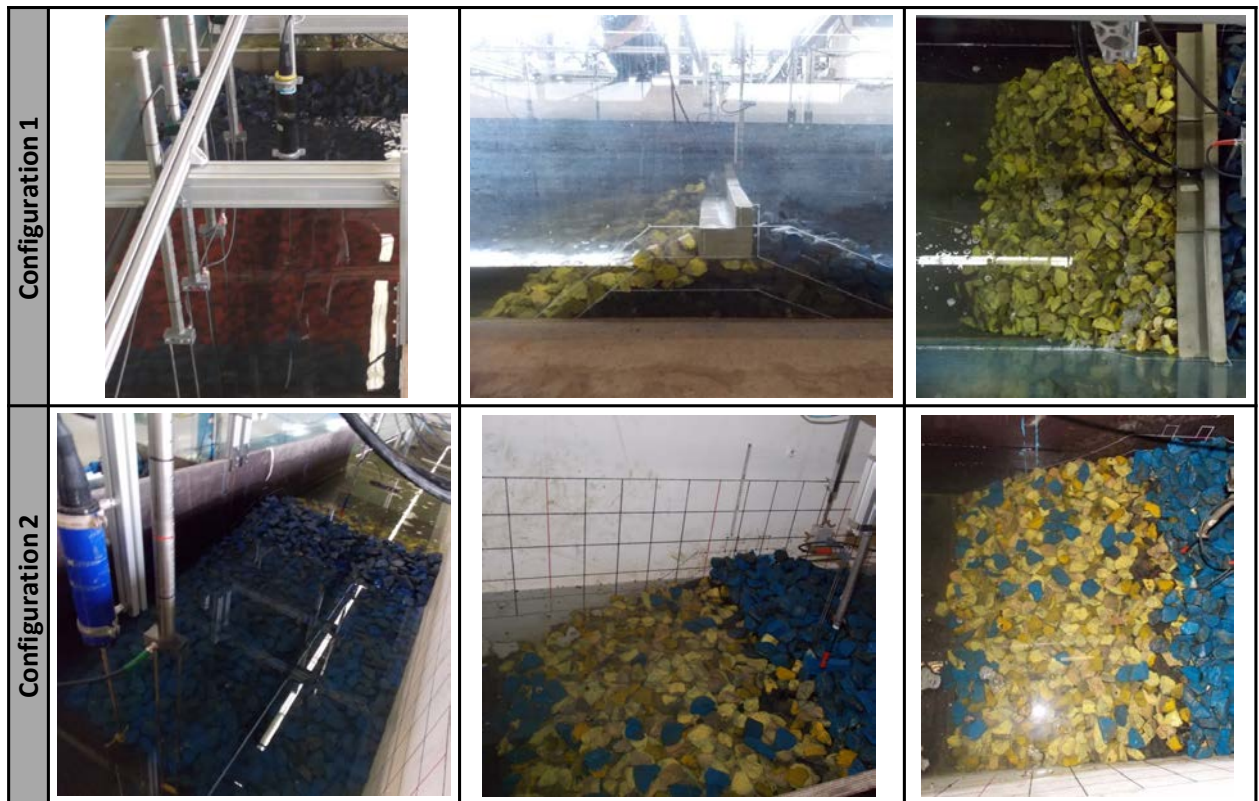


Figure E 9: Damage of configurations 1 and 2 due to solitary wave with $H=0.125$ m (Test 20140807_02)



Figure E 10: Damage of configurations 1 and 2 due to solitary wave with $H=0.150$ m (Test 20140807_03)



Figure E 11: Damage of configurations 3 and 4 due to solitary wave with $H=0.050\text{ m}$ (Test 20150106_01)



Figure E 12: Damage of configurations 3 and 4 due to solitary wave with $H=0.075$ m (Test 20150106_02)



Figure E 13: Damage of configurations 3 and 4 due to solitary wave with $H=0.100\text{ m}$ (Test 20150107_01)



Figure E 14: Damage of configurations 3 and 4 due to solitary wave with $H=0.125$ m (Test 20150108_01)

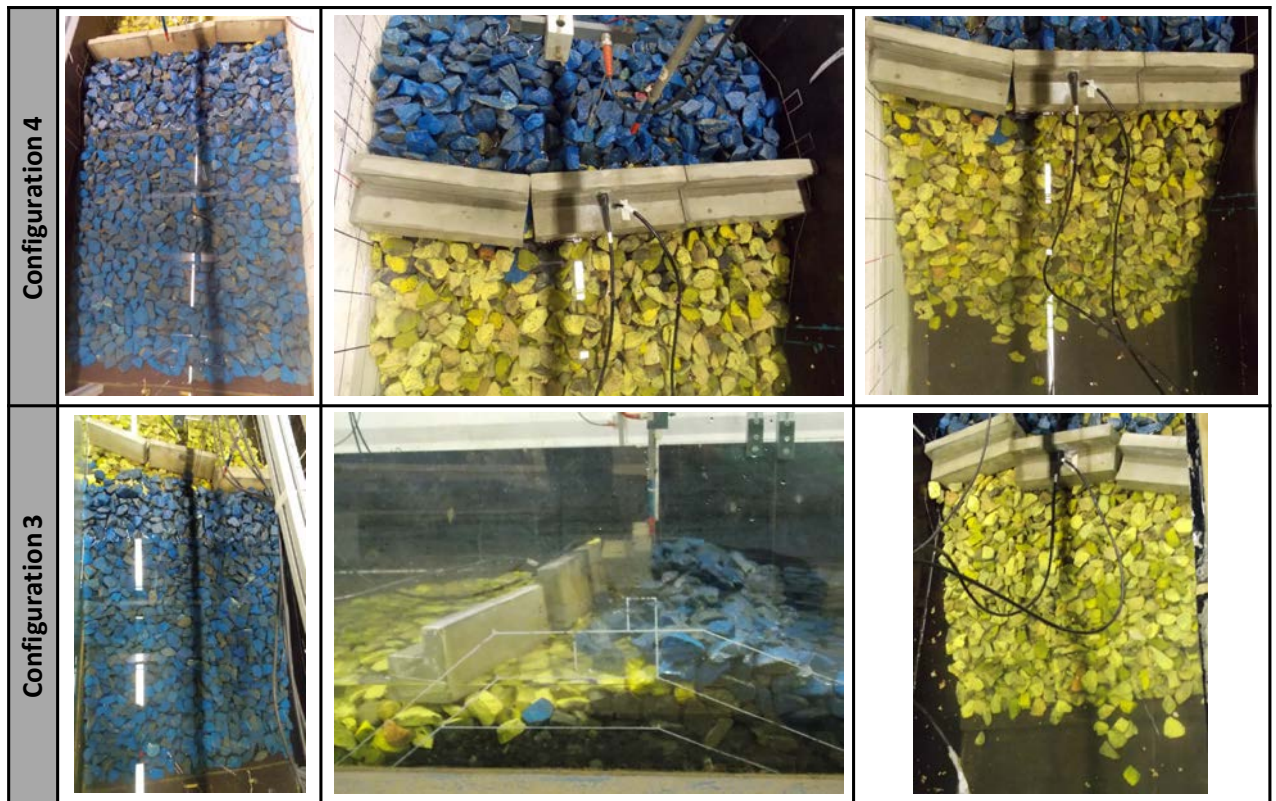


Figure E 15: Damage of configurations 3 and 4 due to solitary wave with $H=0.150$ m (Test 20150108_02)

Review and reference page

Document information									
Document title Deliverable D7 Results of the laboratory analysis and wave flume tests					Document No. 20120768-D7-R				
Type of document Report			Distribution Unlimited			Date 28.05.2015		Rev. No & date 0	
Client CONCERT-Japan Joint Call Secretariat									
Keywords									
Geographical information									
Country, County					Offshore area				
Municipality					Field name				
Location					Location				
Map					Field, Block No.				
UTM-coordinates									
Document control									
Quality assurance according to NS-EN ISO9001									
Rev.	Reason for revision	Self review by:		Colleague review by:		Independent review by:		Inter-disciplinary review by:	
0	Original document	A.S.-C.	A.K.	C.H.					

Document approved for release	Date 28.05.2015	Sign. Project Manager Carl Bonnevie Harbitz
--------------------------------------	---------------------------	---

NGI



**Middle East
Technical University**
Civil Engineering
Department



CONCERT JAPAN
Connecting and Coordinating
European Research and Technology Development with Japan
concertjapan.eu